



This is to certify that the
thesis entitled

EFFECTS OF HETEROGENEITY ON GROUNDWATER
FLOW AND CONTAMINANT TRANSPORT – A
VISUALIZATION LIBRARY

presented by

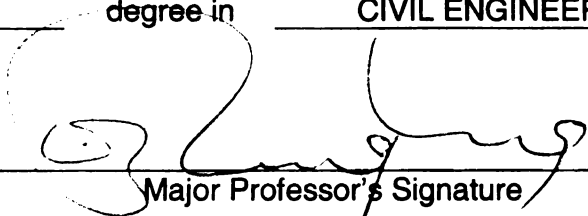
PRASANNA V SAMPATH


has been accepted towards fulfillment
of the requirements for the

MS

degree in

CIVIL ENGINEERING


Major Professor's Signature


Date

MSU is an Affirmative Action/Equal Opportunity Institution

LIBRARY
Michigan State
University

PLACE IN RETURN BOX to remove this checkout from your record.
TO AVOID FINES return on or before date due.
MAY BE RECALLED with earlier due date if requested.

DATE DUE	DATE DUE	DATE DUE

**EFFECTS OF HETEROGENEITY ON GROUNDWATER FLOW AND
CONTAMINANT TRANSPORT – A VISUALIZATION LIBRARY**

By

Prasanna V Sampath

A THESIS

**Submitted to
Michigan State University
in partial fulfillment of the requirements
for the degree of**

MASTER OF SCIENCE

Department of Civil and Environmental Engineering

2006

Abstract

EFFECTS OF HETEROGENEITY ON GROUNDWATER FLOW AND CONTAMINANT TRANSPORT – A VISUALIZATION LIBRARY

By

Prasanna V Sampath

It is well known that the subsurface environment is strongly heterogeneous with respect to geological, hydrological, and chemical properties. These heterogeneities are often “random” and can sometimes vary by several orders of magnitude over short distances. Data limitations, in addition to the fact that the subsurface environment is invisible, make the prediction of contaminant transport very difficult. This thesis presents a comprehensive visualization library, consisting of approximately 50 high-resolution numerical simulations and visualizations, which systematically explore the effects of heterogeneity on groundwater flow and transport. In particular, this thesis studies the effects of spatial heterogeneity, temporal variability, multi-scale heterogeneity and their complex non-linear interactions. This thesis also investigates the applicability of effective macrodispersion models for predicting plume transport, and the probabilistic structure of parameters like head, concentration, seepage flux, and solute flux through high-resolution Monte Carlo simulations. Several interesting conclusions emerge from these visualizations, such as the relative importance of porosity and partitioning coefficient while considering the impact of interacting heterogeneities, the irreversibility of plume transport due to interaction between temporal variability and spatial heterogeneity, the effectiveness of macrodispersion models in the presence of multi-scale heterogeneity, and the skewed, non-stationary nature of concentration uncertainty.

ACKNOWLEDGEMENTS

I owe my gratitude to all the people who have helped me during the course of my graduate study. My heartfelt gratitude goes to Dr. Shu-Guang Li, my adviser and committee chair, for his support and guidance. His advice and untiring help have played a huge role in the successful completion of my thesis.

I thank Dr. Roger Wallace profusely for serving in my committee and for his expert criticism of my writing. His invaluable comments made it possible for me to fine-tune the thesis. I also thank Dr. Phanikumar Mantha for serving in my committee. I also wish to thank Dr. Qun Liu for helping out with IGW-related issues.

I thank National Science Foundation (NSF) for funding my research. I thank all my research group mates, Soheil Afshari, Andreanne Simard, David Ni, and Hassan Abbas for their cooperation.

Finally, and most importantly, I want to thank my parents for encouraging me at each step of this journey.

TABLE OF CONTENTS

LIST OF TABLES.....	ix
LIST OF FIGURES.....	xii
Introduction.....	1
1 REAL WORLD HETEROGENEITY	8
2 RANDOM FIELD REPRESENTATION OF HETEROGENEITY.....	10
2.1 BORDEN AQUIFER, CANADA.....	10
2.1.1 <i>Problem statement</i>	10
2.1.2 <i>Key observations</i>	10
2.1.3 <i>Additional observations and discussion</i>	11
2.2 MULTIPLE REALIZATIONS.....	14
2.2.1 <i>Problem statement</i>	14
2.2.2 <i>Key observations</i>	14
2.2.3 <i>Additional observations and discussion</i>	14
2.3 EFFECT OF CORRELATION SCALES (λ).....	17
2.3.1 <i>Problem statement</i>	17
2.3.2 <i>Key observations</i>	17
2.3.3 <i>Additional observations and discussion</i>	17
2.4 EFFECT OF $\ln K$ VARIANCE.....	20
2.4.1 <i>Problem statement</i>	20
2.4.2 <i>Key observations</i>	20
2.4.3 <i>Additional observations and discussion</i>	20
2.5 RANDOM FIELD MODELS.....	23
2.5.1 <i>Problem statement</i>	23
2.5.2 <i>Key observations</i>	23
2.5.3 <i>Additional observations and discussion</i>	23
2.6 RANDOM FIELD GENERATION ALGORITHMS	25
2.6.1 <i>Problem statement</i>	25
2.6.2 <i>Key observations</i>	25
2.6.3 <i>Additional observations and discussion</i>	25
2.7 UNCONDITIONAL AND CONDITIONAL SIMULATIONS	28
2.7.1 <i>Problem statement</i>	28
2.7.2 <i>Key observations</i>	28
2.7.3 <i>Additional observations and discussion</i>	28

3 SPATIAL HETEROGENEITY.....	31
3.1 EFFECTS OF HETEROGENEITY OF HYDRAULIC CONDUCTIVITY	31
3.1.1 <i>Problem statement</i>	31
3.1.2 <i>Key observations</i>	31
3.1.3 <i>Additional observations and discussion</i>	32
3.1.4 <i>Mathematical interpretation</i>	33
3.2 EFFECTS OF HETEROGENEITY OF HYDRAULIC CONDUCTIVITY – WITH AND WITHOUT PORE-SCALE DISPERSION	38
3.2.1 <i>Problem statement</i>	38
3.2.2 <i>Key observations</i>	38
3.2.3 <i>Additional observations and discussion</i>	38
3.2.4 <i>Mathematical interpretation</i>	39
3.3 INTERACTIONS BETWEEN CONDUCTIVITY AND POROSITY HETEROGENEITIES	44
3.3.1 <i>Problem statement</i>	44
3.3.2 <i>Key observations</i>	44
3.3.3 <i>Additional observations and discussion</i>	44
3.3.4 <i>Mathematical interpretation</i>	45
3.4 INTERACTIONS BETWEEN CONDUCTIVITY AND PARTITIONING COEFFICIENT HETEROGENEITIES.....	49
3.4.1 <i>Problem statement</i>	49
3.4.2 <i>Key observations</i>	49
3.4.3 <i>Additional observations and discussion</i>	50
3.4.4 <i>Mathematical interpretation</i>	50
3.5 INTERACTIONS BETWEEN CONDUCTIVITY, POROSITY AND PARTITIONING COEFFICIENT HETEROGENEITIES	54
3.5.1 <i>Problem statement</i>	54
3.5.2 <i>Key observations</i>	54
3.5.3 <i>Additional observations and discussion</i>	55
3.5.4 <i>Mathematical interpretation</i>	56
3.6 EFFECT OF CORRELATION SCALE (λ) OF CONDUCTIVITY HETEROGENEITY	62
3.6.1 <i>Problem statement</i>	62
3.6.2 <i>Key observations</i>	62
3.6.3 <i>Additional observations and discussion</i>	62
3.7 EFFECT OF CORRELATION SCALE (λ) OF CONDUCTIVITY HETEROGENEITY	66
3.7.1 <i>Problem statement</i>	66
3.7.2 <i>Key observations</i>	66
3.7.3 <i>Additional observations and discussion</i>	66
3.8 EFFECTS OF ANISOTROPIC HETEROGENEITIES.....	70
3.8.1 <i>Problem statement</i>	70
3.8.2 <i>Key observations</i>	70
3.8.3 <i>Additional observations and discussion</i>	71
3.9 EFFECTS OF ANISOTROPIC HETEROGENEITIES.....	75
3.9.1 <i>Problem statement</i>	75

3.9.2 Key observations.....	75
3.9.3 Additional observations and discussion.....	75
4 TEMPORAL VARIABILITY	80
4.1 UNCONFINED AQUIFERS WITH INCREASING TRANSMISSIVITIES	80
4.1.1 Problem statement	80
4.1.2 Key observations.....	80
4.1.3 Additional observations and discussion.....	80
4.1.4 Mathematical interpretation	81
4.2 UNCONFINED AQUIFERS WITH INCREASING SPECIFIC YIELDS ...	85
4.2.1 Problem statement	85
4.2.2 Key observations.....	85
4.2.3 Additional observations and discussion.....	85
4.2.4 Mathematical interpretation	86
4.3 CONFINED AQUIFERS WITH INCREASING CONDUCTIVITIES	90
4.3.1 Problem statement	90
4.3.2 Key observations.....	90
4.3.3 Additional observations and discussion.....	90
4.3.4 Mathematical interpretation	91
4.4 CONFINED AQUIFERS WITH INCREASING STORAGE COEFFICIENTS.....	95
4.4.1 Problem statement	95
4.4.2 Key observations.....	95
4.4.3 Additional observations and discussion.....	95
4.4.4 Mathematical interpretation	96
4.5 COMPARISON BETWEEN UNCONFINED AND CONFINED AQUIFERS	100
4.5.1 Problem statement	100
4.5.2 Key observations.....	100
4.5.3 Additional observations and discussion.....	100
4.5.4 Mathematical interpretation	101
4.6 BOUNDARIES WITH DECREASING FREQUENCIES OF VARIABILITY	104
4.6.1 Problem statement	104
4.6.2 Key observations.....	104
4.6.3 Additional observations and discussion.....	104
4.6.4 Mathematical interpretation	105
4.7 BOUNDARIES WITH INCREASING EXTENTS OF PENETRATION INTO THE AQUIFER	109
4.7.1 Problem statement	109
4.7.2 Key observations.....	109
4.7.3 Additional observations and discussion.....	109
4.7.4 Mathematical interpretation	110
4.8 PLUME TRANSPORT - COMPARISON BETWEEN HOMOGENEOUS AND HETEROGENEOUS AQUIFERS.....	114
4.8.1 Problem statement	114

4.8.2 Key observations.....	114
4.8.3 Additional observations and discussion.....	114
4.9 PLUME TRANSPORT - COMPARISON BETWEEN HETEROGENEOUS AQUIFERS WITH AND WITHOUT EQUILIBRIUM SORPTION.....	118
4.9.1 Problem statement	118
4.9.2 Key observations.....	118
4.9.3 Additional observations and discussion.....	118
4.10 PLUME TRANSPORT - COMPARISON BETWEEN AQUIFERS WITH AND WITHOUT INTERACTING HETEROGENEITIES	122
4.10.1 Problem statement	122
4.10.2 Key observations.....	122
4.10.3 Additional observations and discussion.....	122
5 MACRODISPERSION.....	126
5.1 A MACRODISPERSION MODEL FOR PLUME MIGRATION IN WEAKLY HETEROGENEOUS MEDIA ($\ln K$ VARIANCE 0.5) WITH PORE- SCALE DISPERSION.....	126
5.1.1 Problem statement	126
5.1.2 Key observations.....	126
5.1.3 Additional observations and discussion.....	127
5.1.4 Mathematical interpretation.....	128
5.2 A MACRODISPERSION MODEL FOR PLUME MIGRATION IN MODERATELY HETEROGENEOUS MEDIA ($\ln K$ VARIANCE 1.0) WITH PORE-SCALE DISPERSION	132
5.2.1 Problem statement	132
5.2.2 Key observations.....	132
5.2.3 Additional observations and discussion.....	133
5.2.4 Mathematical interpretation.....	134
5.3 A MACRODISPERSION MODEL FOR PLUME MIGRATION IN STRONGLY HETEROGENEOUS MEDIA ($\ln K$ VARIANCE 2.0) WITH PORE-SCALE DISPERSION	139
5.3.1 Problem statement	139
5.3.2 Key observations.....	139
5.3.3 Additional observations and discussion.....	140
5.3.4 Mathematical interpretation.....	141
5.4 A MACRODISPERSION MODEL FOR PLUME MIGRATION IN VERY STRONGLY HETEROGENEOUS MEDIA ($\ln K$ VARIANCE 4.0) WITH PORE-SCALE DISPERSION	145
5.4.1 Problem statement	145
5.4.2 Key observations.....	145
5.4.3 Additional observations and discussion.....	146
5.4.4 Mathematical interpretation.....	147
5.5 A MACRODISPERSION MODEL FOR PLUME MIGRATION IN STRONGLY HETEROGENEOUS MEDIA ($\ln K$ VARIANCE 2.0) WITHOUT PORE-SCALE DISPERSION	151
5.5.1 Problem statement	151

5.5.2 Key observations.....	151
5.5.3 Additional observations and discussion.....	152
5.5.4 Mathematical interpretation.....	153
6 EFFECTS OF MULTI-SCALE HETEROGENEITY	157
6.1 EFFECTS OF MULTIPLE SCALES OF HETEROGENEITY	157
6.1.1 Problem statement	157
6.1.2 Key observations.....	157
6.1.3 Additional observations and discussion.....	158
6.2 MACRODISPERSION IN THE PRESENCE OF MULTIPLE SCALES OF HETEROGENEITY	161
6.2.1 Problem statement	161
6.2.2 Key observations.....	161
6.2.3 Additional observations and discussion.....	161
6.2.4 Mathematical interpretation.....	163
7 MONTE CARLO SIMULATIONS	167
7.1 EFFECTS OF HYDRAULIC CONDUCTIVITY HETEROGENEITY – DIFFERENT REALIZATIONS.....	167
7.1.1 Problem statement	167
7.1.2 Key observations.....	167
7.1.3 Additional observations and discussion.....	167
7.2 EFFECTS OF HYDRAULIC CONDUCTIVITY HETEROGENEITY – DIFFERENT REALIZATIONS.....	170
7.2.1 Problem statement	170
7.2.2 Key observations.....	170
7.2.3 Additional observations and discussion.....	170
7.3 MONTE CARLO SIMULATION – MEAN, VARIANCE AND COVARIANCE	173
7.3.1 Problem statement	173
7.3.2 Key observations.....	173
7.3.3 Additional observations and discussion.....	173
7.4 MONTE CARLO SIMULATION – PROBABILITY DISTRIBUTIONS AND BREAKTHROUGH CURVES	177
7.4.1 Problem statement	177
7.4.2 Key observations.....	177
7.4.3 Additional observations and discussion.....	178
8 CONCLUSIONS	181
9 REFERENCES.....	185

LIST OF TABLES

Table 2.1.1 Model parameters and inputs for cross-section A-A '	12
Table 2.1.1 Model parameters and inputs for cross-section B-B '	12
Table 2.2 Model parameters and inputs	15
Table 2.3 Model parameters and inputs	18
Table 2.4 Model parameters and inputs	21
Table 2.5 Model parameters and inputs	23
Table 2.6 Model parameters and inputs	25
Table 2.7 Model parameters and inputs	29
Table 3.1 Model parameters and inputs	35
Table 3.2 Model parameters and inputs	41
Table 3.3 Model parameters and inputs	46
Table 3.4 Model parameters and inputs	51
Table 3.5 Model parameters and inputs	57
Table 3.6 Model parameters and inputs	64
Table 3.7 Model parameters and inputs	68
Table 3.8 Model parameters and inputs	72
Table 3.9 Model parameters and inputs	77
Table 4.1 Model parameters and inputs	82
Table 4.2 Model parameters and inputs	87
Table 4.3 Model parameters and inputs	92
Table 4.4 Model parameters and inputs	97
Table 4.5 Model parameters and inputs	102
Table 4.6 Model parameters and inputs	106
Table 4.7 Model parameters and inputs	111
Table 4.8.1 Model parameters and inputs	115
Table 4.8.2 Temporally varying boundary conditions	115
Table 4.9.1 Model parameters and inputs	119

Table 4.9.2 Temporally varying boundary conditions.....	120
Table 4.10.1 Model parameters and inputs.....	123
Table 4.10.2 Temporally varying boundary conditions.....	124
Table 5.1 Model parameters and inputs.....	129
Table 5.2 Model parameters and inputs.....	136
Table 5.3 Model parameters and inputs.....	143
Table 5.4 Model parameters and inputs.....	149
Table 5.5 Model parameters and inputs.....	155
Table 6.1 Model parameters and inputs.....	159
Table 6.2 Model parameters and inputs.....	165
Table 7.1 Model parameters and inputs.....	168
Table 7.2 Model parameters and inputs.....	171
Table 7.3.1 Model parameters and inputs.....	174
Table 7.3.2 Maximum and minimum values for plotting	175
Table 7.4 Model parameters and inputs.....	179

LIST OF FIGURES

Figure 1.1 Gravel pit at Phoenix, Arizona showing natural variability consisting of several layers of coarse and fine grained material of varying thickness (Modified from <i>Groundwater hydrology</i> , Bouwer, 1978).....	8
Figure 1.2 "Permeability and porosity of cores collected at 1-ft intervals from borehole (IL056) in the Mt. Simon aquifer in Illinois (date from Bakr, 1976)." (Modified from <i>Stochastic Subsurface Hydrology</i> , Gelhar, 1993).....	9
Figure 2.1 Snapshot of the visualization.....	13
Figure 2.2 Snapshot of the visualization.....	16
Figure 2.3 Snapshot of the visualization.....	19
Figure 2.4 Snapshot of the visualization.....	22
Figure 2.4 Snapshot of the visualization.....	24
Figure 2.6 Snapshot of the visualization.....	27
Figure 2.7 Snapshot of the visualization.....	30
Figure 3.1 Snapshot of the visualization.....	37
Figure 3.2 Snapshot of the visualization.....	43
Figure 3.3 Snapshot of the visualization showing spatial variation of n	48
Figure 3.4 Snapshot of the visualization showing spatial variation of K_d	53
Figure 3.5.1 Snapshot of the visualization.....	59
Figure 3.5.2 Spatial variation of n	60
Figure 3.5.3 Spatial variation of K_d	61
Figure 3.6 Snapshot of the visualization.....	65
Figure 3.7 Snapshot of the visualization.....	69
Figure 3.8 Snapshot of the visualization.....	74
Figure 3.9 Snapshot of the visualization.....	79
Figure 4.1 Snapshot of the visualization.....	84
Figure 4.2 Snapshot of the visualization.....	89
Figure 4.3 Snapshot of the visualization.....	94
Figure 4.4 Snapshot of the visualization.....	99

Figure 4.5 Snapshot of the visualization.....	103
Figure 4.6 Snapshot of the visualization.....	108
Figure 4.7 Snapshot of the visualization.....	113
Figure 4.8 Snapshot of the visualization.....	117
Figure 4.9 Snapshot of the visualization.....	121
Figure 4.10 Snapshot of the visualization.....	125
Figure 5.1 Snapshot of the visualization.....	131
Figure 5.2 Snapshot of the visualization.....	138
Figure 5.3 Snapshot of the visualization.....	144
Figure 5.4 Snapshot of the visualization.....	150
Figure 5.5 Snapshot of the visualization.....	156
Figure 6.1 Snapshot of the visualization.....	160
Figure 6.2 Snapshot of the visualization.....	166
Figure 7.1 Snapshot of the visualization.....	169
Figure 7.2 Snapshot of the visualization.....	172
Figure 7.3 Snapshot of the visualization.....	176
Figure 7.4 Snapshot of the visualization.....	180

Introduction

The study of the subsurface environment is both challenging and exciting, because of its inherent complexities and heterogeneities. In the past, most research that investigated the effects of heterogeneity employed theoretical analyses based on a number of highly restrictive assumptions, such as stationarity, ergodicity, scale disparity, linearization, and small perturbation. These assumptions severely limit our ability to understand the effects of heterogeneity on groundwater flow and transport in real world scenarios. With the advent of extremely efficient computers, and through the introduction of Interactive Groundwater (IGW) – A real-time modeling paradigm (*Li and Liu, 2003; Li and Liu, 2006*), some of the limitations listed above are overcome. Taking advantage of these recent developments, this thesis systematically explores the effects of heterogeneity on groundwater flow and transport using high-resolution numerical simulations and visualizations.

The need to visualize

More than a couple of decades of research have gone into understanding the influence of heterogeneities on groundwater flow and transport. However, data limitations, in addition to the fact that the subsurface environment is invisible to the human eye, have made it difficult to physically understand groundwater dynamics. The objective of this research is to create a comprehensive library covering different aspects of stochastic subsurface hydrology, using a set of high-resolution numerical simulations and visualizations. This library systematically explores the effects of heterogeneities, interactions between aquifer parameters and temporal variability, and multi-scale effects. Macrodispersion models and

Monte Carlo simulations are also visualized in this thesis. Sharing information in the form of a visualization library has been made possible by the rapid development of computers and the Internet.

Chapter 1 of this thesis illustrates the variability of aquifers in the real world, while Chapter 2 deals with the representation of heterogeneity using random field models. The effects of spatial heterogeneity and interactions with other aquifer parameters, such as porosity and partitioning coefficient are explored in Chapter 3. The effects of temporal variability and its interaction with spatial heterogeneity are dealt with in Chapter 4. Chapter 5 is devoted towards the use of macrodispersion models, while Chapter 6 illustrates the effects of multiple scales of heterogeneity. Stochastic methods like Monte Carlo simulations are discussed in Chapter 7.

Factors influencing groundwater flow and transport

There are spatial and temporal factors that influence plume transport in the subsurface environment. Spatial factors are those that vary in the spatial domain of the aquifer matrix, such as conductivity, porosity, and partitioning coefficient. Temporal factors are those that vary with time, such as the frequency of oscillation of a time-variable boundary condition. This thesis explores, in detail, these heterogeneities and their effect on groundwater flow and transport. The application of macrodispersion models and Monte Carlo simulations are also studied.

Random field representation of heterogeneity

In the real world, the subsurface environment is extremely complex and variable. In order to create an “accurate” model, it is necessary to obtain data samples, which can characterize the type and extent of the variability. The type of variability that has the most influence is the conductivity of the aquifer, although there are other variabilities, such as porosity and partitioning coefficient. The accuracy of the model depends on the resolution of the data. Higher resolution data, in general, will provide better accuracy. High-resolution data is not available at all times since data acquisition is costly and time consuming. However, it is possible to predict the internal structure of the aquifer using statistical methods on available data. The most common method adopted is to obtain the mean, variance, covariance, and correlation scale of the heterogeneity of the aquifer properties. Using this information, a random field can be generated that has the same statistical properties as the data set. Chapter 2 deals exclusively with the use of random field models, algorithms, and unconditional and conditional simulations to represent real world heterogeneity.

Effects of spatial heterogeneity

The main parameter of interest in groundwater hydrology is the hydraulic conductivity of the aquifer. The effect of heterogeneity of this parameter is studied in Section 3.1.

Another parameter of interest in a groundwater model is the pore-scale dispersivity. This parameter is needed in order to compensate for spatial averaging. However, the introduction of pore-scale dispersivity into the model lowers the maximum concentration

of the plume. Section 3.2 deals with the effect of pore-scale dispersivity on plume transport.

Generally, the conductivity in a domain is modeled as a spatially varying parameter, while the values of porosity and partitioning coefficient used in models are assumed to be constant over the modeling domain. This assumption can be questioned since it is known that porosity and partitioning coefficient are correlated with the conductivity. Porosity and partitioning coefficient are, in general, positively and negatively correlated with conductivity respectively. These correlations affect plume spreading. The effects of these correlations are explored in Sections 3.3, 3.4, and 3.5.

The correlation scale of heterogeneity plays a very important role in the spreading of plumes. Depending on whether the correlation scale is smaller, of the same size, or larger than the initial size of the plume, the plume can spread in drastically different ways. This difference can be attributed to the effect of correlation scales on the formation of “preferential” paths for plume transport. Further complications can arise if the heterogeneity is anisotropic. Strongly anisotropic heterogeneity can result in varied degrees of plume spreading, depending on the direction of flow. Sections 3.6, 3.7, 3.8, and 3.9 elucidate the effect of correlation scales on plume transport.

Effects of temporal variability

While spatial heterogeneity is very important, temporal variability can also result in complex groundwater flow situations. A sinusoidally oscillating boundary condition can

affect the head in the aquifer, and hence the direction of flow. The effect of such a boundary on an aquifer is dependent on the type of aquifer, as well as its transmissivity and storage properties. Unconfined aquifers are usually affected less than a confined aquifer of similar transmissivity, due to the drastically different storage properties of the two aquifers. Unconfined aquifers release water by draining of the inter-granular pore space. On the other hand, confined aquifers release water by elastic expansion of the aquifer matrix and decompression of water. Therefore, confined aquifers have to drain a larger area to obtain the same amount of water as an unconfined aquifer. The sinusoidally oscillating boundary condition is characterized by an amplitude and a time period. The magnitude of the amplitude and time period has an impact on the area of aquifer affected. Chapter 4 explores the effects of temporal variability on groundwater flow and transport.

Macrodispersion model

In order to characterize the spatial heterogeneity in an aquifer, data is required. Data acquisition is economically not feasible in all situations. Therefore, it becomes essential to characterize the aquifer using other means. One of the statistical means to characterize the aquifer is Gelhar's asymptotic macrodispersion model (*Gelhar and Axness, 1983a*). This model approximates the complex heterogeneous field with pore-scale dispersion coefficient to a simpler homogenous field with an effective macrodispersion coefficient. One of the basic assumptions of this model is that the heterogeneous field has a relatively small $\ln K$ variance. The advantage of this model is that the complex heterogeneities are "lumped" together into an equivalent coefficient, making the process of modeling much simpler. However, this model is only able to predict the average concentration over a

large spatial area. In reality, the concentration fluctuates, which is extremely important when the maximum concentration is to be estimated. Chapter 5 elucidates the application of macrodispersion models to predict plume transport in heterogeneous media and evaluates the effectiveness of these models.

Effects of multi-scale heterogeneity

Uniquely characterizing spatial heterogeneity is extremely difficult, since it requires high-resolution data. It becomes even more difficult because spatial heterogeneity exists on many scales. Modeling all the scales of heterogeneity is impossible. Smaller scales of heterogeneity within larger scales have a significant impact on plume spreading. Usually, available data is “coarse,” allowing modeling of larger scales. While the larger scales provide the “trend” or the general path of transport, it is the smaller scales that determine the amount of spreading. Therefore, the ability to characterize these smaller scales is important. This can be achieved by using Gelhar’s macrodispersion model. Although Gelhar’s model assumes a homogeneous field with macrodispersion, a moderately heterogeneous field with a large scale of heterogeneity is a close approximation. Chapter 6 deals with effects of multiple scales of heterogeneity on plume transport.

Monte Carlo simulations

Despite the use of various methods to characterize the aquifer structure, due to the inherent complexity of the medium, there is an element of uncertainty in the results obtained. It is in this context that stochastic methods are needed. Stochastic methods make it possible to quantify the uncertainty, using techniques like Monte Carlo

simulations. In spite of characterizing aquifer structure using a random field model, each realization of this random field is only one of an infinite number of possible situations. Therefore, the results obtained from one realization are not the “truth.” Neither is it possible to determine what the truth is. A Monte Carlo simulation, which consecutively generates infinite realizations, is a technique used to obtain the probability of occurrence of an event. The results obtained from each realization are used to update the statistics of the probability distribution. After a sufficiently large number of realizations, the probability distribution “stabilizes.” This result gives not only the probability of occurrence, but also the standard deviation. This technique is very useful for probabilistic analysis and risk estimation, and is discussed in Chapter 7.

Each Chapter in this thesis, with the exception of Chapter 1, consists of a number of Sections, which are further divided into sub-sections. Each Section is devoted to a visualization, which attempts to explain certain aspects of flow and transport. Each Section is divided into the following sub-sections: Problem statement, Key observations, Additional observations and discussion, Mathematical interpretation (if applicable), and Model parameters and inputs. A snapshot of the visualization and a URL to view the visualization on the Internet are also provided in every Section.

It is the intention of this visualization library to provide a systematic “reference manual” for students, researchers, and practitioners of groundwater modeling. Images in this thesis are presented in color. The visualization library can be accessed on the Internet at <http://www.egr.msu.edu/igw/DL/SSH>

1 REAL WORLD HETEROGENEITY

The subsurface environment is inherently heterogeneous with respect to geologic, hydrologic and chemical properties. Aquifer properties such as hydraulic conductivity and partitioning coefficient can sometimes vary by several orders of magnitude over surprisingly short distances.

Figure 1.1 shows a typical aquifer outcrop in a gravel pit at Phoenix, Arizona (*Groundwater hydrology*, Bouwer, 1978). Note that there are several layers of various aquifer materials of varying thickness in the picture.



Figure 1.1 Gravel pit at Phoenix, Arizona showing natural variability consisting of several layers of coarse and fine grained material of varying thickness (Modified from *Groundwater hydrology*, Bouwer, 1978)

Figure 1.2 shows the range of porosity and permeability values collected at 1 foot intervals from a borehole in Mt. Simon aquifer, Illinois (*Stochastic Subsurface Hydrology*, Gelhar, 1993). While porosity varies over a wide range, permeability varies by several orders of magnitude.

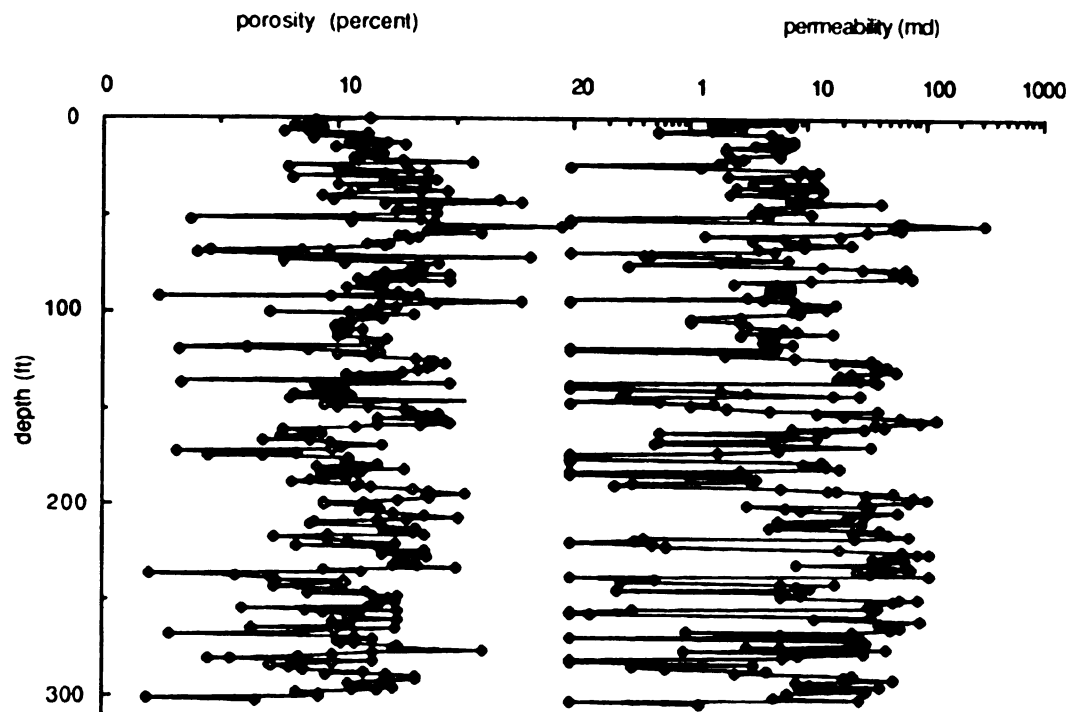


Figure 1.2 "Permeability and porosity of cores collected at 1-ft intervals from borehole (IL056) in the Mt. Simon aquifer in Illinois (date from Bakr, 1976)."
(Modified from *Stochastic Subsurface Hydrology*, Gelhar, 1993)

From Figures 1.1 and 1.2 it is clear that natural variability in the horizontal and vertical directions is significant. A set of pictures on other real world aquifers can be accessed at the following address:

URL: <http://www.egr.msu.edu/igw/DL/SSH/RWH>

2 RANDOM FIELD REPRESENTATION OF HETEROGENEITY

2.1 BORDEN AQUIFER, CANADA

2.1.1 Problem statement

This video demonstrates the multiple realizations for the statistical parameters of the Borden aquifer, Canada (*Sudicky*, 1986). Details are provided in Tables 2.1.1 and 2.1.2.

2.1.2 Key observations

The following observations can be made from the video:

- A random field is characterized by a set of statistical parameters, such as mean, variance and correlation scale.
- Multiple realizations of the Borden aquifer data share the same “texture” as the data.
- In spite of having the same structure, each realization is different from other realizations.
- An infinite number of realizations exist that satisfy the same statistical parameters; hence, uniquely characterizing aquifer structure with limited data is impossible.
- All the realizations statistically represent the truth. None of them can deterministically represent the truth.

2.1.3 Additional observations and discussion

Any aquifer can be statistically represented using a mean, ln K variance and a correlation scale. A brief description of these parameters is given below:

- Mean – Is the geometric mean of the data, which represents the average conditions that exist in the aquifer
- Correlation scale – Is a measure of the spatial distance across which the aquifer properties are supposed to be correlated. This parameter can be different in all three directions making the aquifer anisotropic. However, in most cases, the horizontal correlation scales (λ_x and λ_y) are assumed to be constant. Vertical correlation scale (λ_z) is in general smaller than the horizontal correlation scales. Correlation scales give an idea about the “texture” or “pattern” of variability.
- Variance – Is a measure of how variable the aquifer properties are with respect to the mean. A higher variance means higher variability of aquifer properties and vice versa.

The Borden aquifer is a test site, which generated a large amount of hydraulic conductivity data with extremely fine resolution. Using this data, Sudicky (1986) performed a statistical analysis to obtain the mean, variance and correlation scale for this site. Given these parameters, it is possible to create a random field that statistically represents the Borden aquifer.

Table 2.1.1 Model parameters and inputs for cross-section A-A '

Parameter	All realizations
Geometric mean hydraulic conductivity, K_g (cm/s)	9.75×10^{-3}
$\ln K$ variance	0.38
Correlation scale, λ_x (m)	2.8
Correlation scale, λ_z (m)	0.12
Size of model (m)	19 x 1.75
Covariance function	Exponential
Grid	761 x 71
Cell size, Δx (m)	0.025 x 0.025

Table 2.1.1 Model parameters and inputs for cross-section B-B '

Parameter	All realizations
Geometric mean hydraulic conductivity, K_g (cm/s)	9.75×10^{-3}
$\ln K$ variance	0.38
Correlation scale, λ_x (m)	2.8
Correlation scale, λ_z (m)	0.12
Size of model (m)	12 x 1.75
Covariance function	Exponential
Grid	481 x 71
Cell size, Δx (m)	0.025 x 0.025

The model parameters and inputs are explained below:

- The $\ln K$ field is a normally distributed random field. Therefore, there is an equal probability of the plume encountering a 'low' K zone or a 'high' K zone.
- The heterogeneous conductivity field is uniquely characterized by the following set of statistical parameters: geometric mean (K_g) of K , correlation scale, $\ln K$ variance and covariance.
- The geometric mean, $\ln K$ variance, and correlation scale is constant for all cases.
- The covariance function for all realizations is exponential.
- The cell size, Δx , is selected such that the correlation scale, λ , is resolved; typically, Δx is at least 3 to 4 times smaller than the correlation scale.

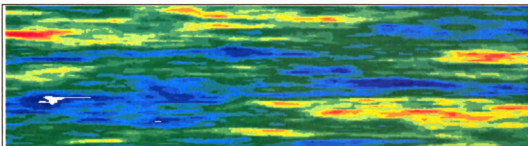


Figure 2.1 Snapshot of the visualization

For a detailed visualization, access the following addresses:

URL: <http://www.egr.msu.edu/igw/DL/SSH/RFRH/RFRH00.htm>

URL: <http://www.egr.msu.edu/igw/DL/SSH/RFRH/RFRH0.htm>

2.2 MULTIPLE REALIZATIONS

2.2.1 Problem statement

This video demonstrates the multiple realizations that are possible from a given set of statistical parameters. Details are provided in Table 2.2.

2.2.2 Key observations

The following observations can be made from the video:

- The statistical properties of all realizations are identical; each realization has the same underlying statistical “structure.”
- In spite of having the same structure, each realization is different from other realizations.
- An infinite number of realizations exist that satisfy the same statistical parameters; hence, uniquely characterizing aquifer structure with limited data is impossible.

2.2.3 Additional observations and discussion

Since aquifer properties vary dramatically within very short distances, a point-to-point detailed description of the aquifer structure is impossible. With available data, statistical parameters such as mean, variance, and correlation scale can be obtained. Using these parameters, a random field model can be created. Infinite realizations of the random field, which satisfy the statistical parameters, can be created. Although each of these realizations is created from the same underlying statistical structure, they are different from each other.

Table 2.2 Model parameters and inputs

Parameter	All realizations
Geometric mean hydraulic conductivity, K_g (m/day)	10
$\ln K$ variance	1.0
Correlation scale, λ (m)	5
Size of model (m)	100 x 100
Covariance function	Exponential
Grid	203 x 203
Cell size, Δx (m)	1 x 1

The model parameters and inputs are explained below:

- The $\ln K$ field is a normally distributed random field. Therefore, there is an equal probability of the plume encountering a 'low' K zone or a 'high' K zone.
- The heterogeneous conductivity field is uniquely characterized by the following set of statistical parameters: geometric mean (K_g) of K , correlation scale, variance and covariance.
- The geometric mean, $\ln K$ variance, and correlation scale is constant for all cases.
- The covariance function for all realizations is exponential.
- The cell size, Δx , is selected such that the correlation scale, λ , is resolved; typically, Δx is at least 3 to 4 times smaller than the correlation scale.

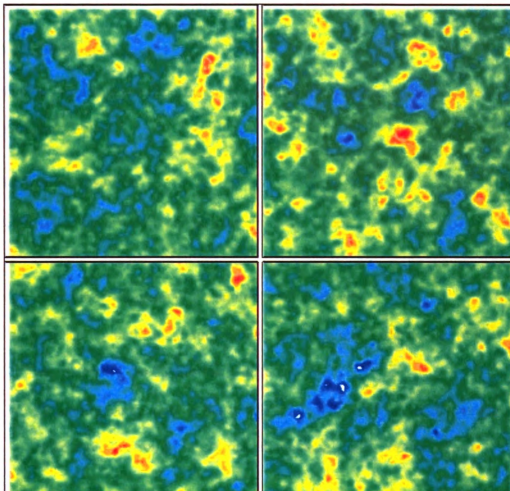


Figure 2.2 Snapshot of the visualization

For a detailed visualization, access the following address:

URL: <http://www.cgr.msu.edu/jgw/DL/SSH/RFRH/RFRH1.htm>

2.3 EFFECT OF CORRELATION SCALES (λ)

2.3.1 Problem statement

This video demonstrates the effect of correlation scales on the aquifer texture. Details are provided in Table 2.3.

2.3.2 Key observations

The following observations can be made from the video:

- Correlation scales are an important statistical property of the aquifer, which determine the texture of the aquifer's heterogeneity.
- Depending on the magnitude of the correlation scales, the texture of the heterogeneity can be drastically different.
- Depending on the ratio of the correlation scales, aquifers can be isotropic, anisotropic or strongly anisotropic in the horizontal or vertical planes.

2.3.3 Additional observations and discussion

Given the statistical parameters of an aquifer, the aquifer structure can be determined.

The parameter that controls the “texture” of the aquifer is the correlation scale.

Case 1: The correlation scales, λ_x and λ_y , are 5 m in both directions for this aquifer. This isotropic structure is most commonly found in the horizontal plane.

Case 2: The correlation scales, λ_x and λ_y , are 30 m and 5 m respectively. This aquifer structure is anisotropic, and is most commonly found in a vertical cross-section.

Case 3: The correlation scales, λ_x and λ_y , are 100 m and 5 m respectively. This aquifer structure is strongly anisotropic, and is most commonly found in a vertical cross-section. Such an aquifer is called “perfectly” stratified.

Case 4: The correlation scales, λ_x and λ_y , are 5 m and 100 m respectively. This aquifer structure is strongly anisotropic and not very commonly found.

Table 2.3 Model parameters and inputs

Parameter	Case 1	Case 2	Case 3	Case 4
Geometric mean hydraulic conductivity, K_g (m/day)	10	10	10	10
ln K variance	1.0	1.0	1.0	1.0
Correlation scale, λ_x (m)	5	30	100	5
Correlation scale, λ_y (m)	5	5	5	100
Size of model (m)	100 x 100	100 x 100	100 x 100	100 x 100
Covariance function	Exponential	Exponential	Exponential	Exponential
Grid	203 x 203	203 x 203	203 x 203	203 x 203
Cell size, Δx (m)	1 x 1	1 x 1	1 x 1	1 x 1

The model parameters and inputs are explained below:

- The ln K field is a normally distributed random field. Therefore, there is an equal probability of the plume encountering a ‘low’ K zone or a ‘high’ K zone.
- The heterogeneous conductivity field is uniquely characterized by the following set of statistical parameters: geometric mean (K_g) of K , correlation scale, variance and covariance.
- The geometric mean and ln K variance is constant for all cases.
- The correlation scales, λ_x and λ_y , are 5m and 5m, 30 m and 5 m, 100 m and 5 m, and 5 m and 100 m for cases 1, 2, 3, and 4 respectively.

- The covariance function for all realizations is exponential.
- The cell size, Δx , is selected such that the correlation scale, λ , is resolved; typically, Δx is at least 3 to 4 times smaller than the correlation scale.

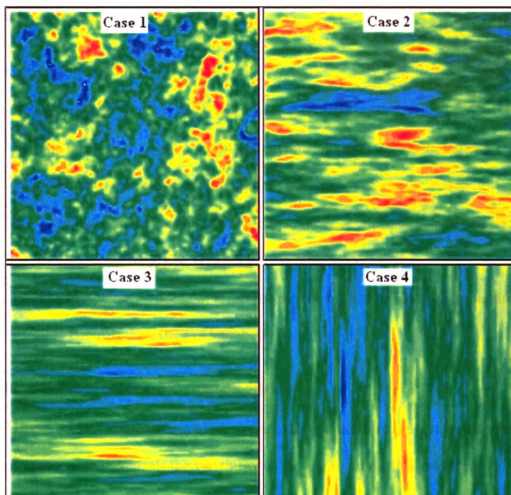


Figure 2.3 Snapshot of the visualization

For a detailed visualization, access the following address:

URL: <http://www.egr.msu.edu/igw/DL/SSH/RFRH/RFRH2.htm>

2.4 EFFECT OF $\ln K$ VARIANCE

2.4.1 Problem statement

This video demonstrates the effect of $\ln K$ variance on the degree of variability in the aquifer. Details are provided in Table 2.4.

2.4.2 Key observations

The following observations can be made from the video:

- The $\ln K$ variance is an important statistical property of the aquifer, which determines the degree of variability in the aquifer.
- Depending on the magnitude of the $\ln K$ variance, aquifers can be weakly, moderately, strongly or very strongly heterogeneous.
- The $\ln K$ variance does not affect the pattern of heterogeneity in the aquifer, it only controls the extent of variability.

2.4.3 Additional observations and discussion

Given the statistical parameters of an aquifer, the aquifer structure can be determined.

The parameter that controls the variability of the aquifer is the $\ln K$ variance.

Case 1: The $\ln K$ variance is 0.5 for this aquifer. This aquifer is weakly heterogeneous.

Case 2: The $\ln K$ variance is 1.0 for this aquifer. This aquifer is moderately heterogeneous.

Case 3: The $\ln K$ variance is 2.0 for this aquifer. This aquifer is moderately to strongly heterogeneous.

Case 4: $\ln K$ variance is 4.0 for this aquifer. This aquifer is strongly heterogeneous.

Table 2.4 Model parameters and inputs

Parameter	Case 1	Case 2	Case 3	Case 4
Geometric mean hydraulic conductivity, K_g (m/day)	10	10	10	10
$\ln K$ variance	0.5	1.0	1.5	2.0
Correlation scale, λ_x (m)	5	5	5	5
Size of model (m)	100 x 100	100 x 100	100 x 100	100 x 100
Covariance function	Exponential	Exponential	Exponential	Exponential
Grid	203 x 203	203 x 203	203 x 203	203 x 203
Cell size, Δx (m)	1 x 1	1 x 1	1 x 1	1 x 1

The model parameters and inputs are explained below:

- The $\ln K$ field is a normally distributed random field. Therefore, there is an equal probability of the plume encountering a 'low' K zone or a 'high' K zone.
- The heterogeneous conductivity field is uniquely characterized by the following set of statistical parameters: geometric mean (K_g) of K , correlation scale, variance and covariance.
- The geometric mean and correlation scale is constant for all cases.
- The $\ln K$ variance is 0.5, 1.0, 2.0, and 4.0 for cases 1, 2, 3, and 4 respectively.
- The covariance function for all realizations is exponential.
- The cell size, Δx , is selected such that the correlation scale, λ , is resolved; typically, Δx is at least 3 to 4 times smaller than the correlation scale.

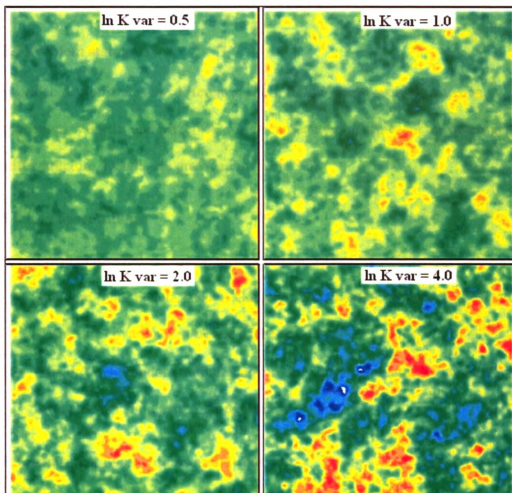


Figure 2.4 Snapshot of the visualization

For a detailed visualization, access the following address:

URL: <http://www.egr.msu.edu/jgw/DL/SSH/RFRH/RFRH3.htm>

2.5 RANDOM FIELD MODELS

2.5.1 Problem statement

This video demonstrates the different random field models, such as Gaussian, Exponential, Whittle, and Mizell-A, which can be used to represent the heterogeneity in aquifer structure. Details are provided in Table 2.5.

2.5.2 Key observations

The following observations can be made from the video:

- Random field models, such as Gaussian, Exponential, Whittle, and Mizell-A, define the covariance structure of the aquifer.
- The different random field models produce aquifer structures that are very similar to each other for a particular realization.

2.5.3 Additional observations and discussion

Given the statistical parameters of an aquifer, the aquifer structure can be modeled using a number of random field models. Depending on the type of model, the data interpolation is done using different sets of equations. Expectedly, the aquifer structures generated by each model, for a particular realization, are very similar to each other.

Table 2.5 Model parameters and inputs

Parameter	Case 1	Case 2	Case 3	Case 4
Geometric mean hydraulic conductivity, K_g (m/day)	10	10	10	10
$\ln K$ variance	1.0	1.0	1.0	1.0
Correlation scale, λ_x (m)	5	5	5	5
Size of model (m)	100 x 50	100 x 50	100 x 50	100 x 50
Covariance function	Gaussian	Exponential	Whittle	Mizell-A
Grid	203 x 102	203 x 102	203 x 102	203 x 102

Cell size, Δx (m)	1 x 1	1 x 1	1 x 1	1 x 1
---------------------------	-------	-------	-------	-------

The model parameters and inputs are explained below:

- The $\ln K$ field is a normally distributed random field. Therefore, there is an equal probability of the plume encountering a ‘low’ K zone or a ‘high’ K zone.
- The heterogeneous conductivity field is uniquely characterized by the following set of statistical parameters: geometric mean (K_g) of K , correlation scale, variance and covariance.
- The geometric mean, $\ln K$ variance, and correlation scale is constant for all cases.
- The covariance function is Gaussian, Exponential, Whittle, and Mizell-A for cases 1, 2, 3, and 4 respectively.
- The cell size, Δx , is selected such that the correlation scale, λ , is resolved; typically, Δx is at least 3 to 4 times smaller than the correlation scale.

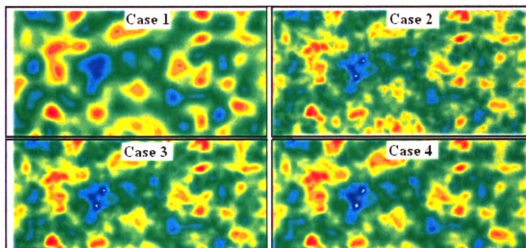


Figure 2.4 Snapshot of the visualization

For a detailed visualization, access the following address:

URL: <http://www.egr.msu.edu/igw/DL/SSH/RFRH/RFRH5.htm>

2.6 RANDOM FIELD GENERATION ALGORITHMS

2.6.1 Problem statement

This video demonstrates the different random field generation algorithms, such as Spectral algorithm, Sequential Gaussian simulation, Turnings Bands algorithm, and Simulated Annealing, which can be used to represent the heterogeneity in aquifer structure. Details are provided in Table 2.6.

2.6.2 Key observations

The following observations can be made from the video:

- The different random field generation algorithms produce aquifer structures that are very similar to each other for a particular realization.

2.6.3 Additional observations and discussion

Given the statistical parameters of an aquifer, the aquifer structure can be modeled using a number of random field generation algorithms. These algorithms in turn use a random field model to generate the random field. Depending on the type of algorithm, the data interpolation is done using different sets of equations. Expectedly, the aquifer structures generated by each algorithm, for a particular realization, are very similar to each other.

Table 2.6 Model parameters and inputs

Parameter	Case 1	Case 2	Case 3	Case 4
Geometric mean hydraulic conductivity, K_g (m/day)	10	10	10	10
ln K variance	0.5	0.5	0.5	0.5
Correlation scale, λ_x (m)	5	5	5	5
Size of model (m)	100 x 50	100 x 50	100 x 50	100 x 50
Covariance function	Exponential	Exponential	Exponential	Exponential
Random field algorithm	Spectral	Sequential Gaussian	Turning Bands	Simulated

	algorithm	algorithm	algorithm	Annealing
Grid	203 x 102	203 x 102	203 x 102	203 x 102
Cell size, Δx (m)	1 x 1	1 x 1	1 x 1	1 x 1

The model parameters and inputs are explained below:

- The $\ln K$ field is a normally distributed random field. Therefore, there is an equal probability of the plume encountering a 'low' K zone or a 'high' K zone.
- The heterogeneous conductivity field is uniquely characterized by the following set of statistical parameters: geometric mean (K_g) of K , correlation scale, variance and covariance.
- The geometric mean, $\ln K$ variance, correlation scale, and covariance function is constant for all cases.
- The random field algorithm is Spectral algorithm, Sequential Gaussian simulation, and Turnings Bands algorithm, and Simulated Annealing for cases 1, 2, 3, and 4 respectively.
- The cell size, Δx , is selected such that the correlation scale, λ , is resolved; typically, Δx is at least 3 to 4 times smaller than the correlation scale.

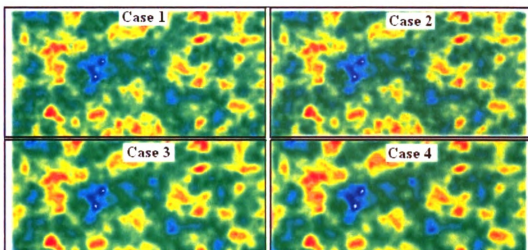


Figure 2.6 Snapshot of the visualization

For a detailed visualization, access the following address:

URL: <http://www.cgr.msu.edu/igw/DL/SSH/RFRH/RFRH6.htm>

2.7 UNCONDITIONAL AND CONDITIONAL SIMULATIONS

2.7.1 Problem statement

This video demonstrates the effect of conditioning of data on the aquifer texture. The effect of extent of conditioning is also shown. Details are provided in Table 2.7.

2.7.2 Key observations

The following observations can be made from the video:

- Unconditional simulations can predict the extent and texture of variability in the aquifer, but do not satisfy the data at the data points.
- Conditional simulations can predict the extent and texture of variability in the aquifer, and also satisfy the data at the data points.
- By increasing the number of data points, conditional simulations become increasingly better representations of “reality.”

2.7.3 Additional observations and discussion

Given a set of data for representing the variability in an aquifer, two methods can be used to represent the aquifer structure: a) Unconditional simulations, b) Conditional simulations. Unconditional simulations can predict the variability in an aquifer, but are not constrained by the data at the data points. On the other hand, conditional simulations can predict the variability, and are also constrained by the data. This makes conditional simulations a better representation of the “real” aquifer. Obviously, the effectiveness of conditional simulations increases by increasing the number of data points.

Table 2.7 Model parameters and inputs

Parameter	"Truth"
Geometric mean hydraulic conductivity, K_g (m/day)	10
$\ln K$ variance	2.0
Correlation scale, λ (m)	10
Size of model (m)	100 x 75
Covariance function	Exponential
Grid	201 x 151
Cell size, Δx (m)	0.5 x 0.5

The model parameters and inputs are explained below:

- The $\ln K$ field is a normally distributed random field. Therefore, there is an equal probability of the plume encountering a 'low' K zone or a 'high' K zone.
- The heterogeneous conductivity field is uniquely characterized by the following set of statistical parameters: geometric mean (K_g) of K , correlation scale, variance and covariance.
- The geometric mean, $\ln K$ variance, correlation scale, and covariance function is constant for all cases.
- The cell size, Δx , is selected such that the correlation scale, λ , is resolved; typically, Δx is at least 3 to 4 times smaller than the correlation scale.

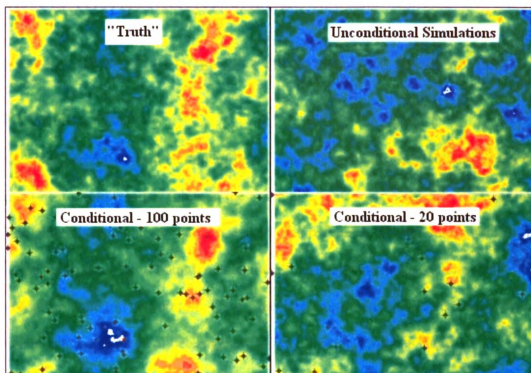


Figure 2.7 Snapshot of the visualization

For a detailed visualization, access the following address:

URL: <http://www.egr.msu.edu/igw/DL/SSH/RFRH/RFRH4.htm>

3 SPATIAL HETEROGENEITY

3.1 EFFECTS OF HETEROGENEITY OF HYDRAULIC CONDUCTIVITY

3.1.1 Problem statement

This video demonstrates the effect of heterogeneous hydraulic conductivity media on the transport of a conservative solute in the absence of pore-scale dispersion. The initial size of the plume is much larger than the scale of heterogeneity. The modeling domain consists of constant head boundaries on the left and right extremes, and no-flow boundaries at the top and bottom. Case 1 has a homogeneous field; and cases 2 through 4 show increasing degrees of heterogeneity. Details are provided in Table 3.1.

3.1.2 Key observations

The following observations can be made from the video:

- Although there is no pore-scale dispersion, the plume spreads because of heterogeneity. This large-scale spreading is called macrodispersion.
- As long as the plume encounters heterogeneity, it continues to spread.
- Plume spreading increases with increasing $\ln K$ variance.
- Longitudinal spreading is significantly greater than transverse spreading.
- Mean displacement remains largely unaffected, despite the heterogeneity.
- Transport through heterogeneous media results in complex irregular plumes; in homogeneous media the plume remains regular.

3.1.3 Additional observations and discussion

The pattern of plume spreading shows a clear trend. The plume does not spread at all when the $\ln K$ variance is 0.0, and spreads the most when the $\ln K$ variance is 3.0. Even though the plume spreading is enhanced, the mean plume displacement is largely unaffected. The fingers of the plume contain the maximum mass of the plume, but are concentrated over a small spatial area. The tails have less mass, but are elongated. Consequently, the center of mass, and thus mean displacement, remains the same, irrespective of the $\ln K$ variance.

The effect of the symmetric $\ln K$ field on plume spreading is asymmetric. The fingers (leading edge) of the plume are shorter than the tails (trailing edge) of the plume, which results in a skewed plume. This can be explained very simply. High K zones are convergent zones, through which the plume prefers to travel, and in which it converges. Convergence is the opposite of spreading. Therefore, shorter fingers are found. In contrast, low K zones are zones of divergence, which impede the movement of the plume. When a low K zone is encountered, the plume travels around it rather than through it and this results in spreading. If a part of the plume reaches the low K zones, it gets 'trapped' due to the extremely low velocities in that zone. The bulk of the plume continues moving, while the portion trapped in the low K zone is released slowly; thus contributing to tail elongation.

3.1.4 Mathematical interpretation

Mathematically, these processes can be explained using the following equations. In a heterogeneous field, in the absence of pore-scale dispersion, the conservative solute concentration at any point for any irregular plume realization is given by:

$$\frac{\partial C}{\partial t} + \frac{\partial u_i C}{\partial x_i} = 0, \quad (3.1.1)$$

where:

C - Concentration

u_i - Seepage velocity.

To determine large-scale behavior, the method of perturbation is used, and on performing local spatial averaging, we get the following:

$$\frac{\partial \bar{C}}{\partial t} + \frac{\partial \bar{u} \bar{C}}{\partial x_i} = \frac{\partial}{\partial x_i} \left(-\overline{u'_i C'} \right), \quad (3.1.2)$$

where:

\bar{C} - Mean concentration

C' - Perturbation to mean concentration

\bar{u} - Mean seepage velocity

u'_i - Perturbation to mean seepage velocity.

This term, $\left(-\overline{u'_i C'} \right)$, reflects the effects of heterogeneity.

It can be shown (*Gelhar and Axness, 1983a*) that:

$$-\overline{u'_i C'} \approx A_{ii} \bar{u} \frac{\partial \bar{C}}{\partial x_i}. \quad (3.1.3a)$$

The coefficient A_{ii} is called macrodispersivity and is given by (*Gelhar, 1993*):

$$A_{11} = \sigma_{\ln K}^2 \lambda; \quad A_{22} = \frac{\sigma_{\ln K}^2}{8} (\alpha_L + \alpha_T), \quad (3.1.3b)$$

where:

$\sigma_{\ln K}^2$ - $\ln K$ variance

λ - Correlation scale

A_{11} - Longitudinal macrodispersivity

A_{22} - Transverse macrodispersivity

α_L - Longitudinal pore-scale dispersivity

α_T - Transverse pore-scale dispersivity

Substituting (3.1.3a) into (3.1.2) yields:

$$\frac{\partial \bar{C}}{\partial t} + \frac{\partial \bar{u} \bar{C}}{\partial x_i} = \frac{\partial}{\partial x_i} \left(A_{ii} \bar{u} \frac{\partial \bar{C}}{\partial x_i} \right). \quad (3.1.4)$$

This is the classical advection-dispersion equation. The additional term, $\frac{\partial}{\partial x_i} \left(A_{ii} \bar{u} \frac{\partial \bar{C}}{\partial x_i} \right)$,

in (3.1.4) represents macrodispersion. From (3.1.3b), it is evident that with increasing $\ln K$ variance, the longitudinal component of macrodispersion will increase. However, there will be no effect on transverse macrodispersion, since no pore-scale dispersion is present.

The mean velocity (\bar{u}) controls the mean displacement of the plume. Darcy's equation gives the seepage velocity of the flow as:

$$u_i = \frac{K}{n} \frac{\partial h}{\partial x_i},$$

where:

K - Mean conductivity

n - Porosity.

The mean velocity is given by:

$$\bar{u} = \frac{\bar{K}}{n} \frac{\partial \bar{h}}{\partial x_i} + \frac{\overline{K' \frac{\partial h'}{\partial x_i}}}{n}. \quad (3.1.5)$$

Gelhar (1993, equation 4.1.48) showed that:

$$\bar{K} \approx K_g \left(1 + \frac{\sigma_{\ln K}^2}{2} \right); \quad \overline{K' \frac{\partial h'}{\partial x_i}} \approx \left(\frac{-\sigma_{\ln K}^2}{2} \frac{\partial \bar{h}}{\partial x_i} \right), \quad (3.1.6)$$

where:

K' - Perturbation to mean conductivity

\bar{h} - Mean hydraulic head

h' - Perturbation to mean hydraulic head

K_g - Geometric mean of hydraulic conductivity.

Substituting (3.1.6) into (3.1.5), we get:

$$\bar{u} \approx \frac{K_g}{n} \frac{\partial \bar{h}}{\partial x_i}. \quad (3.1.7)$$

Since the geometric mean hydraulic conductivity and mean hydraulic gradient are the same for all cases, \bar{u} is the same. As a result, the mean plume displacement remains largely unaffected.

Table 3.1 Model parameters and inputs

Parameter	Case 1	Case 2	Case 3	Case 4
Geometric mean hydraulic conductivity, K_g (m/day)	10	10	10	10
$\ln K$ variance	0.0	0.5	1.0	3.0
Correlation scale, λ (m)	NA	2	2	2

Porosity, n	0.3	0.3	0.3	0.3
Local pore-scale dispersivity	0	0	0	0
Head difference (m)	1	1	1	1
Size of model (m)	200 x 50	200 x 50	200 x 50	200 x 50
Covariance function	NA	Exponential	Exponential	Exponential
Approximate initial plume size (m)	10	10	10	10
Grid	401 x 407	401 x 407	401 x 407	401 x 407
Cell size, Δx (m)	0.5 x 0.5	0.5 x 0.5	0.5 x 0.5	0.5 x 0.5
Time step, Δt (days)	1	1	1	1

The model parameters and inputs are explained below:

- The $\ln K$ field is a normally distributed random field. Therefore, there is an equal probability of the plume encountering a ‘low’ K zone or a ‘high’ K zone.
- The heterogeneous conductivity field is uniquely characterized by the following set of statistical parameters: geometric mean (K_g) of K , correlation scale, variance and covariance.
- The geometric mean is constant for all cases, while the $\ln K$ variance increases from 0 to 3.
- The correlation scale does not apply to case 1 and is a constant for cases 2, 3 and 4.
- The covariance function for cases 2, 3 and 4 is exponential.
- The cell size, Δx , is selected such that the correlation scale, λ , is resolved; typically, Δx is at least 3 to 4 times smaller than the correlation scale.
- The time step, Δt , is selected such that a particle of the plume travels a distance that is less than λ in one time step.

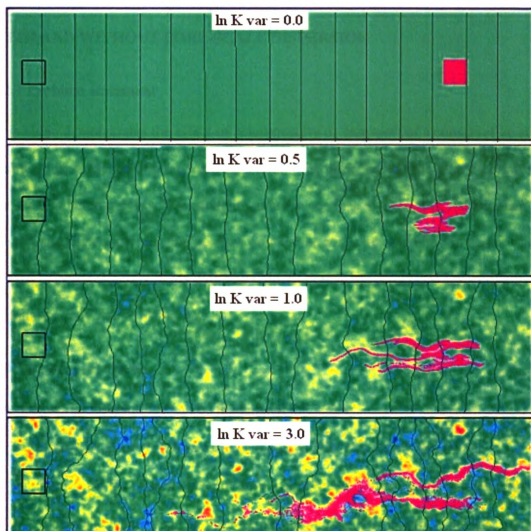


Figure 3.1 Snapshot of the visualization

For a detailed visualization, access the following address:

URL: <http://www.egr.msu.edu/igw/DL/SSH/EHST/EHST1.htm>

3.2 EFFECTS OF HETEROGENEITY OF HYDRAULIC CONDUCTIVITY – WITH AND WITHOUT PORE-SCALE DISPERSION

3.2.1 Problem statement

This video demonstrates the effect of heterogeneity on transport of a conservative solute plume in the presence of pore-scale dispersion. The initial size of the plume is larger than the scale of heterogeneity. The modeling domain consists of constant head boundaries on the left and right extremes, and no-flow boundaries at the top and bottom. Cases 1 and 2 consist of heterogeneous fields with and without pore-scale dispersion respectively.

Details are provided in Table 3.2.

3.2.2 Key observations

The following observations can be made from the video:

- Transport through heterogeneous media causes large scale spreading.
- Pore-scale dispersion does not have a significant impact on overall spreading.
- Pore-scale dispersion has little impact on longitudinal macrodispersion, while it has a relatively greater impact on transverse macrodispersion.
- Pore-scale dispersion significantly reduces the concentration variability, and thus enhances the degree of dilution.

3.2.3 Additional observations and discussion

Since the two models have the same realization, the degree of macrodispersion is the same. The difference lies in the ‘smearing’ of the plume. When there is pore-scale dispersion, the plume is slightly larger (or smeared) than when there is none. This

smearing is both longitudinal and transverse. The absence of pore-scale dispersion results in numerous fingers and tails; hence, the variance of concentration is higher.

Pore-scale dispersion is represented numerically by the longitudinal and transverse dispersivities. The amount of dispersion is obtained by multiplying the dispersivity by the velocity in a particular cell in the grid. Since the $\ln K$ field is fixed for a particular realization, the velocities in each cell of the grid are also fixed.

Physically, pore-scale dispersion can be understood as a measure of our uncertainty or ignorance about the complex pore geometry. If it is possible to map out the microscopic pore structure, and resolve it numerically, a purely advective model can predict plume spreading accurately. This is, however, impossible. Moreover, we do not care about that level of detail, making it necessary to have a numerical correction factor called pore-scale dispersion.

3.2.4 Mathematical interpretation

The similarity in spreading between the two situations can be explained mathematically. Similarly, a mathematical argument can be posed for the need to incorporate pore-scale dispersion if risk based assessment is to be performed.

In a heterogeneous field, in the presence of pore-scale dispersion, the conservative solute concentration at any point for any irregular plume realization is given by:

$$\frac{\partial C}{\partial t} + \frac{\partial u_i C}{\partial x_i} = \frac{\partial}{\partial x_i} \left(D_{ij} \frac{\partial C}{\partial x_j} \right), \quad (3.2.1)$$

where:

C - Concentration

u_i - Seepage velocity

D_{ij} - Dispersion coefficient.

3.2.4.1 Impact of pore-scale dispersion on macrodispersion

For a heterogeneous K field with pore-scale dispersion, applying the perturbation theory, (3.2.1) is modified as follows:

$$\frac{\partial \bar{C}}{\partial t} + \frac{\partial \bar{u} \bar{C}}{\partial x_i} = \frac{\partial}{\partial x_i} \left(D_{ij} \frac{\partial C}{\partial x_j} + \left(-\bar{u}_i \bar{C} \right) \right). \quad (3.2.2)$$

Substituting (3.1.3a) into (3.2.2), we get:

$$\frac{\partial \bar{C}}{\partial t} + \frac{\partial \bar{u} \bar{C}}{\partial x_i} = \frac{\partial}{\partial x_i} \left(D_{ij} \frac{\partial C}{\partial x_j} + \left(A_{ii} \bar{u} \frac{\partial \bar{C}}{\partial x_i} \right) \right). \quad (3.2.3)$$

The additional term, $\frac{\partial}{\partial x_i} \left(A_{ii} \bar{u} \frac{\partial \bar{C}}{\partial x_i} \right)$, in (3.2.3) represents macrodispersion. From (3.1.3b),

it is apparent that the local dispersivities do not have any impact on longitudinal macrodispersion. However, they have some effect on transverse macrodispersion. The magnitude of macrodispersion is larger than pore-scale dispersion. Therefore, the plume in case 2 has the same longitudinal extent as in case 1, while it is slightly smeared in the transverse direction.

3.2.4.2 Impact of pore-scale dispersion on concentration variance

Kapoor and Gelhar (1994) showed that:

$$\frac{\partial \sigma_C^2}{\partial t} + \bar{u} \frac{\partial \sigma_C^2}{\partial x_i} = \bar{u} A_{ij} \frac{\partial^2 \sigma_C^2}{\partial x_i \partial x_j} + 2 \bar{u} A_{ij} \left(\frac{\partial \bar{C}}{\partial x_i} \frac{\partial \bar{C}}{\partial x_j} \right), \quad (3.2.4)$$

$$\frac{\partial \sigma_C^2}{\partial t} + \bar{u} \frac{\partial \sigma_C^2}{\partial x_i} = \bar{u} (A_{ij} + \alpha_{ij}) \frac{\partial^2 \sigma_C^2}{\partial x_i \partial x_j} + 2\bar{u} A_{ij} \left(\frac{\partial \bar{C}}{\partial x_i} \frac{\partial \bar{C}}{\partial x_j} \right) - \chi \sigma_C^2, \quad (3.2.5)$$

$$\chi \equiv \frac{2\bar{u}\alpha_{ij}}{(\Delta_i^C)^2}, \quad (3.2.6)$$

where:

σ_C^2 - Concentration variance

χ - Variance decay coefficient

Δ_i^C - Concentration microscale.

The concentration variance without and with pore-scale dispersion is given in (3.2.4) and (3.2.5) respectively. These equations are necessary in order to perform a risk-based assessment of the plume concentration. The sharp peaks and valleys of concentration in the plume are smoothed when pore-scale dispersion is present, resulting in a decrease in the concentration variance. This can be mathematically proven using (3.2.5).

Table 3.2 Model parameters and inputs

Parameter	Case 1	Case 2
Geometric mean hydraulic conductivity, K_g (m/day)	10	10
ln K variance	3.0	3.0
Correlation scale, λ (m)	2	2
Porosity, n	0.3	0.3
Longitudinal pore-scale dispersivity (m)	0	0.01
Transverse pore-scale dispersivity (m)	0	0.001
Head difference (m)	1	1
Size of model (m)	200 x 50	200 x 50
Covariance function	Exponential	Exponential
Approximate initial plume size (m)	10	10
Grid	401 x 407	401 x 407

Cell size, Δx (m)	0.5 x 0.5	0.5 x 0.5
Time step, Δt (days)	1	1

The model parameters and inputs are explained below:

- The $\ln K$ field is a normally distributed random field. Therefore, there is an equal probability of the plume encountering a 'low' K zone or a 'high' K zone.
- The heterogeneous conductivity field is uniquely characterized by the following set of statistical parameters: geometric mean (K_g) of K , correlation scale, variance and covariance.
- The geometric mean, $\ln K$ and correlation scale are constant for all cases.
- The covariance function for both cases is exponential.
- Case 1 has no longitudinal and transverse dispersivities, while the corresponding values for case 2 are 0.01 m and 0.001 m.
- The cell size, Δx , is selected such that the correlation scale, λ , is resolved.
Typically, Δx is at least 3 to 4 times smaller than the correlation scale.
- The time step, Δt , is selected such that a particle of the plume travels a distance that is less than λ in one time step.

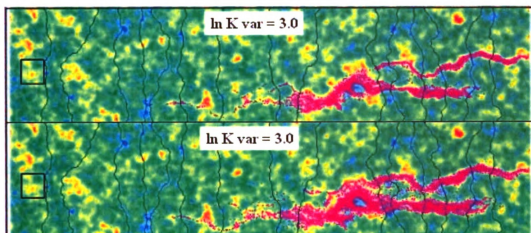


Figure 3.2 Snapshot of the visualization

For a detailed visualization, access the following address:

URL: <http://www.egr.msu.edu/igw/DL/SSH/EHST/EHST2.htm>

3.3 INTERACTIONS BETWEEN CONDUCTIVITY AND POROSITY HETEROGENEITIES

3.3.1 Problem statement

This video demonstrates the impact of interactions between conductivity and porosity heterogeneities on the spreading of a conservative solute plume. The modeling domain consists of constant head boundaries on the left and right extremes, and no-flow boundaries at the top and bottom. Details are provided in Table 3.3.

3.3.2 Key observations

The following observations can be made from the video:

- Interaction between conductivity (K) and porosity (n) heterogeneities has a significant impact on plume spreading.
- In most situations n is positively correlated with K , which results in less plume spreading compared to when there is no heterogeneity in n .
- When n is negatively correlated with K , plume spreading is greater compared to when there is no heterogeneity in n .
- When n and K are independent of each other, plume spreading is less than case 1, although in general, this might not be the case.

3.3.3 Additional observations and discussion

Case 1: Even though K varies continuously over space, n remains constant throughout the field. This is not a commonly encountered situation. In the absence of sufficient data, n is assumed to be constant throughout the field.

Case 2: In a more common situation, n interacts positively with K . When n increases, the seepage velocity decreases. The seepage velocity is given by q/n , where q is the Darcy velocity. When n increases, the seepage velocity decreases, resulting in less plume spreading. Hence, the plume spreads lesser than in case 1.

Case 3: In this case, n interacts negatively with K . This means that n decreases when K increases. This relatively uncommon situation results in enhanced spreading of the plume. The eventual size of the plume is greater in comparison to case 1.

Case 4: When n varies with no relationship to K , velocity variability is random. The plume spreading is dependent on $\ln n$ realization.

Giving n a single value ignores the variability, results in increasing or reducing plume spreading. The video shows that the effect on plume spreading is significant.

3.3.4 Mathematical interpretation

The interaction between n and K is modeled using the following equations (*Paulson, 2002*):

$$\frac{n}{n_m} = \left(e^{\pm \alpha f} + w \right), \quad (3.3.1)$$

where:

n - Porosity

n_m - Mean value of porosity

α - Correlation factor

$$f' - \ln K$$

w - White noise.

The positive sign in the formula is applicable for positive correlation (case 2) and the negative sign is applicable for negative correlation (case 3). The correlation factor is computed by using the coefficient of variation, which is defined as the ratio of standard deviation of porosity to the Mean porosity. The value of α controls the variation in n . The value of α at any point is given by the ratio of coefficient of variation to f' . w is the random white noise for normalized n .

Table 3.3 Model parameters and inputs

Parameter	Case 1	Case 2	Case 3	Case 4
Geometric mean hydraulic conductivity, K_g (m/day)	10	10	10	10
$\ln K$ variance	2.0	2.0	2.0	2.0
Correlation scale, λ (m)	2	2	2	2
Mean porosity, n_m	0.25	0.25	0.25	0.25
Coefficient of variation – n and K	NA	0.27	0.25	0.10 ($\ln n$ variance)
Correlation - n and K	NA	Positive	Negative	None
White noise, w	NA	0	0	0
Local pore-scale dispersivity	0	0	0	0
Head difference (m)	1	1	1	1
Size of model (m)	200 x 50	200 x 50	200 x 50	200 x 50
Covariance function	Exponential	Exponential	Exponential	Exponential
Approximate initial plume size (m)	10	10	10	10
Grid	401 x 407	401 x 407	401 x 407	401 x 407
Cell size, Δx (m)	0.5 x 0.5	0.5 x 0.5	0.5 x 0.5	0.5 x 0.5
Time step, Δt (days)	1	1	1	1

The model parameters and inputs are explained below:

- The $\ln K$ field is a normally distributed random field. Therefore, there is an equal probability of the plume encountering a ‘low’ K zone or a ‘high’ K zone.

- The heterogeneous conductivity field is uniquely characterized by the following set of statistical parameters: geometric mean (K_g) of K , correlation scale, variance and covariance.
- The geometric mean, $\ln K$ and correlation scale are constant for all cases.
- The covariance function for all cases is exponential.
- The interactions between n and K are characterized by a coefficient of variation and the type of correlation.
- The cell size, Δx , is selected such that the correlation scale, λ , is resolved.
Typically, Δx is at least 3 to 4 times smaller than the correlation scale.
- The time step, Δt , is selected such that a particle of the plume travels a distance that is less than λ in one time step.

The video shows only the variation of K over space. The variation of n over space is shown below. Notice that, even though the cases look very different from each other, the head contours are the same. The head is dependent only on K . Since the $\ln K$ realization is the same for all cases, the head contours are identical.

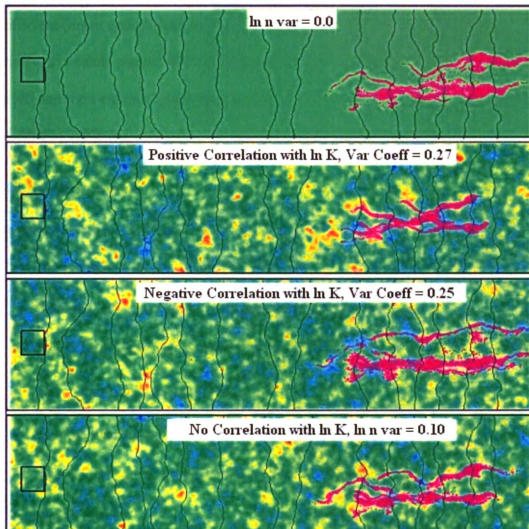


Figure 3.3 Snapshot of the visualization showing spatial variation of n

For a detailed visualization, access the following address:

URL: <http://www.egr.msu.edu/igw/DL/SSH/NIT/NIT3.htm>

3.4 INTERACTIONS BETWEEN CONDUCTIVITY AND PARTITIONING COEFFICIENT HETEROGENEITIES

3.4.1 Problem statement

This video demonstrates the impact of interactions between conductivity and partitioning coefficient (linear equilibrium sorption) heterogeneities on the spreading of a conservative solute plume. The modeling domain consists of constant head boundaries on the left and right extremes, and no-flow boundaries at the top and bottom. Details are provided in Table 3.4.

3.4.2 Key observations

The following observations can be made from the video:

- Interaction between conductivity (K) and partitioning coefficient (K_d) heterogeneities has a significant impact on plume spreading.
- When K_d is positively correlated with K , plume spreading is reduced than when there is no heterogeneity in K_d .
- In most situations K_d is negatively correlated with K , which results in significantly greater plume spreading compared to when there is no heterogeneity in K_d .
- When K_d and K are independent of each other, plume spreading is less than case 1, although in general, this might not be the case.
- Chemical heterogeneity (K_d) causes physical plume dispersion.

3.4.3 Additional observations and discussion

Case 1: Even though K varies continuously over space, K_d remains constant throughout the field. This is not a commonly encountered situation. In the absence of sufficient data, K_d is assumed to be constant throughout the field.

Case 2: In this case, K_d interacts positively with K . This means that K_d increases when K increases. This relatively uncommon situation results in a decrease in plume spreading. The eventual size of the plume is underestimated in comparison to case 1.

Case 3: In a more common situation, K_d interacts negatively with K . When K_d decreases, the retardation factor decreases and hence the contaminant velocity increases and vice versa, which results in increased spreading. The actual size of the plume is larger than in comparison to case 1. The tails, in particular, are longer due to higher retardation factors.

Case 4: When K_d varies with no relationship to the K , velocity variability is random. The plume spreading is dependent on $\ln K_d$ realization.

Giving K_d a single value ignores the variability, results in increasing or reducing plume spreading. The video illustrates that the effect of variability in K_d can be important.

3.4.4 Mathematical interpretation

The interaction between partitioning coefficient and conductivity are modeled using the following equations (*Paulson*, 2002):

$$\frac{K_d}{K_{dm}} = \left(e^{\pm \alpha f'} + w \right), \quad (2.4.1)$$

where:

K_d – Partitioning coefficient

K_{dm} – Mean value of Partitioning coefficient

α – Correlation factor

f' – $\ln K$

w – White noise.

The positive sign in the formula is applicable for positive correlation (case 2) and the negative sign is applicable for negative correlation (case 3). The correlation factor is computed by using the coefficient of variation, which is defined as the ratio of standard deviation of partitioning coefficient to the mean partitioning coefficient. The value of α controls the variation in K_d . The value of α at any point is given by the ratio of coefficient of variation to f' . w is the random white noise for normalized K_d .

Table 3.4 Model parameters and inputs

Parameter	Case 1	Case 2	Case 3	Case 4
Geometric mean hydraulic conductivity, K_g (m/day)	10	10	10	10
$\ln K$ variance	2.0	2.0	2.0	2.0
Correlation scale, λ (m)	2	2	2	2
Porosity, n	0.3	0.3	0.3	0.3
Mean partitioning coefficient, K_{dm} (m ³ /g)	10^{-7}	10^{-7}	10^{-7}	10^{-7}
Coefficient of variation – K_d and K	NA	1.65	1.47	1.50 ($\ln K_d$ variance)
Correlation - K_d and K	NA	Positive	Negative	None
White noise, w	NA	0	0	0
Local pore-scale dispersivity	0	0	0	0

Head difference (m)	1	1	1	1
Size of model (m)	200 x 50	200 x 50	200 x 50	200 x 50
Covariance function	Exponential	Exponential	Exponential	Exponential
Approximate initial plume size (m)	10	10	10	10
Grid	401 x 407	401 x 407	401 x 407	401 x 407
Cell size, Δx (m)	0.5 x 0.5	0.5 x 0.5	0.5 x 0.5	0.5 x 0.5
Time step, Δt (days)	2	2	2	2

The model parameters and inputs are explained below:

- The $\ln K$ field is a normally distributed random field. Therefore, there is an equal probability of the plume encountering a 'low' K zone or a 'high' K zone.
- The heterogeneous conductivity field is uniquely characterized by the following set of statistical parameters: geometric mean (K_g) of K , correlation scale, variance and covariance.
- The geometric mean, $\ln K$ and correlation scale are constant for all cases.
- The covariance function for all cases is exponential.
- The interactions between K_d and K are characterized by a coefficient of variation and the type of correlation.
- The cell size, Δx , is selected such that the correlation scale, λ , is resolved.
Typically, Δx is at least 3 to 4 times smaller than the correlation scale.
- The time step, Δt , is selected such that a particle of the plume travels a distance that is less than λ in one time step.

The video shows only the variation of K over space. The variation of K_d over space is shown below. Notice that, even though the cases look very different from each other, the head contours are the same. The head is dependent only on K . Since the $\ln K$ realization is the same for all cases, the head contours are identical.

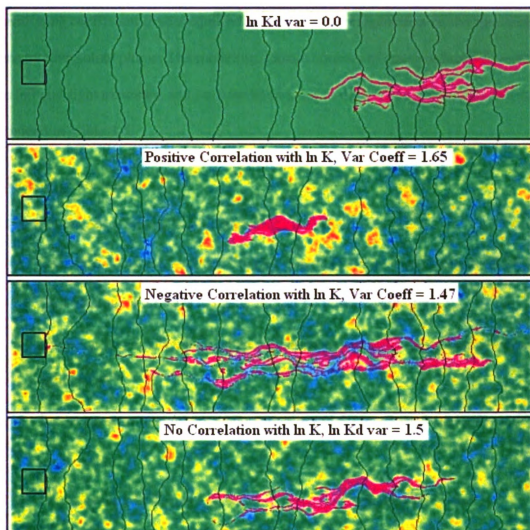


Figure 3.4 Snapshot of the visualization showing spatial variation of K_d

For a detailed visualization, access the following address:

URL: <http://www.egr.msu.edu/igw/DL/SSH/NIT/NIT4.htm>

3.5 INTERACTIONS BETWEEN CONDUCTIVITY, POROSITY AND PARTITIONING COEFFICIENT HETEROGENEITIES

3.5.1 Problem statement

This video demonstrates the impact of interactions between conductivity, porosity and partitioning coefficient (linear equilibrium sorption) heterogeneities on the spreading of a conservative solute plume. The modeling domain consists of constant head boundaries on the left and right extremes, and no-flow boundaries at the top and bottom. Details are provided in Table 3.5.

3.5.2 Key observations

The following observations can be made from the video:

- Interaction between conductivity (K), porosity (n) and partitioning coefficient (K_d) heterogeneities has a drastic impact on plume spreading.
- Plume spreading decreases when variability of n (positive correlation with K) is considered.
- Plume spreading increases when variability of K_d (negative correlation with K) is considered.
- Heterogeneity in K_d has a greater influence on plume spreading than heterogeneity in n .

3.5.3 Additional observations and discussion

Case 1: Even though K varies continuously over space, n and K_d remain constant throughout the field. This is not a commonly encountered situation. In the absence of sufficient data, n and K_d is assumed to be constant throughout the field.

Case 2: In this case, n interacts positively with K , while K_d remains constant throughout. This means that n increases when K increases. This results in less extensive spreading. In comparison to case 1, the plume is slightly smaller.

Case 3: In a more common situation, n remains constant throughout, while K_d interacts negatively with K , meaning that K_d will decrease with increase in K . When K_d decreases, the retardation factor decreases and hence the contaminant velocity increases, resulting in enhanced spreading. The size of the plume is significantly larger than in case 1, and the tails, in particular, are longer due to higher retardation factors. This indicates that K_d heterogeneity has a significant impact on plume spreading.

Case 4: This is the most commonly encountered situation. Porosity interacts positively with K , while K_d interacts negatively with K . The resulting plume is considerably larger than in case 1, which is the result of heterogeneity in K_d . However, in comparison to case 3, the plume is slightly smaller, due to the variability in n .

A comparison of the four situations shows that the effect of the interaction between K , n and K_d is worth considering. Wherever possible, the effect of variability in all three must

be considered. In most cases, only the variability in K is considered. If the variability in n is ignored, spreading of the plume is enhanced. If the variability in K_d is ignored, spreading of the plume is reduced. If both are ignored, spreading of the plume is reduced, indicating that the effect of heterogeneity in K_d is much greater than heterogeneity in n .

3.5.4 Mathematical interpretation

The interactions between porosity, partitioning coefficient and conductivity are modeled using the following equations (*Paulson, 2002*):

$$\frac{n}{n_m} = \left(e^{\pm \alpha f'} + w \right), \quad (3.5.1)$$

$$\frac{K_d}{K_{dm}} = \left(e^{\pm \alpha f'} + w \right), \quad (3.5.2)$$

where:

n – Porosity

n_m – Mean value of porosity

K_d – Partitioning coefficient

K_{dm} – Mean value of Partitioning coefficient

α – Correlation factor

f' – $\ln K$

w – White noise.

Porosity is positively correlated with conductivity (cases 2, 4), while partitioning coefficient is negatively correlated (cases 3, 4). The correlation factor is computed by

using the coefficient of variation, which is defined as the ratio of standard deviation of porosity (or partitioning coefficient) to the Mean porosity (or partitioning coefficient).

The value of α controls the variation in n (or K_d). The value of α at any point is given by the ratio of coefficient of variation to f' . w is the random white noise for normalized n (or K_d).

Table 3.5 Model parameters and inputs

Parameter	Case 1	Case 2	Case 3	Case 4
Geometric mean hydraulic conductivity, K_g (m/day)	10	10	10	10
ln K Variance	2.0	2.0	2.0	2.0
Correlation scale, λ (m)	2	2	2	2
Mean porosity, n	0.25	0.25	0.25	0.25
Coefficient of variation - n and K	0.0	0.27	0.0	0.27
Correlation - n and K	NA	Positive	NA	Positive
Partitioning coefficient, K_d (m ³ /g)	10^{-7}	10^{-7}	10^{-7}	10^{-7}
Coefficient of variation - K_d and K	0.0	0.0	1.47	1.47
Correlation - K_d and K	NA	NA	Negative	Negative
Local pore-scale dispersivity	0	0	0	0
Head difference (m)	1	1	1	1
Size of model (m)	200 x 50	200 x 50	200 x 50	200 x 50
Covariance function	Exponential	Exponential	Exponential	Exponential
Approximate initial plume size (m)	10	10	10	10
Grid	401 x 407	401 x 407	401 x 407	401 x 407
Cell size, Δx (m)	0.5 x 0.5	0.5 x 0.5	0.5 x 0.5	0.5 x 0.5
Time step, Δt (days)	2	2	2	2

The model parameters and inputs are explained below:

- The ln K field is a normally distributed random field. Therefore, there is an equal probability of the plume encountering a 'low' K zone or a 'high' K zone.
- The heterogeneous conductivity field is uniquely characterized by the following set of statistical parameters: geometric mean (K_g) of K , correlation scale, variance and covariance.

- The geometric mean, $\ln K$ and correlation scale are constant for all cases.
- The covariance function for all cases is exponential.
- The interactions between n and K , and between K_d and K are characterized by a coefficient of variation and the type of correlation. Only 4 of the 16 possible situations are modeled, since those are the most commonly encountered situations.
- The cell size, Δx , is selected such that the correlation scale, λ , is resolved.
Typically, Δx is at least 3 to 4 times smaller than the correlation scale.
- The time step, Δt , is selected such that a particle of the plume travels a distance that is less than λ in one time step.

The video shows only the variation of K over space. The variations of n and K_d over space are shown below. Notice that, even though the cases look very different from each other, the head contours are the same. The head is dependent only on K . Since the $\ln K$ realization is the same for all cases, the head contours are identical.

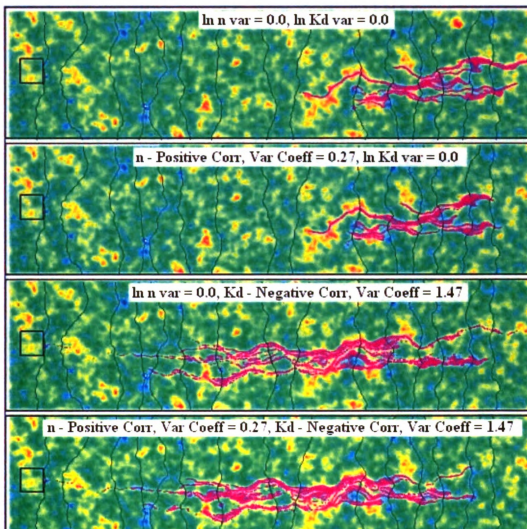


Figure 3.5.1 Snapshot of the visualization

For a detailed visualization, access the following address:

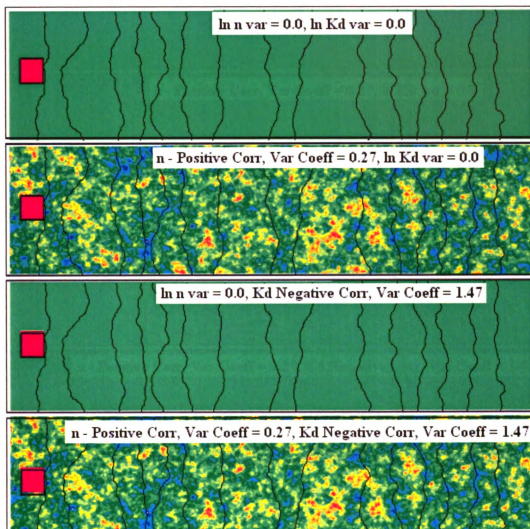


Figure 3.5.2 Spatial variation of n

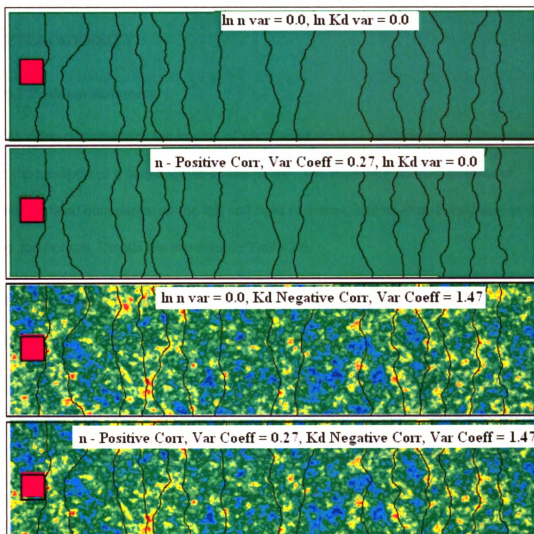


Figure 3.5.3 Spatial variation of K_d

3.6 EFFECT OF CORRELATION SCALE (λ) OF CONDUCTIVITY HETEROGENEITY

3.6.1 Problem statement

This video demonstrates the impact of correlation scale (λ) of conductivity heterogeneity on the transport of a conservative solute plume. The modeling domain consists of constant head boundaries on the left and right extremes, and no-flow boundaries at the top and bottom. Details are provided in Table 3.6.

3.6.2 Key observations

The following observations can be made from the video:

- Correlation scale, λ , has a significant impact on plume transport.
- When the correlation scale is much smaller than the plume source size, the plume spreads in longitudinal and transverse directions. The center of mass of the plume moves, in general, along a straight line. The plume boundary displays small scale irregularities.
- When the correlation scale is of the order of the plume source size, the longitudinal spreading is greater than in case 1, transverse spreading is lesser than in case 1 and the mean plume displacement is greater than in case 1. The center of mass moves in general, along a meandering path. The irregularities of the plume boundary are of a larger scale than in case 1.

3.6.3 Additional observations and discussion

The two cases differ only in the magnitude of their correlation scales. However, the plumes look completely different. In case 1, the plume spreading is apparent in both

directions. Since the scale of heterogeneity is much smaller than the plume source size, small preferential channels are formed, which ‘shred’ the plume into numerous fingers and tails. Since the plume travels a distance equal to at least 50λ , the plume has the opportunity to encounter the full range of conductivities. This is reflected in the mean velocity of the plume and the mean plume displacement.

In case 2, where the correlation scale is about the size of the plume source, the plume moves predominantly along a preferential channel (higher K regions). In comparison to case 1, the width of the preferential channel is larger, and the plume is ‘sucked’ into it. In any preferential channel, the streamlines of flow tend to converge, resulting in longitudinal stretching and transverse compression of the plume. Therefore, we see that the longitudinal spreading is greater than in case 1, and the transverse spreading is lesser than in case 1. Since the plume encounters only the higher range of conductivities, the mean velocity of the plume will be higher than in case 1; therefore, the mean plume displacement is also much higher.

Data limitation can seriously impair the ability to accurately characterize the aquifer. Correlation scales are determined from field data using standard statistical methods. When data is limited, the correlation scale will be overestimated. This results in overestimation of the mean plume displacement and longitudinal spreading and underestimation of transverse spreading.

Table 3.6 Model parameters and inputs

Parameter	Case 1	Case 2
Geometric mean hydraulic conductivity, K_g (m/day)	10	10
$\ln K$ variance	2.0	2.0
Correlation scale, λ (m)	1	5
Porosity, n	0.3	0.3
Local pore-scale dispersivity	0	0
Head difference (m)	1	1
Size of model (m)	200 x 50	200 x 50
Covariance function	Exponential	Exponential
Approximate initial size of plume (m)	10	10
Grid	801 x 201	801 x 201
Cell size, Δx (m)	0.25 x 0.25	0.25 x 0.25
Time step, Δt (days)	1	1

The model parameters and inputs are explained below:

- The $\ln K$ field is a normally distributed random field. Therefore, there is an equal probability of the plume encountering a 'low' K zone or a 'high' K zone.
- The heterogeneous conductivity field is uniquely characterized by the following set of statistical parameters: geometric mean (K_g) of K , correlation scale, variance and covariance.
- The geometric mean and $\ln K$ variance are constant for all cases..
- The correlation scale is 1 m for case 1 and 5 m for Case 2.
- The covariance function for both cases is exponential.
- The cell size, Δx , is selected such that the correlation scale, λ , is resolved.

Typically, Δx is at least 3 to 4 times smaller than the correlation scale.

- The time step, Δt , is selected such that a particle of the plume travels a distance that is less than λ in one time step.

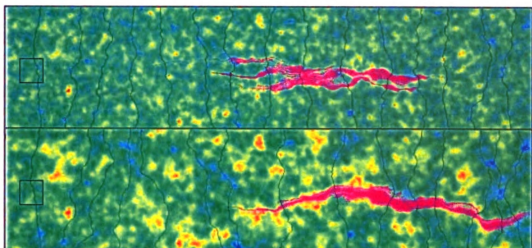


Figure 3.6 Snapshot of the visualization

For a detailed visualization, access the following address:

URL: <http://www.egr.msu.edu/igw/DL/SSH/EHST/EHST7.htm>

3.7 EFFECT OF CORRELATION SCALE (λ) OF CONDUCTIVITY HETEROGENEITY

3.7.1 Problem statement

This video demonstrates the impact of correlation scale (λ) of conductivity heterogeneity on the spreading of a conservative solute plume. The modeling domain consists of constant head boundaries on the left and right extremes, and no-flow boundaries at the top and bottom. Details are provided in Table 3.7.

3.7.2 Key observations

The following observations can be made from the video:

- Correlation scale, λ , has a significant impact on plume spreading.
- When the correlation scale is much smaller than the source size of the plume, the plume encounters a significant amount of heterogeneity and spreads as a result.
- When the correlation scale is comparable to or larger than the plume source size, the plume moves predominantly through preferential channels resulting in enhanced longitudinal spreading and increased mean plume displacement.
- Enhanced longitudinal spreading causes ‘negative’ transverse dispersion, which means that the eventual size of the plume is smaller than the source size of the plume, in the transverse direction.

3.7.3 Additional observations and discussion

The two models differ only in their correlation scale. However, the plumes look completely different. In case 1, the plume exhibits more detailed spreading in both directions while in case 2, the plume spreading is prominent in the longitudinal direction

and minimal in the transverse direction. When the correlation scale is smaller than the source size, the plume encounters more variability. As a result, the plume exhibits numerous fingers and tails. The mean displacement is lower than in case 2, because the chance of the plume encountering a low K zone is as high as that of encountering a high K zone. Hence, the mean velocity of the plume is lower.

When the correlation scale is larger than the size of the plume, plume migration is highly dependent on the $\ln K$ realization. If the plume source is located in a zone of low K , the plume will remain trapped for a long time. Conversely, if the source is located in a zone of high K , the plume moves rapidly. Plume spreading also depends on how large the correlation scale is, in comparison to the source size. Predicting the plume migration is error-prone if λ is many orders of magnitude larger than the source. In case 2, λ is approximately the same size as the size of the plume source. Hence, the chance of getting trapped in a low K zone is not drastically increased. In this particular realization, the high K zones are well connected, forming high-velocity preferential channels. The plume travels almost completely through these channels. The chance of encountering a low K zone is minimized and as a result, the transverse spreading is considerably reduced. It is obvious that the mean velocity of the plume will be higher than in case 1, because it travels mostly through preferential channels. Therefore, the mean displacement is also much higher.

Correlation scales are determined from field data using statistical methods. Data limitation can seriously impair the ability to characterize the aquifer. In the absence of

data, the correlation scale of the variability can be overestimated. This results in serious overestimation of the mean plume displacement and underestimation of plume spreading in the transverse direction.

Table 3.7 Model parameters and inputs

Parameter	Case 1	Case 2
Geometric mean hydraulic conductivity, K_g (m/day)	10	10
$\ln K$ variance	2.0	2.0
Correlation scale, λ (m)	1	10
Porosity, n	0.3	0.3
Local pore-scale dispersivity	0	0
Head difference (m)	1	1
Size of model (m)	200 x 50	200 x 50
Covariance function	Exponential	Exponential
Approximate initial size of plume (m)	10	10
Grid	801 x 201	801 x 201
Cell size, Δx (m)	0.25 x 0.25	0.25 x 0.25
Time step, Δt (days)	1	1

The model parameters and inputs are explained below:

- The $\ln K$ field is a normally distributed random field. Therefore, there is an equal probability of the plume encountering a ‘low’ K zone or a ‘high’ K zone.
- The heterogeneous conductivity field is uniquely characterized by the following set of statistical parameters: geometric mean (K_g) of K , correlation scale, variance and covariance. The geometric mean and $\ln K$ variance are constant for all cases.
- The correlation scale is 1 m for case 1 and 10 m for case 2.
- The covariance function for both cases is exponential.
- The cell size, Δx , is selected such that the correlation scale, λ , is resolved.

Typically, Δx is at least 3 to 4 times smaller than the correlation scale.

- The time step, Δt , is selected such that a particle of the plume travels a distance that is less than λ in one time step.

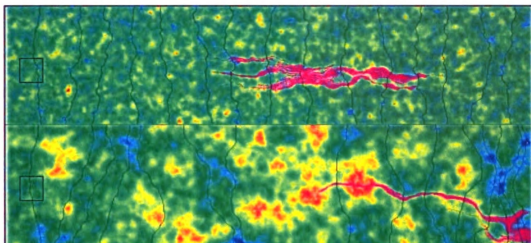


Figure 3.7 Snapshot of the visualization

For a detailed visualization, access the following address:

URL: <http://www.egr.msu.edu/igw/DL/SSH/EHST/EHST8.htm>

3.8 EFFECTS OF ANISOTROPIC HETEROGENEITIES

3.8.1 Problem statement

This video demonstrates the effects of anisotropic heterogeneities on the spreading of a conservative solute plume. This type of anisotropic heterogeneity is most commonly found in vertical cross-sections. The modeling domain consists of constant head boundaries on the left and right extremes, and no-flow boundaries at the top and bottom. Details are provided in Table 3.8.

3.8.2 Key observations

The following observations can be made from the video:

- Anisotropic heterogeneities have a drastic impact on plume spreading.
- Increasing horizontal correlation scales correspond to increasingly higher degrees of stratification, resulting in less plume spreading in the transverse direction.
- Longitudinal spreading is dependent on the $\ln K$ realization.
- The vertical correlation scale is of the same order as the plume source size, but the horizontal correlation scale controls plume spreading.
- Plume spreading is most pronounced for the smallest horizontal correlation scale (100 m), since the high K zones are not well connected. The longitudinal spreading is prominent.
- For the largest horizontal correlation scale (5000 m), the plume migration is controlled, for the most part, by the preferential channels, which extend longitudinally for about 5000 m. This implies that, once a preferential channel is

entered, the plume can travel for a very long distance within that channel, thus minimizing transverse spreading.

3.8.3 Additional observations and discussion

Case 1: The correlation scale is 100 m in the horizontal direction and 10 m in the vertical direction. The plume spreads to a great extent in the longitudinal direction, since the high *K* zones are not well connected. The mass of the plume is concentrated in the leading edges, and the plume tails are elongated.

Case 2: The correlation scale is 500 m in the horizontal direction and 10 m in the vertical direction. The plume spreads to a lesser extent in the longitudinal direction, since the high *K* zones are connected better than in case 1. The mass of the plume is not concentrated as much in the leading edges as in case 1. The highly skewed plume spreading seen in case 1 is not observed.

Case 3: The correlation scale is 1000 m in the horizontal direction and 10 m in the vertical direction. The plume spreads to a lesser extent in the longitudinal direction, since a longer high *K* zone (1000 m) is present than in case 1. The mass of the plume is not concentrated as much in the leading edges as in case 1. The highly skewed plume spreading seen in case 1 is not observed. In comparison to case 2, there is little difference in longitudinal and transverse spreading.

Case 4: The correlation scale is 5000 m in the horizontal direction and 10 m in the vertical direction. The plume spreads the least in the longitudinal direction, since an

extremely long high K zone (5000 m) is present. The plume spreads approximately equally about its mean. This is evidenced by the presence of a number of small fingers and tails that are not elongated. In comparison to cases 2 and 3, the plume appears different, especially in the longitudinal direction.

A comparison of the four situations shows that the effect of anisotropic heterogeneities on plume spreading is drastic. The most common places where such heterogeneity is encountered are vertical cross-sections. It is interesting to note that, with increasing stratification, the head contours approach a uniform distribution, as though the field were homogeneous. However, the spreading of the plume indicates that the velocity vectors differ greatly. The differential rates of advection are responsible for the spreading of the plume.

Table 3.8 Model parameters and inputs

Parameter	Case 1	Case 2	Case 3	Case 4
Geometric mean hydraulic conductivity, K_g (m/day)	10	10	10	10
ln K Variance	2.0	2.0	2.0	2.0
Correlation scale, λ_x (m)	100	500	1000	5000
Correlation scale, λ_z (m)	10	10	10	10
Porosity, n	0.3	0.3	0.3	0.3
Pore-scale dispersivity	0	0	0	0
Head difference (m)	1	1	1	1
Size of model (m)	200 x 50	200 x 50	200 x 50	200 x 50
Covariance function	Exponential	Exponential	Exponential	Exponential
Approximate initial plume size (m)	10	10	10	10
Grid	401 x 407	401 x 407	401 x 407	401 x 407
Cell size, Δx (m)	0.5 x 0.5	0.5 x 0.5	0.5 x 0.5	0.5 x 0.5
Time step, Δt (days)	1	1	1	1

The model parameters and inputs are explained below:

- The $\ln K$ field is a normally distributed random field. Therefore, there is an equal probability of the plume encountering a 'low' K zone or a 'high' K zone.
- The heterogeneous conductivity field is uniquely characterized by the following set of statistical parameters: geometric mean (K_g) of K , correlation scale, variance and covariance.
- The geometric mean and $\ln K$ variance are constant for all cases.
- The horizontal correlation scales vary from 100 m to 5000 m, while the vertical correlation scales remain constant at 10 m.
- The covariance function for all cases is exponential.
- The cell size, Δx , is selected such that the correlation scale, λ , is resolved.
Typically, Δx is at least 3 to 4 times smaller than the correlation scale.
- The time step, Δt , is selected such that a particle of the plume travels a distance that is less than λ in one time step.

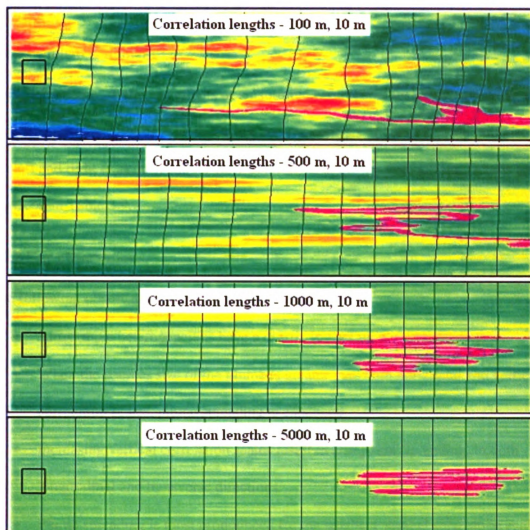


Figure 3.8 Snapshot of the visualization

For a detailed visualization, access the following address:

URL: <http://www.egr.msu.edu/igw/DL/SSH/EHST/EHST14.htm>

3.9 EFFECTS OF ANISOTROPIC HETEROGENEITIES

3.9.1 Problem statement

This video demonstrates the effects of anisotropic heterogeneities on the spreading of a conservative solute plume. The modeling domain consists of constant head boundaries on the left and right extremes, and no-flow boundaries at the top and bottom. Details are provided in Table 3.9.

3.9.2 Key observations

The following observations can be made from the video:

- Anisotropic heterogeneities have a drastic impact on plume spreading.
- When the sources size of the plume is greater than both horizontal and vertical correlation scales, plume spreading is enhanced.
- Increasing vertical correlation scales result in less plume spreading, in both longitudinal and transverse directions.
- Plume spreading is most pronounced for the smallest vertical correlation scale (2 m), since the high K zones are not well connected in the transverse direction, resulting in significant spreading.
- For the largest horizontal correlation scale (25 m), the plume migration is controlled, for the most part, by the $\ln K$ realization, which in turn, governs the location of preferential channels.

3.9.3 Additional observations and discussion

Case 1: The correlation scale is 20 m in the horizontal direction and 2 m in the vertical direction. This correlation structure is similar to what is found in a vertical cross-section.

However, it is not perfectly stratified, resulting in elongated plumes. The plume spreads to a great extent in the longitudinal direction, since the high K zones are not well connected in the transverse direction. The magnitude of transverse spreading is less in comparison to that of longitudinal spreading.

Case 2: The correlation scale is 20 m in the horizontal direction and 5 m in the vertical direction. This correlation structure is similar to what is found in a vertical cross-section. However, it is not perfectly stratified, resulting in elongated plumes, although less elongated than in case 1. The plume spreads to a less extent in the longitudinal direction, since the high K zones are connected better than in case 1.

Case 3: The correlation scale is 20 m in the horizontal direction and 10 m in the vertical direction. This correlation structure is commonly found in a horizontal view. Plume migration is controlled by the $\ln K$ realization. If a low K zone is encountered, the plume is trapped, and is released slowly at later points in time. The horizontal correlation scale is such that both low K and high K zones have to be encountered. This means that the different parts of the plume move at significantly different velocities, which means that the longitudinal spreading will be enhanced.

Case 4: The correlation scale is 20 m in the horizontal direction and 25 m in the vertical direction. This correlation structure is commonly found in a horizontal view. Plume migration is controlled by the $\ln K$ realization. If a low K zone is encountered, the plume is trapped, and is released slowly at later points in time. The horizontal correlation scale

is such that both low K and high K zones have to be encountered. This means that the different parts of the plume move at significantly different velocities, and longitudinal spreading will be enhanced. In comparison to case 3, the spreading is less extensive, since the plume does not encounter the different heterogeneities.

A comparison of the four situations shows that the effect of anisotropic heterogeneities on plume spreading is drastic. With increasing correlation scales, plume spreading is reduced in the transverse direction, since it becomes difficult to encounter the heterogeneities. The differential rates of advection are responsible for the spreading of the plume.

Table 3.9 Model parameters and inputs

Parameter	Case 1	Case 2	Case 3	Case 4
Geometric mean hydraulic conductivity, K_g (m/day)	10	10	10	10
$\ln K$ Variance	2.0	2.0	2.0	2.0
Correlation scale, λ_x (m)	20	20	20	20
Correlation scale, λ_z (m)	2	5	10	25
Porosity, n	0.3	0.3	0.3	0.3
Pore-scale dispersivity	0	0	0	0
Head difference (m)	1	1	1	1
Size of model (m)	200 x 50	200 x 50	200 x 50	200 x 50
Covariance function	Exponential	Exponential	Exponential	Exponential
Approximate initial plume size (m)	10	10	10	10
Grid	401 x 407	401 x 407	401 x 407	401 x 407
Cell size, Δx (m)	0.5 x 0.5	0.5 x 0.5	0.5 x 0.5	0.5 x 0.5
Time step, Δt (days)	1	1	1	1

The model parameters and inputs are explained below:

- The $\ln K$ field is a normally distributed random field. Therefore, there is an equal probability of the plume encountering a 'low' K zone or a 'high' K zone.

- The heterogeneous conductivity field is uniquely characterized by the following set of statistical parameters: geometric mean (K_g) of K , correlation scale, variance and covariance.
- The geometric mean and $\ln K$ variance are constant for all cases.
- The vertical correlation scales vary from 2 m to 25 m, while the horizontal correlation scales remain constant at 20 m.
- The covariance function for all cases is exponential.
- The cell size, Δx , is selected such that the correlation scale, λ , is resolved.
Typically, Δx is at least 3 to 4 times smaller than the correlation scale.
- The time step, Δt , is selected such that a particle of the plume travels a distance that is less than λ in one time step.

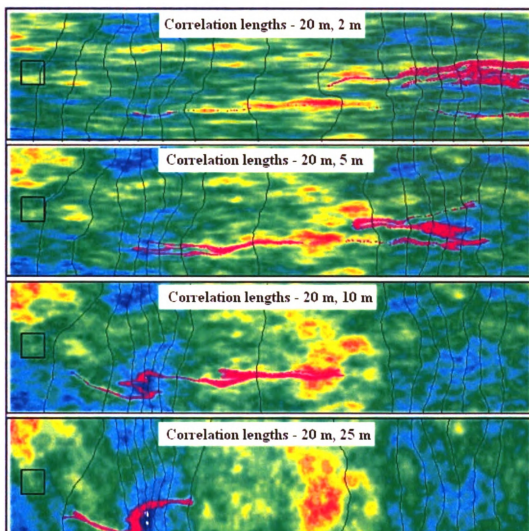


Figure 3.9 Snapshot of the visualization

For a detailed visualization, access the following address:

URL: <http://www.egr.msu.edu/jgw/DL/SSH/EHST/EHST15.htm>

4 TEMPORAL VARIABILITY

4.1 UNCONFINED AQUIFERS WITH INCREASING TRANSMISSIVITIES

4.1.1 Problem statement

This video demonstrates the effect of a sinusoidally oscillating boundary condition on the hydraulic head in unconfined aquifers with increasing transmissivities. The modeling domain consists of a time-variable head boundary on the left extreme, and a no-flow boundary on the right. Details are provided in Table 4.1.

4.1.2 Key observations

The following observations can be made from the video:

- Sinusoidal oscillation at the boundary affects the head in the aquifer sinusoidally.
- As distance from the boundary increases, the effect on the head decreases.
- The area that is influenced by the boundary is called the “response zone”. The response zone depends on several parameters, such as transmissivity, storage coefficient, frequency of oscillations, amplitude of oscillations, and distance from the boundary.
- Lower transmissivity values result in a smaller response zone.

4.1.3 Additional observations and discussion

Case 1: The average transmissivity is $2 \text{ m}^2/\text{day}$ and the specific yield is 0.1. The sinusoidal oscillation of head in the river is characterized by an amplitude of 5 m and a time period of 1 day. Since the aquifer material is not highly transmissive, the resulting transient head distribution in the aquifer is concentrated in a small zone very close to the

river. Beyond approximately 20 m from the river, the oscillating head in the river produces no visible effect on the head in the aquifer.

Case 2: The average transmissivity is $20 \text{ m}^2/\text{day}$ and the specific yield is 0.1. The sinusoidal oscillation of head in the river is characterized by an amplitude of 5 m and a time period of 1 day. Since the aquifer material is more transmissive than in case 1, the resulting transient head distribution in the aquifer is concentrated in a larger zone compared to case 1. Beyond approximately 50 m from the river, the oscillating head in the river produces no visible effect on the head in the aquifer.

Case 3: The average transmissivity is $200 \text{ m}^2/\text{day}$ and the specific yield is 0.1. The sinusoidal oscillation of head in the river is characterized by an amplitude of 5 m and a time period of 1 day. Since the aquifer material is more transmissive than in cases 1 and 2, the resulting transient head distribution in the aquifer is concentrated in a larger zone compared to cases 1 and 2. Beyond approximately 100 m from the river, the oscillating head in the river produces no visible effect on the head in the aquifer.

4.1.4 Mathematical interpretation

The head change in an aquifer connected to a surface water body with a sinusoidally oscillating stage was studied by Ferris (1951), and is given by:

$$s(x, t) = s_r \exp\left(-\sqrt{\frac{\omega S_y x^2}{2T}}\right) \sin\left(\omega t - \sqrt{\frac{\omega S_y x^2}{2T}}\right), \quad (4.1)$$

where:

s - Head change in the aquifer

s_r - Amplitude of stage change in the surface water body

ω - Frequency of stage change

x - Distance from the boundary

T - Transmissivity of aquifer

t - Time

S_y - Storage coefficient (specific yield) of aquifer

Equation 4.1 shows that the head change in the aquifer varies sinusoidally with the same frequency as the stage in the surface water body, but with a time lag. The amplitude of variation is damped exponentially with distance away from the boundary. The amplitude is dependent on aquifer properties such as transmissivity and storage coefficient. When transmissivity increases, amplitude also increases, and when storage coefficient increases, amplitude decreases.

Table 4.1 Model parameters and inputs

Parameter	Case 1	Case 2	Case 3
Average transmissivity, T (m^2/day)	2	20	200
Specific yield, S_y	0.1	0.1	0.1
Storage coefficient, S	NA	NA	NA
Porosity, n	0.3	0.3	0.3
Starting head - aquifer (m)	5	5	5
Mean head - river (m)	5	5	5
Amplitude, s_r (m)	5	5	5
Time period (days)	1	1	1
Size of model (m)	500 x 10	500 x 10	500 x 10
Grid	251 x 6	251 x 6	251 x 6
Cell size, Δx (m)	2 x 2	2 x 2	2 x 2
Time step, Δt (days)	0.1	0.1	0.1

The model parameters and inputs are explained below:

- The average transmissivity values are $2 \text{ m}^2/\text{d}$, $20 \text{ m}^2/\text{d}$, and $200 \text{ m}^2/\text{d}$ for cases 1, 2, and 3 respectively, and specific yields are 0.1 for all cases.
- The sinusoidal oscillation in the river is characterized by the following parameters: amplitude of 5 m and a time period of 1 day.
- The time step, Δt , is selected such that the temporal variability of head in the river is resolved. The head in the river varies sinusoidally over a time period of 1 day, and hence a time step of 0.1 days is selected.

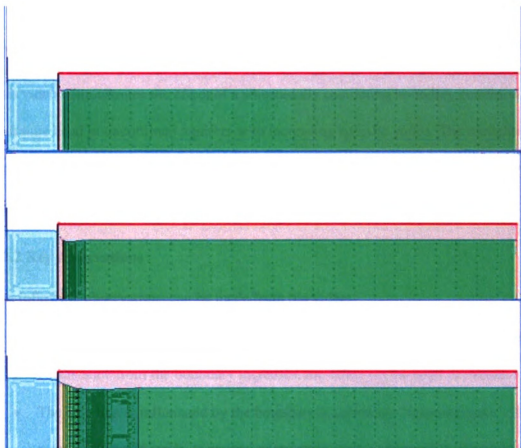


Figure 4.1 Snapshot of the visualization

For a detailed visualization, access the following address:

URL: <http://www.cgr.msu.edu/igw/DL/SSH/TV/TV9.htm>

4.2 UNCONFINED AQUIFERS WITH INCREASING SPECIFIC YIELDS

4.2.1 Problem statement

This video demonstrates the effect of a sinusoidally oscillating boundary condition on the hydraulic head in unconfined aquifers with increasing specific yields. The modeling domain consists of a time-variable head boundary on the left extreme, and a no-flow boundary on the right. Details are provided in Table 4.2.

4.2.2 Key observations

The following observations can be made from the video:

- Sinusoidal oscillation at the boundary affects the head in the aquifer sinusoidally.
- As distance from the boundary increases, the effect on the head decreases.
- The area that is influenced by the boundary is called the “response zone”. The response zone depends on several parameters, such as transmissivity, storage coefficient, frequency of oscillations, amplitude of oscillations, and distance from the boundary.
- Higher specific yield values result in a smaller response zone.

4.2.3 Additional observations and discussion

Case 1: The average transmissivity is $200 \text{ m}^2/\text{d}$ and the specific yield is 0.01. The sinusoidal oscillation of head in the river is characterized by an amplitude of 5 m and a time period of 1 day. The resulting transient head distribution in the aquifer is concentrated in a zone close to the river. Beyond approximately 250 m from the river, the oscillating head in the river produces no visible effect on the head in the aquifer.

Case 2: The average transmissivity is $200 \text{ m}^2/\text{d}$ and the specific yield is 0.1. The sinusoidal oscillation of head in the river is characterized by an amplitude of 5 m and a time period of 1 day. The resulting transient head distribution in the aquifer looks very similar to case 1. The higher specific yield compared to case 1, decreases the area influenced by the river. Beyond approximately 100 m from the river, the oscillating head in the river produces no visible effect on the head in the aquifer.

Case 3: The average transmissivity is $200 \text{ m}^2/\text{d}$ and the specific yield is 0.3. The sinusoidal oscillation of head in the river is characterized by an amplitude of 5 m and a time period of 1 day. The resulting transient head distribution in the aquifer looks very similar to cases 1 and 2. The higher specific yield of 0.3 compared to cases 1 and 2, decreases the area influenced by the river. Beyond approximately 60 m from the river, the oscillating head in the river produces no visible effect on the head in the aquifer.

4.2.4 Mathematical interpretation

The head change in an aquifer connected to a surface water body with a sinusoidally oscillating stage was studied by Ferris (1951), and is given by:

$$s(x,t) = s_r \exp\left(-\sqrt{\frac{\omega S_y x^2}{2T}}\right) \sin\left(\omega t - \sqrt{\frac{\omega S_y x^2}{2T}}\right), \quad (4.2)$$

where:

s - Head change in the aquifer

s_r - Amplitude of stage change in the surface water body

ω - Frequency of stage change

x - Distance from the boundary

T - Transmissivity of aquifer

t - Time

S_y - Storage coefficient (specific yield) of aquifer

Equation 4.2 shows that the head change in the aquifer varies sinusoidally with the same frequency as the stage in the surface water body, but with a time lag. The amplitude of variation is dampened exponentially with distance away from the boundary. The amplitude is dependent on aquifer properties such as transmissivity and storage coefficient. When transmissivity increases, amplitude also increases, and when storage coefficient increases, amplitude decreases.

Table 4.2 Model parameters and inputs

Parameter	Case 1	Case 2	Case 3
Average transmissivity, T (m^2/day)	200	200	200
Specific yield, S_y	0.01	0.1	0.3
Storage coefficient, S	NA	NA	NA
Porosity, n	0.3	0.3	0.3
Starting head - aquifer (m)	5	5	5
Mean head - river (m)	5	5	5
Amplitude, s_r (m)	5	5	5
Time period (days)	1	1	1
Size of model (m)	500 x 10	500 x 10	500 x 10
Grid	251 x 6	251 x 6	251 x 6
Cell size, Δx (m)	2 x 2	2 x 2	2 x 2
Time step, Δt (days)	0.1	0.1	0.1

The model parameters and inputs are explained below:

- The transmissivity is $200 \text{ m}^2/\text{d}$ for all cases; specific yield is 0.01, 0.1, and 0.3 for cases 1, 2, and 3 respectively.

- The sinusoidal oscillation in the river is characterized by the following parameters: amplitude of 5 m and a time period of 1 day.
- The time step, Δt , is selected such that the temporal variability of head in the river is resolved. The head in the river varies sinusoidally over a time period of 1 day, and hence a time step of 0.1 days is selected.

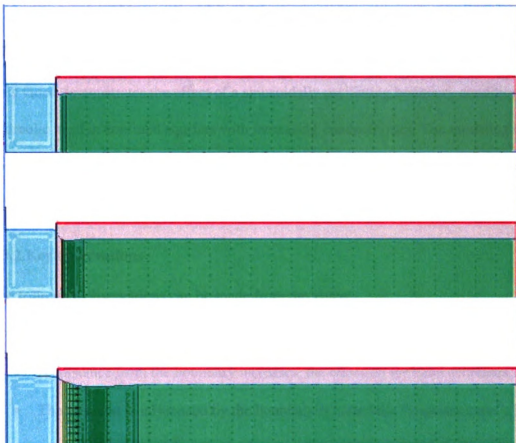


Figure 4.2 Snapshot of the visualization

For a detailed visualization, access the following address:

URL: <http://www.egr.msu.edu/igw/DL/SSH/TV/TV10.htm>

4.3 CONFINED AQUIFERS WITH INCREASING CONDUCTIVITIES

4.3.1 Problem statement

This video demonstrates the effect of a sinusoidally oscillating boundary condition on the hydraulic head in confined aquifers with increasing conductivities. The modeling domain consists of a time-variable head boundary on the left extreme, and a no-flow boundary on the right. Details are provided in Table 4.3.

4.3.2 Key observations

The following observations can be made from the video:

- Sinusoidal oscillation at the boundary affects the head in the aquifer sinusoidally.
- As distance from the boundary increases, the effect on the head decreases.
- The area that is influenced by the boundary is called the “response zone”. The response zone depends on several parameters, such as transmissivity, storage coefficient, frequency of oscillations, amplitude of oscillations, and distance from the boundary.
- Lower transmissivity values result in a smaller response zone.

4.3.3 Additional observations and discussion

Case 1: The transmissivity is $0.2 \text{ m}^2/\text{d}$ and the storage coefficient is 2×10^{-4} . The sinusoidal oscillation of head in the river is characterized by an amplitude of 5 m and a time period of 1 day. Since the aquifer material is not highly transmissive, the resulting transient head distribution in the aquifer is concentrated in a small zone very close to the river. Beyond approximately 75 m from the river, the oscillating head in the river produces no visible effect on the head in the aquifer.

Case 2: The transmissivity is $2 \text{ m}^2/\text{day}$ and the storage coefficient is 2×10^{-4} . The sinusoidal oscillation of head in the river is characterized by an amplitude of 5 m and a time period of 1 day. Since the aquifer material is more transmissive than in case 1, the resulting transient head distribution in the aquifer is concentrated in a larger zone compared to case 1. Beyond approximately 200 m from the river, the oscillating head in the river produces no visible effect on the head in the aquifer.

Case 3: The transmissivity is $20 \text{ m}^2/\text{day}$ and the storage coefficient is 2×10^{-4} . The sinusoidal oscillation of head in the river is characterized by an amplitude of 5 m and a time period of 1 day. Since the aquifer material is more transmissive than in cases 1 and 2, the resulting transient head distribution in the aquifer is concentrated in a larger zone compared to cases 1 and 2. The variable head in the river affects the head in the entire modeled area (450 m).

4.3.4 Mathematical interpretation

The head change in an aquifer connected to a surface water body with a sinusoidally oscillating stage was studied by Ferris (1951), and is given by:

$$s(x,t) = s_r \exp\left(-\sqrt{\frac{\omega S x^2}{2T}}\right) \sin\left(\omega t - \sqrt{\frac{\omega S x^2}{2T}}\right), \quad (4.3)$$

where:

s - Head change in the aquifer

s_r - Amplitude of stage change in the surface water body

ω - Frequency of stage change

x - Distance from the boundary

T - Transmissivity of aquifer

t - Time

S - Storage coefficient of aquifer

Equation 4.3 shows that the head change in the aquifer varies sinusoidally with the same frequency as the stage in the surface water body, but with a time lag. The amplitude of variation is dampened exponentially with distance away from the boundary. The amplitude is dependent on aquifer properties such as transmissivity and storage coefficient. When transmissivity increases, amplitude also increases, and when storage coefficient increases, amplitude decreases.

Table 4.3 Model parameters and inputs

Parameter	Case 1	Case 2	Case 3
Transmissivity, T (m^2/day)	0.2	2	20
Storage coefficient, S	2×10^{-4}	2×10^{-4}	2×10^{-4}
Porosity, n	0.3	0.3	0.3
Starting head - aquifer (m)	5	5	5
Mean head - river (m)	5	5	5
Amplitude, s_r (m)	5	5	5
Time period (days)	1	1	1
Size of model (m)	500 x 10	500 x 10	500 x 10
Grid	251 x 6	251 x 6	251 x 6
Cell size, Δx (m)	2 x 2	2 x 2	2 x 2
Time step, Δt (days)	0.1	0.1	0.1

The model parameters and inputs are explained below:

- The transmissivity values are $0.2 \text{ m}^2/\text{d}$, $2 \text{ m}^2/\text{d}$, and $20 \text{ m}^2/\text{d}$ for cases 1, 2, and 3 respectively, and storage coefficients are 2×10^{-4} for all cases.
- The sinusoidal oscillation in the river is characterized by the following parameters: amplitude of 5 m and a time period of 1 day.
- The time step, Δt , is selected such that the temporal variability of head in the river is resolved. The head in the river varies sinusoidally over a time period of 1 day, and hence a time step of 0.1 days is selected.

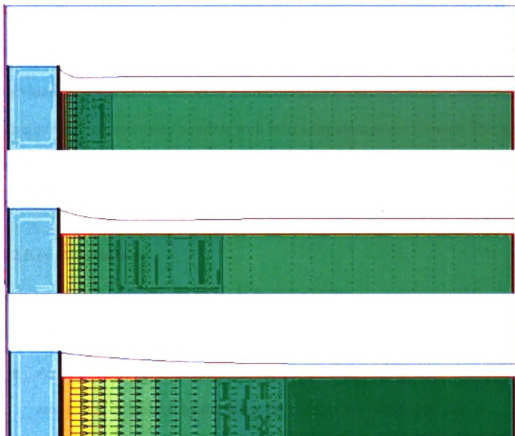


Figure 4.3 Snapshot of the visualization

For a detailed visualization, access the following address:

URL: <http://www.egr.msu.edu/igw/DL/SSH/TV/TV11.htm>

4.4 CONFINED AQUIFERS WITH INCREASING STORAGE COEFFICIENTS

4.4.1 Problem statement

This video demonstrates the effect of a sinusoidally oscillating boundary condition on the hydraulic head in unconfined aquifers with increasing storage coefficients. The modeling domain consists of a time-variable head boundary on the left extreme, and a no-flow boundary at the right. Details are provided in Table 4.4.

4.4.2 Key observations

The following observations can be made from the video:

- Sinusoidal oscillation at the boundary affects the head in the aquifer sinusoidally.
- As distance from the boundary increases, the effect on the head decreases. The area that is influenced by the boundary is called the “response zone”.
- The area that is influenced by the boundary is called the “response zone”. The response zone depends on several parameters, such as transmissivity, storage coefficient, frequency of oscillations, amplitude of oscillations, and distance from the boundary.
- Lower storage coefficient values result in a larger response zone.

4.4.3 Additional observations and discussion

Case 1: The transmissivity is $2 \text{ m}^2/\text{d}$ and storage coefficient is 2×10^{-3} . The sinusoidal oscillation of head in the river is characterized by an amplitude of 5 m and a time period of 1 day. The resulting transient head distribution in the aquifer is spread over a large area. Since the aquifer material can store “less” water, the head in the aquifer is affected in the whole of the modeled area.

Case 2: The transmissivity is $2 \text{ m}^2/\text{d}$ and storage coefficient is 2×10^{-4} . The sinusoidal oscillation of head in the river is characterized by an amplitude of 5 m and a time period of 1 day. The resulting transient head distribution in the aquifer looks very different from case 1. The higher storage coefficient compared to case 1, means that the aquifer can store more water. Therefore, a smaller area is affected. Beyond approximately 150 m from the river, the oscillating head in the river produces no visible effect on the head in the aquifer.

Case 3: The transmissivity is $2 \text{ m}^2/\text{d}$ and storage coefficient is 2×10^{-5} . The sinusoidal oscillation of head in the river is characterized by an amplitude of 5 m and a time period of 1 day. The resulting transient head distribution in the aquifer is concentrated in a small zone very close to the river. The higher storage coefficient compared to cases 1 and 2, has a significant impact on the area influenced by the river. Since the aquifer can store more water than in cases 1 and 2, beyond approximately 150 m from the river, the oscillating head in the river produces no visible effect on the head in the aquifer.

4.4.4 Mathematical interpretation

The head change in an aquifer connected to a surface water body with a sinusoidally oscillating stage was studied by Ferris (1951), and is given by:

$$s(x,t) = s_r \exp\left(-\sqrt{\frac{\omega S x^2}{2T}}\right) \sin\left(\omega t - \sqrt{\frac{\omega S x^2}{2T}}\right), \quad (4.4)$$

where:

s - Head change in the aquifer

s_r - Amplitude of stage change in the surface water body

ω - Frequency of stage change

x - Distance from the boundary

T - Transmissivity of aquifer

t - Time

S - Storage coefficient of aquifer

Equation 4.4 shows that the head change in the aquifer varies sinusoidally with the same frequency as the stage in the surface water body, but with a time lag. The amplitude of variation is dampened exponentially with distance away from the boundary. The amplitude is dependent on aquifer properties such as transmissivity and storage coefficient. When transmissivity increases, amplitude also increases, and when storage coefficient increases, amplitude decreases.

Table 4.4 Model parameters and inputs

Parameter	Case 1	Case 2	Case 3
Transmissivity, T (m^2/day)	2	2	2
Storage coefficient, S	2×10^{-3}	2×10^{-4}	2×10^{-5}
Porosity, n	0.3	0.3	0.3
Starting head - aquifer (m)	5	5	5
Mean head - river (m)	5	5	5
Amplitude, s_r (m)	5	5	5
Time period (days)	1	1	1
Size of model (m)	500 x 10	500 x 10	500 x 10
Grid	251 x 6	251 x 6	251 x 6
Cell size, Δx (m)	2 x 2	2 x 2	2 x 2
Time step, Δt (days)	0.1	0.1	0.1

The model parameters and inputs are explained below:

- The transmissivity is $2 \text{ m}^2/\text{d}$ for all cases; storage coefficient is 2×10^{-3} , 2×10^{-4} and 2×10^{-5} for cases 1, 2 and 3 respectively.
- The sinusoidal oscillation in the river is characterized by the following parameters: amplitude of 5 m and a time period of 1 day.
- The time step, Δt , is selected such that the temporal variability of head in the river is resolved. The head in the river varies sinusoidally over a time period of 1 day, and hence a time step of 0.1 days is selected.

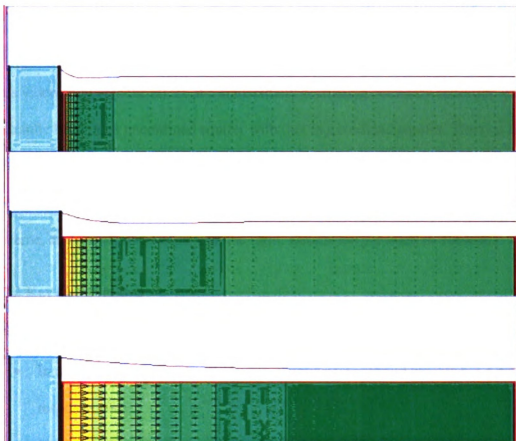


Figure 4.4 Snapshot of the visualization

For a detailed visualization, access the following address:

URL: <http://www.egr.msu.edu/igw/DL/SSH/TV/TV12.htm>

4.5 COMPARISON BETWEEN UNCONFINED AND CONFINED AQUIFERS

4.5.1 Problem statement

This video compares the effect of a sinusoidally oscillating boundary condition on the hydraulic head in an unconfined aquifer with that in a confined aquifer. The two aquifers differ only in the magnitude of their storage properties (specific yield and storage coefficient). The modeling domain consists of a time-variable head boundary on the left extreme, and a no-flow boundary on the right. Details are provided in Table 4.5.

4.5.2 Key observations

The following observations can be made from the video:

- In comparison to a confined aquifer, a similar unconfined aquifer has a smaller response zone.
- Unconfined aquifers release water by draining water-filled pores, while confined aquifers release water by elastic expansion of the aquifer matrix and decompression of water. Therefore, unconfined aquifers are able to drain more water from a unit area of aquifer material per unit decline in head; hence, the smaller response zones.

4.5.3 Additional observations and discussion

Case 1: The average transmissivity of the unconfined aquifer is $20 \text{ m}^2/\text{d}$ and the specific yield is 0.1. The sinusoidal oscillation of head in the river is characterized by an amplitude of 5 m and a time period of 1 day. The response zone is approximately 50 m in length.

Case 2: The transmissivity of the confined aquifer is $20 \text{ m}^2/\text{d}$ and the storage coefficient is 2×10^{-4} . The sinusoidal oscillation of head in the river is characterized by an amplitude of 5 m and a time period of 1 day. The response zone is larger than in case 1, since the confined aquifer has a much lower storage coefficient compared to the unconfined aquifer.

Since storage properties of confined aquifers are smaller than those of unconfined aquifers by several orders of magnitude (typically 2 or more), the response zones are proportionally larger.

3.5.4 Mathematical interpretation

The head change in an aquifer connected to a surface water body with a sinusoidally oscillating stage was studied by Ferris (1951), and is given by:

$$s(x,t) = s_r \exp\left(-\sqrt{\frac{\omega S x^2}{2T}}\right) \sin\left(\omega t - \sqrt{\frac{\omega S x^2}{2T}}\right), \quad (4.5)$$

where:

s - Head change in the aquifer

s_r - Amplitude of stage change in the surface water body

ω - Frequency of stage change

x - Distance from the boundary

T - Transmissivity of aquifer

t - Time

S - Storage coefficient of aquifer

Equation 4.5 shows that the head change in the aquifer varies sinusoidally with the same frequency as the stage in the surface water body, but with a time lag. The amplitude of variation is dampened exponentially with distance away from the boundary. The amplitude is dependent on aquifer properties such as transmissivity and storage coefficient. When all properties of the two aquifers are similar, a decrease in storage coefficient causes an increase in amplitude and size of the response zone.

Table 4.5 Model parameters and inputs

Parameter	Case 1	Case 2
Average transmissivity, T (m^2/day)	20	20
Specific yield, S_y	0.1	NA
Storage coefficient, S	NA	2×10^{-4}
Porosity, n	0.3	0.3
Starting head - aquifer (m)	5	5
Mean head - river (m)	5	5
Amplitude, s_r (m)	5	5
Time period (days)	1	1
Size of model (m)	500 x 10	500 x 10
Grid	251 x 6	251 x 6
Cell size, Δx (m)	2 x 2	2 x 2
Time step, Δt (days)	0.1	0.1

The model parameters and inputs are explained below:

- The transmissivity values are $20 \text{ m}^2/\text{d}$ for both cases; specific yield is 0.1 for case 1 and storage coefficient is 2×10^{-4} for case 2.
- The sinusoidal oscillation in the river is characterized by the following parameters: amplitude of 5 m and a time period of 1 day.
- The time step, Δt , is selected such that the temporal variability of head in the river is resolved. The head in the river varies sinusoidally over a time period of 1 day, and hence a time step of 0.1 days is selected.

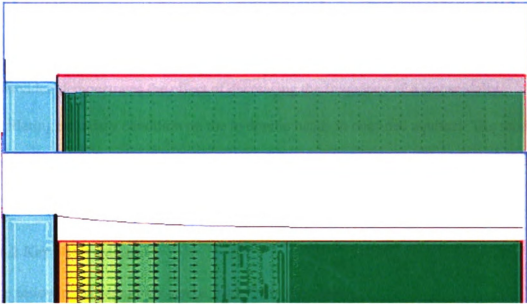


Figure 4.5 Snapshot of the visualization

For a detailed visualization, access the following address:

URL: <http://www.egr.msu.edu/igw/DL/SSH/TV/TV13.htm>

4.6 BOUNDARIES WITH DECREASING FREQUENCIES OF VARIABILITY

4.6.1 Problem statement

This video demonstrates the effect of decreasing the frequency of a sinusoidally oscillating boundary condition on the hydraulic heads in confined aquifers. The modeling domain consists of a time-variable head boundary on the left extreme, and a no-flow boundary on the right. Details are provided in Table 4.6.

4.6.2 Key observations

The following observations can be made from the video:

- Decreasing the frequency of Sinusoidal oscillation at the boundary decreases the frequency of change in head in the aquifer.
- The area influenced by the boundary is called the “response zone”. The response zone depends on several parameters, such as transmissivity, storage coefficient, frequency of oscillations, amplitude of oscillations, and distance from the boundary.
- Smaller values of frequency of oscillation result in a larger response zone.

4.6.3 Additional observations and discussion

Case 1: The transmissivity is $2 \text{ m}^2/\text{d}$ and the storage coefficient is 2×10^{-4} . The sinusoidal oscillation of head in the river is characterized by amplitude of 10 m and time period of 0.25 days. Since the frequency of oscillations is very high, the resulting transient head distribution in the aquifer is concentrated in a small zone close to the river. Beyond approximately 100 m from the river, the oscillating head in the river produces no visible effect on the head in the aquifer.

Case 2: The transmissivity is $2 \text{ m}^2/\text{d}$ and the storage coefficient is 2×10^{-4} . The sinusoidal oscillation of head in the river is characterized by amplitude of 10 m and time period of 1 day. Since the frequency of oscillations is smaller than in case 1, the resulting transient head distribution in the aquifer is concentrated in a larger zone compared to case 1. Beyond approximately 200 m from the river, the oscillating head in the river produces no visible effect on the head in the aquifer.

Case 3: The transmissivity is $2 \text{ m}^2/\text{d}$ and the storage coefficient is 2×10^{-4} . The sinusoidal oscillation of head in the river is characterized by amplitude of 10 m and time period of 10 days. Since the frequency of oscillations is smaller than in cases 1 and 2, the resulting transient head distribution in the aquifer is concentrated in a larger zone compared to cases 1 and 2. The variable head in the river affects the head in the entire modeled area (450 m).

4.6.4 Mathematical interpretation

The head change in an aquifer connected to a surface water body with a sinusoidally oscillating stage was studied by Ferris (1951), and is given by:

$$s(x,t) = s_r \exp\left(-\sqrt{\frac{\omega S x^2}{2T}}\right) \sin\left(\omega t - \sqrt{\frac{\omega S x^2}{2T}}\right), \quad (4.6)$$

where:

s - Head change in the aquifer

s_r - Amplitude of stage change in the surface water body

ω - Frequency of stage change

x - Distance from the boundary

T - Transmissivity of aquifer

t - Time

S - Storage coefficient of aquifer

Equation 4.6 shows that the head change in the aquifer varies sinusoidally with the same frequency as the stage in the surface water body, but with a time lag. The size of the response zone is dependent on aquifer properties, as well as the frequency. When the frequency of variability decreases, the size of the response zone increases.

Table 4.6 Model parameters and inputs

Parameter	Case 1	Case 2	Case 3
Transmissivity, T (m^2/day)	2	2	2
Storage coefficient, S	2×10^{-4}	2×10^{-4}	2×10^{-4}
Porosity, n	0.3	0.3	0.3
Starting head - aquifer (m)	5	5	5
Mean head - river (m)	5	5	5
Amplitude, s_r (m)	10	10	10
Time period (days)	0.25	1	10
Size of model (m)	500 x 10	500 x 10	500 x 10
Grid	251 x 6	251 x 6	251 x 6
Cell size, Δx (m)	2 x 2	2 x 2	2 x 2
Time step, Δt (days)	0.05	0.05	0.05

The model parameters and inputs are explained below:

- The transmissivity and storage coefficient values are $2 \text{ m}^2/\text{d}$ and 2×10^{-4} respectively for all cases.
- The sinusoidal oscillation in the river is characterized by amplitude of 10 m for all cases, and time periods of 0.25, 1, and 10 days for cases 1, 2, and 3 respectively.

- The time step, Δt , is selected such that the temporal variability of head in the river is resolved. The head in the river varies sinusoidally over a time period of 0.25 days, and hence a time step of 0.05 days is selected.

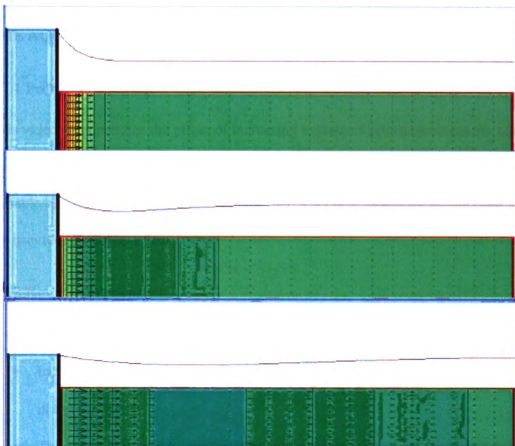


Figure 4.6 Snapshot of the visualization

For a detailed visualization, access the following address:

URL: <http://www.egr.msu.edu/igw/DL/SSH/TV/TV14.htm>

4.7 BOUNDARIES WITH INCREASING EXTENTS OF PENETRATION INTO THE AQUIFER

4.7.1 Problem statement

This video demonstrates the effect of increasing extents of penetration into the aquifer on the hydraulic heads in confined aquifers. The modeling domain consists of a time-variable head boundary on the left extreme, and a no-flow boundary on the right. Details are provided in Table 4.7.

4.7.2 Key observations

The following observations can be made from the video:

- Increasing the extent of penetration into the aquifer has little impact on the head in the aquifer.
- The area influenced by the boundary is called the “response zone”. When the extent of penetration increases, the size of the response zone increases, although the increase is not drastic.

4.7.3 Additional observations and discussion

Case 1: The transmissivity is $2 \text{ m}^2/\text{d}$ and the storage coefficient is 2×10^{-4} . The sinusoidal oscillation of head in the river is characterized by amplitude of 10 m and time period of 1 day. The surface water body penetrates only 5 m of the 20 m thickness of the aquifer.

Beyond approximately 230 m from the river, the oscillating head in the river produces no visible effect on the head in the aquifer. There is considerable head loss under the surface water boundary..

Case 2: The transmissivity is $2 \text{ m}^2/\text{d}$ and the storage coefficient is 2×10^{-4} . The sinusoidal oscillation of head in the river is characterized by amplitude of 10 m and time period of 1 day. The surface water body penetrates only 10 m of the 20 m thickness of the aquifer. Beyond approximately 240 m from the river, the oscillating head in the river produces no visible effect on the head in the aquifer. The small increase in the size of the response zone is due to the lower head loss under the surface water boundary.

Case 3: The transmissivity is $2 \text{ m}^2/\text{d}$ and the storage coefficient is 2×10^{-4} . The sinusoidal oscillation of head in the river is characterized by amplitude of 10 m and time period of 1 day. The surface water body penetrates the entire 20 m thickness of the aquifer. Beyond approximately 250 m from the river, the oscillating head in the river produces no visible effect on the head in the aquifer. Since the surface water body penetrates the entire aquifer, there is no head loss under the boundary. Therefore, to achieve the same head loss as cases 1 and 2, water in a larger area has to be displaced.

4.7.4 Mathematical interpretation

The head change in an aquifer connected to a surface water body with a sinusoidally oscillating stage was studied by Ferris (1951), and is given by:

$$s(x,t) = s_r \exp\left(-\sqrt{\frac{\omega S x^2}{2T}}\right) \sin\left(\omega t - \sqrt{\frac{\omega S x^2}{2T}}\right), \quad (3.7)$$

where:

s - Head change in the aquifer

s_r - Amplitude of stage change in the surface water body

ω - Frequency of stage change

x - Distance from the boundary

T - Transmissivity of aquifer

t - Time

S - Storage coefficient of aquifer

Equation 4.7 shows that the head change in the aquifer varies sinusoidally with the same frequency as the stage in the surface water body, but with a time lag. The size of the response zone is dependent on aquifer properties, as well as the frequency. When the frequency of variability decreases, the size of the response zone increases.

Table 4.7 Model parameters and inputs

Parameter	Case 1	Case 2	Case 3
Transmissivity, T (m^2/day)	2	2	2
Storage coefficient, S	2×10^{-4}	2×10^{-4}	2×10^{-4}
Porosity, n	0.3	0.3	0.3
Starting head - aquifer (m)	5	5	5
Mean head - river (m)	5	5	5
Amplitude, s_r (m)	10	10	10
Time period (days)	1	1	1
Size of model (m)	500 x 10	500 x 10	500 x 10
Grid	251 x 6	251 x 6	251 x 6
Cell size, Δx (m)	2 x 2	2 x 2	2 x 2
Time step, Δt (days)	0.05	0.05	0.05

The model parameters and inputs are explained below:

- The transmissivity and storage coefficient values are $2 \text{ m}^2/\text{day}$ and 2×10^{-4} respectively for all cases.
- The sinusoidal oscillation in the river is characterized by amplitude of 10 m for all cases, and time periods of 0.25, 1, and 10 days for cases 1, 2, and 3 respectively.

- The time step, Δt , is selected such that the temporal variability of head in the river is resolved. The head in the river varies sinusoidally over a time period of 0.25 days, and hence a time step of 0.05 days is selected.

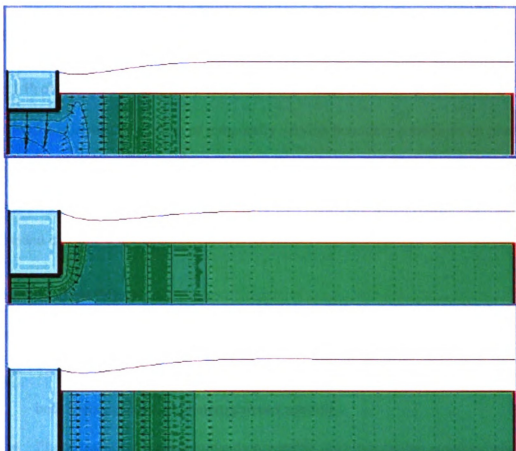


Figure 4.7 Snapshot of the visualization

For a detailed visualization, access the following address:

URL: <http://www.egr.msu.edu/igw/DL/SSH/TV/TV15.htm>

4.8 PLUME TRANSPORT - COMPARISON BETWEEN HOMOGENEOUS AND HETEROGENEOUS AQUIFERS

4.8.1 Problem statement

This video compares the effect of temporally varying boundary conditions on plume transport in homogeneous aquifers with heterogeneous aquifers. The modeling domain consists of a time-variable head boundary on both left and right extremes. Details are provided in Table 4.8.

4.8.2 Key observations

The following observations can be made from the video:

- Temporally varying boundary conditions cause to and fro motion of the plume in both homogeneous and heterogeneous aquifers.
- Plume transport is predominantly reversible in homogeneous aquifers, while it is irreversible in heterogeneous aquifers.
- The plume spreads significantly due to the interaction between spatial heterogeneity and temporal variability. In the absence of spatial heterogeneity, the plume does not spread, but undergoes slight distortion in shape.

4.8.3 Additional observations and discussion

Case 1: The average conductivity of the aquifer is 5 m/day. The temporally varying boundary conditions cause the head in the aquifer to fluctuate. As a result, the flow of groundwater changes direction, resulting in to and fro motion of the plume. However, due to the homogeneous properties of the aquifer, there is no spreading of the plume, apart from a slight distortion in the shape of the plume.

Case 2: The geometric mean conductivity of the aquifer is 5 m/day. The temporally varying boundary conditions cause the head in the aquifer to fluctuate. As a result, the flow of groundwater changes direction, resulting in to and fro motion of the plume. Since the aquifer is heterogeneous, the to and fro motion of the plume is irreversible. When a part of the plume enters a low K zone, it is “trapped” and releases the contaminant slowly. As a result, the plume spreads significantly. Compared to case 1, the plume’s shape is lost and its position in the aquifer is drastically different. Since the aquifer is anisotropic, plume spreading is predominantly in the horizontal plane, and very little in the vertical plane.

Table 4.8.1 Model parameters and inputs

Parameter	Case 1	Case 2
Geometric mean conductivity, K_g (m/day)	5	5
$\ln K$ variance	0.0	2.0
Correlation scale, λ_x (m)	NA	10
Correlation scale, λ_z (m)	NA	3
Porosity, n	0.3	0.3
Size of model (m)	200 x 100	200 x 100
Grid	251 x 126	251 x 126
Cell size, Δx (m)	0.8 x 0.8	0.8 x 0.8
Time step, Δt (days)	10	10

Table 4.8.2 Temporally varying boundary conditions

Time (days)	Left boundary (m)	Right boundary (m)
0	73	75
30	71.5	74
60	70	72.5
90	70	70
120	69	68
150	68.5	67.5
180	67.5	67
210	68	66.5
240	68.5	68
270	69.5	70

300	70.5	71
330	72	73
360	73	75

The model parameters and inputs are explained below:

- The mean conductivity values are 5 m/d for both cases.
- The $\ln K$ variance for case 1 is 0.0 and for case 2 it is 2.0.
- The horizontal correlation scale (λ_x), and vertical correlation scale (λ_z) is 10 m and 3 m respectively for case 2.
- The cell size, Δx , is selected such that the correlation scale, λ , is resolved. Typically, Δx is at least 3 to 4 times smaller than the correlation scale.
- The time step, Δt , is selected such that the temporal variability of head in the river is resolved. Since the variability is 30 days, a time step of 10 days is used.

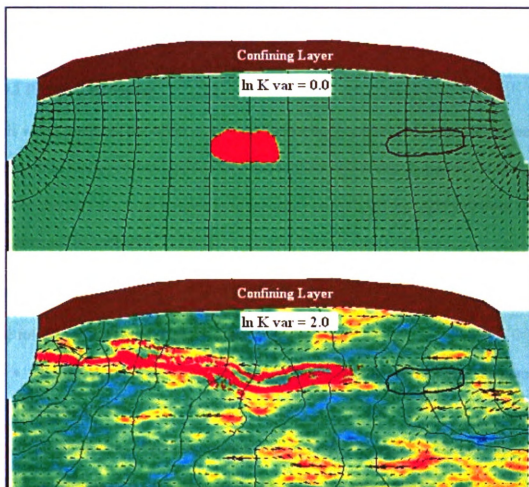


Figure 4.8 Snapshot of the visualization

For a detailed visualization, access the following address:

URL: <http://www.egr.msu.edu/igw/DL/SSH/TV/TV1.htm>

4.9 PLUME TRANSPORT - COMPARISON BETWEEN HETEROGENEOUS AQUIFERS WITH AND WITHOUT EQUILIBRIUM SORPTION

4.9.1 Problem statement

This video compares the effect of temporally varying boundary conditions on plume transport in heterogeneous aquifers with and without equilibrium sorption. The modeling domain consists of a time-variable head boundary on both left and right extremes. Details are provided in Table 4.9.

4.9.2 Key observations

The following observations can be made from the video:

- Temporally varying boundary conditions cause to and fro motion of the plume in the aquifers.
- In the absence of equilibrium sorption, the plume spreads significantly due to the interaction between spatial heterogeneity and temporal variability. The spreading of the plume is irreversible.
- In the presence of equilibrium sorption, the plume spreading is similar as above. However, the extent of the plume is smaller because of retardation.

4.9.3 Additional observations and discussion

Case 1: The geometric mean conductivity of the aquifer is 5 m/day. The temporally varying boundary conditions cause the head in the aquifer to fluctuate. As a result, the flow of groundwater changes direction, resulting in to and fro motion of the plume. Since the aquifer is heterogeneous, the to and fro motion of the plume is irreversible. When a part of the plume enters a low K zone, it is “trapped” and releases the contaminant

slowly. As a result, the plume spreads significantly. Since the aquifer is anisotropic, plume spreading is predominantly in the horizontal plane, and very little in the vertical plane.

Case 2: The geometric mean conductivity of the aquifer is 5 m/day. The temporally varying boundary conditions cause the head in the aquifer to fluctuate. As a result, the flow of groundwater changes direction, resulting in to and fro motion of the plume. Since the aquifer is heterogeneous, the to and fro motion of the plume is irreversible. Due to the presence of retardation in the form of sorption, when a part of the plume enters a low K zone, it is “trapped” and releases the contaminant extremely slowly. However, sorption is uniform throughout the aquifer; therefore, the velocity in the aquifer is lowered throughout. As a result, the plume spreading is lesser than in comparison to case 1. Since the aquifer is anisotropic, plume spreading is predominantly in the horizontal plane, and very little in the vertical plane. Compared to case 1, the plume’s size is slightly smaller.

Table 4.9.1 Model parameters and inputs

Parameter	Case 1	Case 2
Geometric mean conductivity, K_g (m/day)	5	5
$\ln K$ variance	2.0	2.0
Correlation scale, λ_x (m)	10	10
Correlation scale, λ_z (m)	3	3
Partitioning coefficient, K_d (kg/m ³)	0.0	10^{-7}
Porosity, n	0.3	0.3
Size of model (m)	200 x 100	200 x 100
Grid	251 x 126	251 x 126
Cell size, Δx (m)	0.8 x 0.8	0.8 x 0.8
Time step, Δt (days)	10	10

Table 4.9.2 Temporally varying boundary conditions

Time (days)	Left boundary (m)	Right boundary (m)
0	73	75
30	71.5	74
60	70	72.5
90	70	70
120	69	68
150	68.5	67.5
180	67.5	67
210	68	66.5
240	68.5	68
270	69.5	70
300	70.5	71
330	72	73
360	73	75

The model parameters and inputs are explained below:

- The average conductivity values are 5 m/d for both cases.
- The $\ln K$ variance is 2.0 and for both cases.
- The horizontal correlation scale (λ_x) and vertical correlation scale (λ_z), is 10 m and 3 m respectively for both cases.
- The partitioning coefficient is 0.0 for case 1 and 10^{-7} kg/m^3 for case 2.
- The cell size, Δx , is selected such that the correlation scale, λ , is resolved.
Typically, Δx is at least 3 to 4 times smaller than the correlation scale.
- The time step, Δt , is selected such that the temporal variability of head in the river is resolved. Since the variability is 30 days, a time step of 10 days is used.

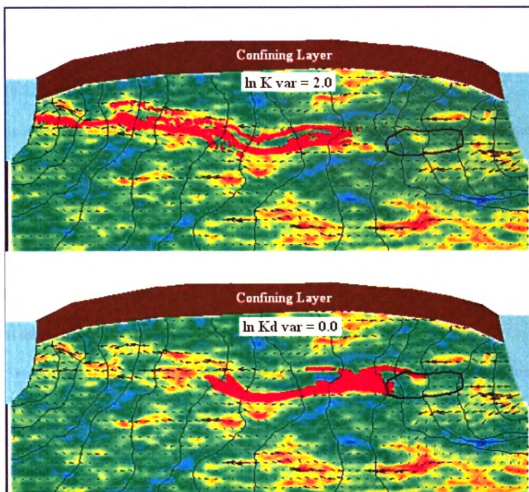


Figure 4.9 Snapshot of the visualization

For a detailed visualization, access the following address:

URL: <http://www.egr.msu.edu/igw/DL/SSH/TV/TV2.htm>

4.10 PLUME TRANSPORT - COMPARISON BETWEEN AQUIFERS WITH AND WITHOUT INTERACTING HETEROGENEITIES

4.10.1 Problem statement

This video compares the effect of temporally varying boundary conditions on plume transport in aquifers with and without interacting heterogeneities. The modeling domain consists of a time-variable head boundary on both left and right extremes. Details are provided in Table 4.10.

4.10.2 Key observations

The following observations can be made from the video:

- Temporally varying boundary conditions cause to and fro motion of the plume in the aquifers.
- Interaction between conductivity and partitioning coefficient heterogeneity in the presence of temporal variability does not have a significant impact on plume transport.

4.10.3 Additional observations and discussion

Case 1: The geometric mean conductivity of the aquifer is 5 m/day. The temporally varying boundary conditions cause the head in the aquifer to fluctuate. As a result, the flow of groundwater changes direction, resulting in to and fro motion of the plume. Since the aquifer is heterogeneous, the to and fro motion of the plume is irreversible. Due to the presence of retardation in the form of sorption, when a part of the plume enters a low K zone, it is “trapped” and releases the contaminant extremely slowly. However, sorption is

uniform throughout the aquifer; therefore, the velocity in the aquifer is lowered throughout.

Case 2: The geometric mean conductivity of the aquifer is 5 m/day. The temporally varying boundary conditions cause the head in the aquifer to fluctuate. As a result, the flow of groundwater changes direction, resulting in to and fro motion of the plume. Since the aquifer is heterogeneous, the to and fro motion of the plume is irreversible. Due to the presence of retardation in the form of sorption, when a part of the plume enters a low K zone, it is “trapped” and releases the contaminant extremely slowly. Since partitioning coefficient is negatively correlated with conductivity, the velocity in the low conductivity zones is lowered drastically. However, in the high conductivity zones, velocity is lowered by much less. As a result, velocity variability is effectively lesser in comparison to case 1; hence, the plume size is marginally larger in case 2.

Table 4.10.1 Model parameters and inputs

Parameter	Case 1	Case 2
Geometric mean conductivity, K_g (m/day)	5	5
ln K variance	2.0	2.0
Correlation scale, λ_x (m)	10	10
Correlation scale, λ_z (m)	3	3
Partitioning coefficient, K_d (kg/m ³)	10^{-7}	10^{-7}
Coefficient of variation – K_d and K	NA	2
Correlation - K_d and K	NA	Negative
Porosity, n	0.3	0.3
Size of model (m)	200 x 100	200 x 100
Grid	251 x 126	251 x 126
Cell size, Δx (m)	0.8 x 0.8	0.8 x 0.8
Time step, Δt (days)	10	10

Table 4.10.2 Temporally varying boundary conditions

Time (days)	Left boundary (m)	Right boundary (m)
0	73	75
30	71.5	74
60	70	72.5
90	70	70
120	69	68
150	68.5	67.5
180	67.5	67
210	68	66.5
240	68.5	68
270	69.5	70
300	70.5	71
330	72	73
360	73	75

The model parameters and inputs are explained below:

- The average conductivity values are 5 m/d for both cases.
- The $\ln K$ variance is 2.0 and for both cases.
- The horizontal correlation scale (λ_x) and vertical correlation scale (λ_z), is 10 m and 3 m respectively for both cases.
- The mean partitioning coefficient is 10^{-7} kg/m³ for both cases.
- The interaction between K_d and K is characterized by a coefficient of variation of 2.0 and a negative correlation.
- The cell size, Δx , is selected such that the correlation scale, λ , is resolved. Typically, Δx is at least 3 to 4 times smaller than the correlation scale.
- The time step, Δt , is selected such that the temporal variability of head in the river is resolved. Since the variability is 30 days, a time step of 10 days is used.

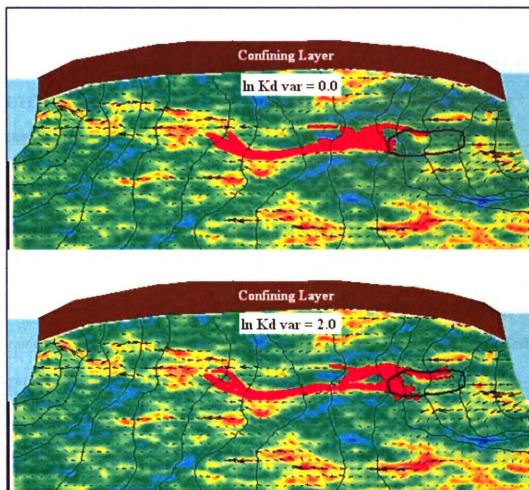


Figure 4.10 Snapshot of the visualization

For a detailed visualization, access the following address:

URL: <http://www.egr.msu.edu/igw/DL/SSH/TV/TV3.htm>

5 MACRODISPERSION

5.1 A MACRODISPERSION MODEL FOR PLUME MIGRATION IN WEAKLY HETEROGENEOUS MEDIA ($\ln K$ VARIANCE 0.5) WITH PORE-SCALE DISPERSION

5.1.1 Problem statement

This video compares two different modeling techniques to predict macrodispersion of a conservative solute plume in a weakly heterogeneous medium. The first technique employs a detailed description of spatial variability of conductivity using statistical parameters, and a pore-scale dispersion coefficient. The second technique uses Gelhar's asymptotic macrodispersion model (*Gelhar and Axness, 1983a*) that consists of a homogeneous medium and a macrodispersion coefficient. This video demonstrates the effectiveness of Gelhar's model in predicting plume spreading. The modeling domain consists of constant head boundaries on the left and right extremes, and no-flow boundaries at the top and bottom; the initial size of the plume is significantly larger than the correlation scale of heterogeneity. Details are provided in Table 5.1.

5.1.2 Key observations

The following observations can be made from the video:

- The macrodispersion model approximately predicts plume location and amount of spreading in both longitudinal and transverse directions.
- The macrodispersion model is unable to predict the irregular shape of the plume, and hence, the maximum concentration and degree of dilution.

Similar experiments with larger perturbations (higher $\ln K$ variance) are shown in subsequent videos.

5.1.3 Additional observations and discussion

Gelhar's macrodispersion model attempts to predict the large-scale spreading that occurs in a heterogeneous field. The underlying assumption for the macrodispersion model is that the conductivity perturbations in the heterogeneous field are small. These perturbations control plume spreading in the heterogeneous field. Longitudinal spreading in the heterogeneous field is greater than transverse spreading. The macrodispersion model predicts that the longitudinal spreading is directly proportional to the correlation scale of heterogeneity and the $\ln K$ variance, and transverse spreading is directly proportional to the pore-scale dispersivity and the $\ln K$ variance. Since the correlation scale is at least two orders of magnitudes larger than pore-scale dispersivity, longitudinal spreading is significantly larger than its transverse counterpart. Therefore, the macrodispersion model is able to predict the overall spreading of the plume approximately.

Since the macrodispersion model consists of a homogeneous medium, the plume obtained is always regular. As a result, the irregular shape of the plume seen in the heterogeneous field is not predicted. The irregular shape of the plume translates to irregular variations of concentration, which are also not predicted. Consequently, the macrodispersion model is unable to accurately predict the maximum concentration and the degree of dilution of the plume.

5.1.4 Mathematical interpretation

The following equations show the relationship between pore-scale dispersion and macrodispersion:

$$\frac{\partial C}{\partial t} + \frac{\partial u_i C}{\partial x_i} = \frac{\partial}{\partial x_i} \left(D_{ij} \frac{\partial C}{\partial x_j} \right), \quad (5.1.1)$$

$$\frac{\partial \bar{C}}{\partial t} + \frac{\partial \bar{u} \bar{C}}{\partial x_i} = \frac{\partial}{\partial x_i} \left(D_{ij} \frac{\partial \bar{C}}{\partial x_j} + \left(-\overline{u_i' C'} \right) \right), \quad (5.1.2)$$

where:

C – Concentration

u_i – Seepage velocity

D_{ij} – Dispersion coefficient.

It can be shown (*Gelhar and Axness, 1983a*) that:

$$-\overline{u_i' C'} \approx A_{ii} \bar{u} \frac{\partial \bar{C}}{\partial x_i}. \quad (5.1.3a)$$

The coefficient A_{ii} is called macrodispersivity and is given by (*Gelhar, 1993*):

$$A_{11} = \sigma_{\ln K}^2 \lambda; \quad A_{22} = \frac{\sigma_{\ln K}^2}{8} (\alpha_L + \alpha_T), \quad (5.1.3b)$$

where:

$\sigma_{\ln K}^2$ – $\ln K$ variance

λ – Correlation scale

A_{11} – Longitudinal macrodispersivity

A_{22} – Transverse macrodispersivity

α_L – Longitudinal dispersivity

α_T – Transverse dispersivity.

Equation (5.1.3b) shows that the longitudinal macrodispersion is unaffected by pore-scale dispersion, whereas transverse macrodispersion is affected. Therefore, the magnitude of longitudinal macrodispersion is many orders of magnitude larger than the transverse macrodispersion. Substituting (5.1.3a) into (5.1.2):

$$\frac{\partial \bar{C}}{\partial t} + \frac{\partial \bar{u} \bar{C}}{\partial x_i} = \frac{\partial}{\partial x_i} \left(D_{ij} \frac{\partial \bar{C}}{\partial x_j} + \left(A_{ij} \bar{u} \frac{\partial \bar{C}}{\partial x_i} \right) \right), \quad (5.1.4)$$

$$\frac{\partial \bar{C}}{\partial t} + \frac{\partial \bar{u} \bar{C}}{\partial t} = (\alpha_{ij} + A_{ij}) \bar{u} \frac{\partial \bar{C}}{\partial x_i}. \quad (5.1.5)$$

The pore-scale dispersivity, α_{ij} , is typically one-hundredth of a meter, while the macrodispersivity, A_{ij} , is approximately one meter. Therefore, macrodispersion is the dominant process and controls the total spreading of the plume.

Equation (5.1.5) simplifies the complex heterogeneous field, represented by (5.1.2). A simple mean macrodispersion model is obtained by replacing the dispersion coefficient with a macrodispersivity value. This model can predict the mean spreading of the plume.

Table 5.1 Model parameters and inputs

Parameter	Case 1	Case 2
Mean hydraulic conductivity, K_g (m/day)	10	10
$\ln K$ variance	0.5	0.0
Correlation scale, λ (m)	1	NA

Porosity, n	0.3	0.3
Longitudinal pore-scale dispersivity (m)	0.01	NA
Transverse pore-scale dispersivity (m)	0.001	NA
Longitudinal macrodispersivity (m)	NA	0.5
Transverse macrodispersivity (m)	NA	0.0008125
Head difference (m)	1	1
Size of model (m)	200 x 50	200 x 50
Covariance function	Exponential	Exponential
Approximate initial size of plume (m)	10	10
Grid	801 x 201	801 x 201
Cell size, Δx (m)	0.25 x 0.25	0.25 x 0.25
Time step, Δt (days)	1	1

The model parameters and inputs are explained below:

- The $\ln K$ field is a normally distributed random field. Therefore, there is an equal probability of the plume encountering a 'low' K zone or a 'high' K zone.
- The heterogeneous conductivity field is uniquely characterized by the following set of statistical parameters: geometric mean (K_g) of K , correlation scale, variance and covariance.
- The geometric mean, $\ln K$ variance and correlation scale are constant for both cases.
- The covariance function for both cases is exponential.
- Case 1 has longitudinal and transverse dispersivities of 0.01 m and 0.001 m respectively, while they do not apply to case 2. The corresponding macrodispersivities for case 2 are 0.5 m and 0.0008125 m.
- The cell size, Δx , is selected such that the correlation scale, λ , is resolved. Typically, Δx is at least 3 to 4 times smaller than the correlation scale.
- The time step, Δt , is selected such that a particle of the plume travels a distance that is less than λ in one time step.

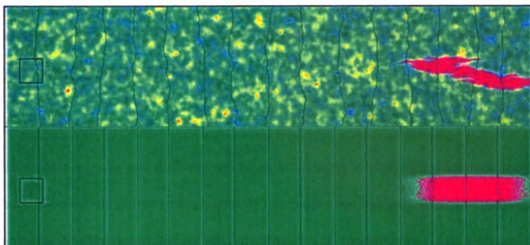


Figure 5.1 Snapshot of the visualization

For a detailed visualization, access the following address:

URL: <http://www.egr.msu.edu/igw/DL/SSH/SMM/SMM9.htm>

5.2 A MACRODISPERSION MODEL FOR PLUME MIGRATION IN MODERATELY HETEROGENEOUS MEDIA ($\ln K$ VARIANCE 1.0) WITH PORE-SCALE DISPERSION

5.2.1 Problem statement

This video compares two different modeling techniques to predict macrodispersion of a conservative solute plume in a moderately heterogeneous medium. The first technique employs a detailed description of spatial variability of conductivity using statistical parameters, and a pore-scale dispersion coefficient. The second technique uses Gelhar's asymptotic macrodispersion model (*Gelhar and Axness, 1983a*) that consists of a homogeneous medium and a macrodispersion coefficient. This video demonstrates the effectiveness of Gelhar's model in predicting plume spreading. The modeling domain consists of constant head boundaries on the left and right extremes, and no-flow boundaries at the top and bottom; the initial size of the plume is significantly larger than the correlation scale of heterogeneity. Details are provided in Table 5.2.

5.2.2 Key observations

The following observations can be made from the video:

- The macrodispersion model approximately predicts plume location and amount of spreading in both longitudinal and transverse directions.
- The macrodispersion model is unable to predict the irregular shape of the plume, and hence the maximum concentration and degree of dilution.

- In comparison to the previous experiment with weakly heterogeneous media, the effectiveness of the macrodispersion model in predicting plume spreading decreases.

Similar experiments with larger perturbations (higher $\ln K$ variance) are shown in subsequent videos.

5.2.3 Additional observations and discussion

Gelhar's macrodispersion model attempts to predict the large-scale spreading that occurs in a heterogeneous field. The underlying assumption for the macrodispersion model is that the conductivity perturbations in the heterogeneous field are small. These perturbations control plume spreading in the heterogeneous field. Longitudinal spreading in the heterogeneous field is greater than transverse spreading. The macrodispersion model predicts that the longitudinal spreading is directly proportional to the correlation scale of heterogeneity and the $\ln K$ variance, and transverse spreading is directly proportional to the pore-scale dispersivity and the $\ln K$ variance. Since the correlation scale is at least two orders of magnitudes larger than pore-scale dispersivity, longitudinal spreading is significantly larger than its transverse counterpart. Therefore, the macrodispersion model is able to predict the overall spreading of the plume approximately.

Since the macrodispersion model consists of a homogeneous medium, the plume obtained is always regular. As a result, the irregular shape of the plume seen in the heterogeneous field is not predicted. The irregular shape of the plume translates to irregular variations in

concentration, which are also not predicted. Consequently, the macrodispersion model is unable to accurately predict the maximum concentration and the degree of dilution of the plume.

In comparison to the previous video, where the $\ln K$ variance was 0.5, this macrodispersion model is not as accurate. Although the model captures the overall extent of the plume, the plume is more irregular, which is not captured by the macrodispersion model. Since a $\ln K$ variance of 1.0 can still be considered only moderately heterogeneous, the predictive ability of Gelhar's model is not seriously hampered.

5.2.4 Mathematical interpretation

The following equations show the relationship between pore-scale dispersion and macrodispersion:

$$\frac{\partial C}{\partial t} + \frac{\partial u_i C}{\partial x_i} = \frac{\partial}{\partial x_i} \left(D_{ij} \frac{\partial C}{\partial x_j} \right), \quad (5.2.1)$$

$$\frac{\partial \bar{C}}{\partial t} + \frac{\partial \bar{u} \bar{C}}{\partial x_i} = \frac{\partial}{\partial x_i} \left(D_{ij} \frac{\partial \bar{C}}{\partial x_j} + \left(-\overline{u_i' C'} \right) \right), \quad (5.2.2)$$

where:

C – Concentration

u_i – Seepage velocity

D_{ij} – Dispersion coefficient.

It can be shown (Gelhar and Axness, 1983a) that:

$$-\overline{u_i' C'} \approx A_{ii} \overline{u} \frac{\partial \overline{C}}{\partial x_i}. \quad (5.2.3a)$$

The coefficient A_{ii} is called macrodispersivity and is given by (Gelhar, 1993):

$$A_{11} = \sigma_{\ln K}^2 \lambda; \quad A_{22} = \frac{\sigma_{\ln K}^2}{8} (\alpha_L + \alpha_T), \quad (5.2.3b)$$

where:

$\sigma_{\ln K}^2$ – $\ln K$ variance

λ – Correlation scale

A_{11} – Longitudinal macrodispersivity

A_{22} – Transverse macrodispersivity

α_L – Longitudinal dispersivity

α_T – Transverse dispersivity.

Equation (5.2.3b) shows that the longitudinal macrodispersion is unaffected by pore-scale dispersion, whereas transverse macrodispersion is affected. Therefore, the magnitude of longitudinal macrodispersion is many orders of magnitude larger than the transverse macrodispersion. Substituting (5.2.3a) into (5.2.2):

$$\frac{\partial \overline{C}}{\partial t} + \frac{\partial \overline{u C}}{\partial x_i} = \frac{\partial}{\partial x_i} \left(D_{ij} \frac{\partial \overline{C}}{\partial x_j} + \left(A_{ii} \overline{u} \frac{\partial \overline{C}}{\partial x_i} \right) \right), \quad (5.2.4)$$

$$\frac{\partial \overline{C}}{\partial t} + \frac{\partial \overline{u C}}{\partial t} = (\alpha_{ij} + A_{ij}) \overline{u} \frac{\partial \overline{C}}{\partial x_i}. \quad (4.2.5)$$

The pore-scale dispersivity, α_{ij} , is typically one-hundredth of a meter, while the macrodispersivity, A_{ij} , is approximately one meter. Therefore, macrodispersion is the dominant process and controls the total spreading of the plume.

Equation (5.2.5) simplifies the complex heterogeneous field, represented by (5.2.2). A simple mean macrodispersion model is obtained by replacing the dispersion coefficient with a macrodispersivity value. This model can predict the mean spreading of the plume.

Table 5.2 Model parameters and inputs

Parameter	Case 1	Case 2
Mean hydraulic conductivity, K_g (m/day)	10	10
$\ln K$ variance	1.0	0.0
Correlation scale, λ (m)	1	NA
Porosity, n	0.3	0.3
Longitudinal pore-scale dispersivity (m)	0.01	NA
Transverse pore-scale dispersivity (m)	0.001	NA
Longitudinal macrodispersivity (m)	NA	1.0
Transverse macrodispersivity (m)	NA	0.001625
Head difference (m)	1	1
Size of model (m)	200 x 50	200 x 50
Covariance function	Exponential	Exponential
Approximate initial size of plume (m)	10	10
Grid	801 x 201	801 x 201
Cell size, Δx (m)	0.25 x 0.25	0.25 x 0.25
Time step, Δt (days)	1	1

The model parameters and inputs are explained below:

- The $\ln K$ field is a normally distributed random field. Therefore, there is an equal probability of the plume encountering a 'low' K zone or a 'high' K zone.

- The heterogeneous conductivity field is uniquely characterized by the following set of statistical parameters: geometric mean (K_g) of K , correlation scale, variance and covariance.
- The geometric mean, $\ln K$ variance and correlation scale are constant for both cases.
- The covariance function for both cases is exponential.
- Case 1 has longitudinal and transverse dispersivities of 0.01 m and 0.001 m respectively, while they do not apply to case 2. The corresponding macrodispersivities for case 2 are 1.0 m and 0.001625 m.
- The cell size, Δx , is selected such that the correlation scale, λ , is resolved. Typically, Δx is at least 3 to 4 times smaller than the correlation scale.
- The time step, Δt , is selected such that a particle of the plume travels a distance that is less than λ in one time step.

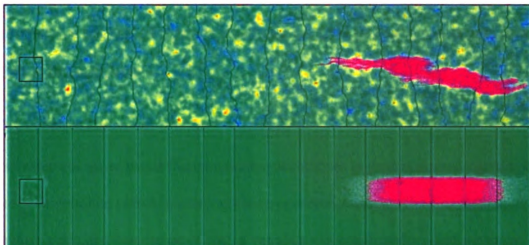


Figure 5.2 Snapshot of the visualization

For a detailed visualization, access the following address:

URL: <http://www.egr.msu.edu/igw/DL/SSH/SMM/SMM10.htm>

5.3 A MACRODISPERSION MODEL FOR PLUME MIGRATION IN STRONGLY HETEROGENEOUS MEDIA ($\ln K$ VARIANCE 2.0) WITH PORE-SCALE DISPERSION

5.3.1 Problem statement

This video compares two different modeling techniques to predict macrodispersion of a conservative solute plume in a strongly heterogeneous medium. The first technique employs a detailed description of spatial variability of conductivity using statistical parameters, and a pore-scale dispersion coefficient. The second technique uses Gelhar's asymptotic macrodispersion model (*Gelhar and Axness, 1983a*) that consists of a homogeneous medium and a macrodispersion coefficient. This video demonstrates the effectiveness of Gelhar's model in predicting plume spreading. The modeling domain consists of constant head boundaries on the left and right extremes, and no-flow boundaries at the top and bottom; the initial size of the plume is significantly larger than the correlation scale of heterogeneity. Details are provided in Table 5.3.

5.3.2 Key observations

The following observations can be made from the video:

- The macrodispersion model approximately predicts plume location and underestimates the amount of spreading in both longitudinal and transverse directions.
- The macrodispersion model is unable to predict the irregular shape of the plume, and hence the maximum concentration and degree of dilution.

- In comparison to previous experiments with weakly and moderately heterogeneous media, the effectiveness of the macrodispersion model in predicting plume spreading decreases drastically.

5.3.3 Additional observations and discussion

Gelhar's macrodispersion model attempts to predict the large-scale spreading that occurs in a heterogeneous field. The underlying assumption for the macrodispersion model is that the conductivity perturbations in the heterogeneous field are small. These perturbations control plume spreading in the heterogeneous field. Longitudinal spreading in the heterogeneous field is greater than transverse spreading. The macrodispersion model predicts that the longitudinal spreading is directly proportional to the correlation scale of heterogeneity and the $\ln K$ variance, and transverse spreading is directly proportional to the pore-scale dispersivity and the $\ln K$ variance. Since the correlation scale is at least two orders of magnitudes larger than pore-scale dispersivity, longitudinal spreading is significantly larger than its transverse counterpart. Therefore, the macrodispersion model is able to predict the overall spreading of the plume approximately.

Since the macrodispersion model consists of a homogeneous medium, the plume obtained is always regular. As a result, the irregular shape of the plume seen in the heterogeneous field is not predicted. The irregular shape of the plume translates to irregular variations in concentration, which are also not predicted. Consequently, the macrodispersion model is unable to accurately predict the maximum concentration and the degree of dilution of the plume.

In comparison to the previous video, where the $\ln K$ variance was 1.0, this macrodispersion model is not as accurate. Although the model captures the overall extent of the plume, the plume is more irregular, which is not captured by the macrodispersion model. The $\ln K$ variance of 2.0 is considered strongly heterogeneous; the predictive ability of Gelhar's model is hampered.

5.3.4 Mathematical interpretation

The following equations show the relationship between pore-scale dispersion and macrodispersion:

$$\frac{\partial C}{\partial t} + \frac{\partial u_i C}{\partial x_i} = \frac{\partial}{\partial x_i} \left(D_{ij} \frac{\partial C}{\partial x_j} \right), \quad (5.3.1)$$

$$\frac{\partial \bar{C}}{\partial t} + \frac{\partial \bar{u} \bar{C}}{\partial x_i} = \frac{\partial}{\partial x_i} \left(D_{ij} \frac{\partial \bar{C}}{\partial x_j} + \left(-\overline{u_i C'} \right) \right), \quad (5.3.2)$$

where:

C – Concentration

u_i – Seepage velocity

D_{ij} – Dispersion coefficient.

It can be shown (*Gelhar and Axness, 1983a*) that:

$$-\overline{u_i C'} \approx A_{ii} \bar{u} \frac{\partial \bar{C}}{\partial x_i}. \quad (5.3.3a)$$

The coefficient A_{ii} is called macrodispersivity and is given by (*Gelhar, 1993*):

$$A_{11} = \sigma_{\ln K}^2 \lambda; \quad A_{22} = \frac{\sigma_{\ln K}^2}{8} (\alpha_L + \alpha_T), \quad (5.3.3b)$$

where:

$\sigma_{\ln K}^2$ – $\ln K$ variance

λ – Correlation scale

A_{11} – Longitudinal macrodispersivity

A_{22} – Transverse macrodispersivity

α_L – Longitudinal dispersivity

α_T – Transverse dispersivity.

Equation (5.3.3b) shows that the longitudinal macrodispersion is unaffected by pore-scale dispersion, whereas transverse macrodispersion is affected. Therefore, the magnitude of longitudinal macrodispersion is many orders of magnitude larger than the transverse macrodispersion. Substituting (5.3.3a) into (5.3.2):

$$\frac{\partial \bar{C}}{\partial t} + \frac{\partial \bar{u} \bar{C}}{\partial x_i} = \frac{\partial}{\partial x_i} \left(D_{ij} \frac{\partial \bar{C}}{\partial x_j} + \left(A_{ij} \bar{u} \frac{\partial \bar{C}}{\partial x_i} \right) \right), \quad (5.3.4)$$

$$\frac{\partial \bar{C}}{\partial t} + \frac{\partial \bar{u} \bar{C}}{\partial t} = (\alpha_{ij} + A_{ij}) \bar{u} \frac{\partial \bar{C}}{\partial x_i}. \quad (5.3.5)$$

The pore-scale dispersivity, α_{ij} , is typically one-hundredth of a meter, while the macrodispersivity, A_{ij} , is approximately one meter. Therefore, macrodispersion is the dominant process and controls the total spreading of the plume.

Equation (5.3.5) simplifies the complex heterogeneous field, represented by (5.3.2). A simple mean macrodispersion model is obtained by replacing the dispersion coefficient with a macrodispersivity value. This model can predict the mean spreading of the plume.

Table 5.3 Model parameters and inputs

Parameter	Case 1	Case 2
Mean hydraulic conductivity, K_g (m/day)	10	10
$\ln K$ variance	2.0	0.0
Correlation scale, λ (m)	1	NA
Porosity, n	0.3	0.3
Longitudinal pore-scale dispersivity (m)	0.01	NA
Transverse pore-scale dispersivity (m)	0.001	NA
Longitudinal macrodispersivity (m)	NA	2.0
Transverse macrodispersivity (m)	NA	0.00325
Head difference (m)	1	1
Size of model (m)	200 x 50	200 x 50
Covariance function	Exponential	Exponential
Approximate initial size of plume (m)	10	10
Grid	801 x 201	801 x 201
Cell size, Δx (m)	0.25 x 0.25	0.25 x 0.25
Time step, Δt (days)	1	1

The model parameters and inputs are explained below:

- The $\ln K$ field is a normally distributed random field. Therefore, there is an equal probability of the plume encountering a ‘low’ K zone or a ‘high’ K zone.
- The heterogeneous conductivity field is uniquely characterized by the following set of statistical parameters: geometric mean (K_g) of K , correlation scale, variance and covariance.
- The geometric mean, $\ln K$ variance and correlation scale are constant for both cases.
- The covariance function for both cases is exponential.

- Case 1 has longitudinal and transverse dispersivities of 0.01 m and 0.001 m respectively, while they do not apply to case 2. The corresponding macrodispersivities for case 2 are 2.0 m and 0.00325 m.
- The cell size, Δx , is selected such that the correlation scale, λ , is resolved. Typically, Δx is at least 3 to 4 times smaller than the correlation scale.
- The time step, Δt , is selected such that a particle of the plume travels a distance that is less than λ in one time step.

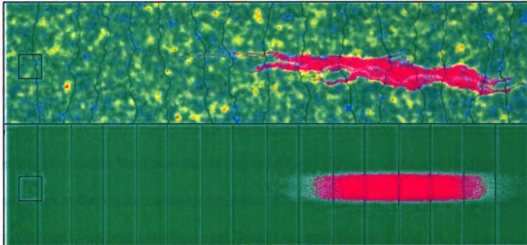


Figure 5.3 Snapshot of the visualization

For a detailed visualization, access the following address:

URL: <http://www.egr.msu.edu/igw/DL/SSH/SMM/SMM11.htm>

5.4 A MACRODISPERSION MODEL FOR PLUME MIGRATION IN VERY STRONGLY HETEROGENEOUS MEDIA ($\ln K$ VARIANCE 4.0) WITH PORE-SCALE DISPERSION

5.4.1 Problem statement

This video compares two different modeling techniques to predict macrodispersion of a conservative solute plume in a very strongly heterogeneous medium. The first technique employs a detailed description of spatial variability of conductivity using statistical parameters, and a pore-scale dispersion coefficient. The second technique uses Gelhar's asymptotic macrodispersion model (*Gelhar and Axness, 1983a*) that consists of a homogeneous medium and a macrodispersion coefficient. This video demonstrates the effectiveness of Gelhar's model in predicting plume spreading. The modeling domain consists of constant head boundaries on the left and right extremes, and no-flow boundaries at the top and bottom; the initial size of the plume is significantly larger than the correlation scale of heterogeneity. Details are provided in Table 5.4.

5.4.2 Key observations

The following observations can be made from the video:

- The macrodispersion model approximately predicts plume location and significantly underestimates the amount of spreading in both longitudinal and transverse directions.
- The macrodispersion model is unable to predict the irregular shape of the plume, and hence the maximum concentration and degree of dilution.

- In comparison to previous experiments with weakly, moderately and strongly heterogeneous media, the effectiveness of the macrodispersion model in predicting plume spreading decreases drastically.

5.4.3 Additional observations and discussion

Gelhar's macrodispersion model attempts to predict the large-scale spreading that occurs in a heterogeneous field. The underlying assumption for the macrodispersion model is that the conductivity perturbations in the heterogeneous field are small. These perturbations control plume spreading in the heterogeneous field. Longitudinal spreading in the heterogeneous field is greater than transverse spreading. The macrodispersion model predicts that the longitudinal spreading is directly proportional to the correlation scale of heterogeneity and the $\ln K$ variance, and transverse spreading is directly proportional to the pore-scale dispersivity and the $\ln K$ variance. Since the correlation scale is at least two orders of magnitudes larger than pore-scale dispersivity, longitudinal spreading is significantly larger than its transverse counterpart. Therefore, the macrodispersion model is able to predict the overall spreading of the plume approximately.

Since the macrodispersion model consists of a homogeneous medium, the plume obtained is always regular. As a result, the irregular shape of the plume seen in the heterogeneous field is not predicted. The irregular shape of the plume translates to irregular variations in concentration, which are also not predicted. Consequently, the macrodispersion model is unable to accurately predict the maximum concentration and the degree of dilution of the plume.

In comparison to the previous video, where the $\ln K$ variance was 2.0, this macrodispersion model is not as accurate. Although the model captures the overall extent of the plume, the plume is more irregular, which is not captured by the macrodispersion model. The $\ln K$ variance of 4.0 is considered very strongly heterogeneous; the predictive ability of Gelhar's model is seriously hampered.

5.4.4 Mathematical interpretation

The following equations show the relationship between pore-scale dispersion and macrodispersion:

$$\frac{\partial C}{\partial t} + \frac{\partial u_i C}{\partial x_i} = \frac{\partial}{\partial x_i} \left(D_{ij} \frac{\partial C}{\partial x_j} \right), \quad (5.4.1)$$

$$\frac{\partial \bar{C}}{\partial t} + \frac{\partial \bar{u} \bar{C}}{\partial x_i} = \frac{\partial}{\partial x_i} \left(D_{ij} \frac{\partial \bar{C}}{\partial x_j} + \left(-\overline{u_i' C'} \right) \right), \quad (5.4.2)$$

where:

C – Concentration

u_i – Seepage velocity

D_{ij} – Dispersion coefficient.

It can be shown (Gelhar and Axness, 1983a) that:

$$-\overline{u_i' C'} \approx A_{ii} \bar{u} \frac{\partial \bar{C}}{\partial x_i}. \quad (5.4.3a)$$

The coefficient A_{ii} is called macrodispersivity and is given by (Gelhar, 1993):

$$A_{11} = \sigma_{\ln K}^2 \lambda; \quad A_{22} = \frac{\sigma_{\ln K}^2}{8} (\alpha_L + \alpha_T), \quad (5.4.3b)$$

where:

$\sigma_{\ln K}^2$ – $\ln K$ variance

λ – Correlation scale

A_{11} – Longitudinal macrodispersivity

A_{22} – Transverse macrodispersivity

α_L – Longitudinal dispersivity

α_T – Transverse dispersivity.

Equation (5.4.3b) shows that the longitudinal macrodispersion is unaffected by pore-scale dispersion, whereas transverse macrodispersion is affected. Therefore, the magnitude of longitudinal macrodispersion is many orders of magnitude larger than the transverse macrodispersion. Substituting (5.4.3a) into (5.4.2):

$$\frac{\partial \bar{C}}{\partial t} + \frac{\partial \bar{u} \bar{C}}{\partial x_i} = \frac{\partial}{\partial x_i} \left(D_{ij} \frac{\partial \bar{C}}{\partial x_j} + \left(A_{ii} \bar{u} \frac{\partial \bar{C}}{\partial x_i} \right) \right), \quad (5.4.4)$$

$$\frac{\partial \bar{C}}{\partial t} + \frac{\partial \bar{u} \bar{C}}{\partial t} = (\alpha_{ij} + A_{ij}) \bar{u} \frac{\partial \bar{C}}{\partial x_i}. \quad (5.4.5)$$

The pore-scale dispersivity, α_{ij} , is typically one-hundredth of a meter, while the macrodispersivity, A_{ij} , is approximately one meter. Therefore, macrodispersion is the dominant process and controls the total spreading of the plume.

Equation (5.4.5) simplifies the complex heterogeneous field, represented by (5.4.2). A simple mean macrodispersion model is obtained by replacing the dispersion coefficient with a macrodispersivity value. This model can predict the mean spreading of the plume.

Table 5.4 Model parameters and inputs

Parameter	Case 1	Case 2
Mean hydraulic conductivity, K_g (m/day)	10	10
$\ln K$ variance	4.0	0.0
Correlation scale, λ (m)	1	NA
Porosity, n	0.3	0.3
Longitudinal pore-scale dispersivity (m)	0.01	NA
Transverse pore-scale dispersivity (m)	0.001	NA
Longitudinal macrodispersivity (m)	NA	4.0
Transverse macrodispersivity (m)	NA	0.0065
Head difference (m)	1	1
Size of model (m)	200 x 50	200 x 50
Covariance function	Exponential	Exponential
Approximate initial size of plume (m)	10	10
Grid	801 x 201	801 x 201
Cell size, Δx (m)	0.25 x 0.25	0.25 x 0.25
Time step, Δt (days)	1	1

The model parameters and inputs are explained below:

- The $\ln K$ field is a normally distributed random field. Therefore, there is an equal probability of the plume encountering a 'low' K zone or a 'high' K zone.
- The heterogeneous conductivity field is uniquely characterized by the following set of statistical parameters: geometric mean (K_g) of K , correlation scale, variance and covariance.
- The geometric mean, $\ln K$ variance and correlation scale are constant for both cases.
- The covariance function for both cases is exponential.

- Case 1 has longitudinal and transverse dispersivities of 0.01 m and 0.001 m respectively, while they do not apply to case 2. The corresponding macrodispersivities for case 2 are 4.0 m and 0.0065 m.
- The cell size, Δx , is selected such that the correlation scale, λ , is resolved. Typically, Δx is at least 3 to 4 times smaller than the correlation scale.
- The time step, Δt , is selected such that a particle of the plume travels a distance that is less than λ in one time step.

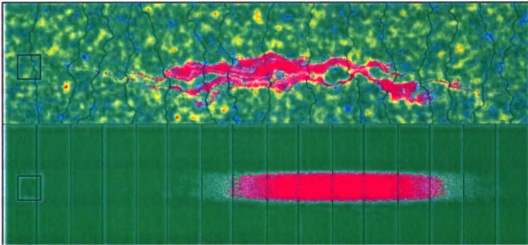


Figure 5.4 Snapshot of the visualization

For a detailed visualization, access the following address:

URL: <http://www.egr.msu.edu/igw/DL/SSH/SMM/SMM12.htm>

5.5 A MACRODISPERSION MODEL FOR PLUME MIGRATION IN STRONGLY HETEROGENEOUS MEDIA ($\ln K$ VARIANCE 2.0) WITHOUT PORE-SCALE DISPERSION

5.5.1 Problem statement

This video compares two different modeling techniques to predict macrodispersion of a conservative solute plume in a strongly heterogeneous medium without pore-scale dispersion. The first technique employs a detailed description of spatial variability of conductivity using statistical parameters. The second technique uses Gelhar's asymptotic macrodispersion model (*Gelhar and Axness, 1983a*) that consists of a homogeneous medium and a macrodispersion coefficient. This video demonstrates the effectiveness of Gelhar's model in predicting plume spreading. The modeling domain consists of constant head boundaries on the left and right extremes, and no-flow boundaries at the top and bottom; the initial size of the plume is significantly larger than the correlation scale of heterogeneity. Details are provided in Table 5.5.

5.5.2 Key observations

The following observations can be made from the video:

- The macrodispersion model approximately predicts plume location but underestimates the amount of spreading in the longitudinal direction.
- The macrodispersion model predicts that there will be no transverse spreading, contrary to the heterogeneous model.
- The macrodispersion model is unable to predict the irregular shape of the plume, and hence the maximum concentration and degree of dilution.

- In comparison to the macrodispersion model in 4.3, the effectiveness of this macrodispersion model in predicting transverse spreading decreases.

5.5.3 Additional observations and discussion

Gelhar's macrodispersion model attempts to predict the large-scale spreading that occurs in a heterogeneous field. The underlying assumption for the macrodispersion model is that the conductivity perturbations in the heterogeneous field are small. These perturbations control plume spreading in the heterogeneous field. Longitudinal spreading in the heterogeneous field is greater than transverse spreading. The macrodispersion model predicts that the longitudinal spreading is directly proportional to the correlation scale of heterogeneity and the $\ln K$ variance, and transverse spreading is directly proportional to the pore-scale dispersivity and the $\ln K$ variance. Since there is no pore-scale dispersivity, the macrodispersion model predicts that there will be no transverse spreading. Since the transverse spreading in the heterogeneous model is not significant, compared to longitudinal spreading, the macrodispersion model is able to predict the overall spreading of the plume approximately.

Since the macrodispersion model consists of a homogeneous medium, the plume obtained is always regular. As a result, the irregular shape of the plume seen in the heterogeneous field is not predicted. The irregular shape of the plume translates to irregular variations in concentration, which are also not predicted. Consequently, the macrodispersion model is unable to accurately predict the maximum concentration and the degree of dilution of the plume.

Although the model captures the overall extent of the plume, the peaks and valleys are sharp, which is not accurately captured by the macrodispersion model. In the absence of pore-scale dispersion, Gelhar's model loses the ability to predict transverse spreading. Despite this limitation, the overall predictive ability is not seriously hampered.

5.5.4 Mathematical interpretation

The following equations show the relationship between pore-scale dispersion and macrodispersion:

$$\frac{\partial C}{\partial t} + \frac{\partial u_i C}{\partial x_i} = \frac{\partial}{\partial x_i} \left(D_{ij} \frac{\partial C}{\partial x_j} \right), \quad (5.5.1)$$

$$\frac{\partial \bar{C}}{\partial t} + \frac{\partial \bar{u} \bar{C}}{\partial x_i} = \frac{\partial}{\partial x_i} \left(D_{ij} \frac{\partial \bar{C}}{\partial x_j} + \left(-\overline{u_i' C'} \right) \right), \quad (5.5.2)$$

where:

C – Concentration

u_i – Seepage velocity

D_{ij} – Dispersion coefficient.

It can be shown (Gelhar and Axness, 1983a) that:

$$-\overline{u_i' C'} \approx A_{ii} u \frac{\partial \bar{C}}{\partial x_i}. \quad (5.5.3a)$$

The coefficient A_{ii} is called macrodispersivity and is given by (Gelhar, 1993):

$$A_{11} = \sigma_{\ln K}^2 \lambda; \quad A_{22} = \frac{\sigma_{\ln K}^2}{8} (\alpha_L + \alpha_T), \quad (5.5.3b)$$

where:

$\sigma_{\ln K}^2$ – $\ln K$ variance

λ – Correlation scale

A_{11} – Longitudinal macrodispersivity

A_{22} – Transverse macrodispersivity

α_L – Longitudinal dispersivity

α_T – Transverse dispersivity.

Equation (5.5.3b) shows that the longitudinal macrodispersion is unaffected by pore-scale dispersion, whereas transverse macrodispersion is affected. Therefore, the magnitude of longitudinal macrodispersion is many orders of magnitude larger than the transverse macrodispersion. Substituting (45.5.3a) into (5.5.2):

$$\frac{\partial \bar{C}}{\partial t} + \frac{\partial \bar{u} \bar{C}}{\partial x_i} = \frac{\partial}{\partial x_i} \left(D_{ij} \frac{\partial \bar{C}}{\partial x_j} + \left(A_{ij} \bar{u} \frac{\partial \bar{C}}{\partial x_i} \right) \right), \quad (5.5.4)$$

$$\frac{\partial \bar{C}}{\partial t} + \frac{\partial \bar{u} \bar{C}}{\partial t} = (\alpha_{ij} + A_{ij}) \bar{u} \frac{\partial \bar{C}}{\partial x_i}. \quad (5.5.5)$$

The pore-scale dispersivity, α_{ij} , is typically one-hundredth of a meter, while the macrodispersivity, A_{ij} , is approximately one meter. Therefore, macrodispersion is the dominant process and controls the total spreading of the plume.

Equation (5.5.5) simplifies the complex heterogeneous field, represented by (5.5.2). A simple mean macrodispersion model is obtained by replacing the dispersion coefficient with a macrodispersivity value. This model can predict the mean spreading of the plume.

Table 5.5 Model parameters and inputs

Parameter	Case 1	Case 2
Mean hydraulic conductivity, K_g (m/day)	10	10
$\ln K$ variance	2.0	0.0
Correlation scale, λ (m)	1	NA
Porosity, n	0.3	0.3
Longitudinal pore-scale dispersivity (m)	0	NA
Transverse pore-scale dispersivity (m)	0	NA
Longitudinal macrodispersivity (m)	NA	2.0
Transverse macrodispersivity (m)	NA	0.0
Head difference (m)	1	1
Size of model (m)	200 x 50	200 x 50
Covariance function	Exponential	Exponential
Approximate initial size of plume (m)	10	10
Grid	801 x 201	801 x 201
Cell size, Δx (m)	0.25 x 0.25	0.25 x 0.25
Time step, Δt (days)	1	1

The model parameters and inputs are explained below:

- The $\ln K$ field is a normally distributed random field. Therefore, there is an equal probability of the plume encountering a ‘low’ K zone or a ‘high’ K zone.
- The heterogeneous conductivity field is uniquely characterized by the following set of statistical parameters: geometric mean (K_g) of K , correlation scale, variance and covariance.
- The geometric mean, $\ln K$ variance and correlation scale are constant for both cases.
- The covariance function for both cases is exponential.
- Cases 1 and 2 do not have longitudinal and transverse pore-scale dispersivities.

The macrodispersivities for case 2 are 2.0 m and 0.0 m.

- The cell size, Δx , is selected such that the correlation scale, λ , is resolved.
Typically, Δx is at least 3 to 4 times smaller than the correlation scale.
- The time step, Δt , is selected such that a particle of the plume travels a distance that is less than λ in one time step.

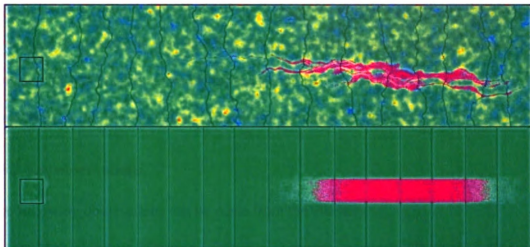


Figure 5.5 Snapshot of the visualization

For a detailed visualization, access the following address:

URL: <http://www.egr.msu.edu/igw/DL/SSH/SMM/SMM13.htm>

6 EFFECTS OF MULTI-SCALE HETEROGENEITY

6.1 EFFECTS OF MULTIPLE SCALES OF HETEROGENEITY

6.1.1 Problem statement

This video demonstrates the effects of multiple scales of heterogeneity, in the absence of pore-scale dispersion, on the spreading of a conservative solute plume. The modeling domain consists of constant head boundaries on the left and right extremes, and no-flow boundaries at the top and bottom. Details are provided in Table 6.1.

6.1.2 Key observations

The following observations can be made from the video:

- Multiple scales of heterogeneity have a drastic impact on plume spreading.
- In case 1, the scale of heterogeneity is much larger than the initial size of the plume. As a result, the plume does not encounter all the heterogeneity, and hence does not spread greatly.
- In case 2, two large scales of heterogeneity are modeled, the smallest scale of heterogeneity is larger than the initial size of the plume. Plume spreading is enhanced in comparison to case 1, though not significantly, because the plume does not encounter all of the heterogeneity.
- In case 3, three scales of heterogeneity are modeled, plume spreading is considerably enhanced. Since the smallest scale of heterogeneity is smaller than the initial size of the plume, the plume encounters all the heterogeneity and hence the spreading is increased.

- Mean plume displacement, for this particular realization, increased as more scales of heterogeneity were modeled.

6.1.3 Additional observations and discussion

Case 1: The correlation scale of heterogeneity is 500 m, which is much larger than the initial size of the plume; therefore the plume does not spread greatly. In such cases, the $\ln K$ realization is an important factor that controls plume migration.

Case 2: The correlation scales of heterogeneity in the first and second scales are 500 m and 100 m respectively. The initial size of the plume is of the order of 100 m. The plume does not exhibit detailed fingers and tails. However, in comparison to case 1, spreading is increased. The mean plume displacement is greater than in case 1, because the plume encounters more preferential paths (high velocity channels).

Case 3: The correlation scales of heterogeneity in the first, second and third scales are 500 m, 100 m, and 10 m respectively. The third scale is smaller than the initial size of the plume; most of the heterogeneity is encountered, and thus plume spreading is greatly enhanced. The mean displacement is greater than in cases 1 and 2, because the plume encounters more preferential paths (high velocity channels).

A comparison of the three cases shows that increasing the number of scales of heterogeneity increases plume spreading. Eliminating smaller scales of heterogeneity from the model underestimates plume spreading. Incorporating smaller scales requires higher-resolution data, which is costly, and perhaps infeasible. When only larger scales are modeled, the detailed structure of the aquifer represented by the smaller scales of

heterogeneity is averaged. In this process of averaging, considerable amount of detail is lost. These details are critical, and make a huge difference in the prediction of plume spreading.

Table 6.1 Model parameters and inputs

Parameter	Case 1	Case 2	Case 3
Geometric mean hydraulic conductivity, K_g (m/day)	10	10	10
$\ln K$ variance (for all scales)	1.0	1.0	1.0
Scale 1 correlation scale, λ (m)	500	500	500
Scale 2 correlation scale, λ (m)	-	100	100
Scale 3 correlation scale, λ (m)	-	-	10
Porosity, n	0.3	0.3	0.3
Pore-scale dispersivity	0	0	0
Head difference (m)	1	1	1
Size of model (m)	2000 x 500	2000 x 500	2000 x 500
Covariance function	Gaussian	Gaussian	Gaussian
Approximate initial plume size (m)	100	100	100
Grid	801 x 201	801 x 201	801 x 201
Cell size, Δx (m)	2.5 x 2.5	2.5 x 2.5	2.5 x 2.5
Time step, Δt (days)	100	100	100

The model parameters and inputs are explained below:

- The $\ln K$ field is a normally distributed random field. Therefore, there is an equal probability of the plume encountering a 'low' K zone or a 'high' K zone.
- The heterogeneous conductivity field is uniquely characterized by the following set of statistical parameters: geometric mean (K_g) of K , correlation scale, variance and covariance.
- The geometric mean and $\ln K$ variance are constant for all cases.
- The first scale of heterogeneity is common to all cases, and has a correlation scale of 500 m.

- The second scale of heterogeneity is applicable only to cases 2 and 3, and has a correlation scale of 100 m.
- The third scale of heterogeneity is applicable only to cases 2 and 3, and has a correlation scale of 10 m.
- The covariance function for all cases is Gaussian.
- The cell size, Δx , is selected such that the correlation scale, λ , is resolved. Typically, Δx is at least 3 to 4 times smaller than the correlation scale.
- The time step, Δt , is selected such that a particle of the plume travels a distance that is less than λ in one time step.

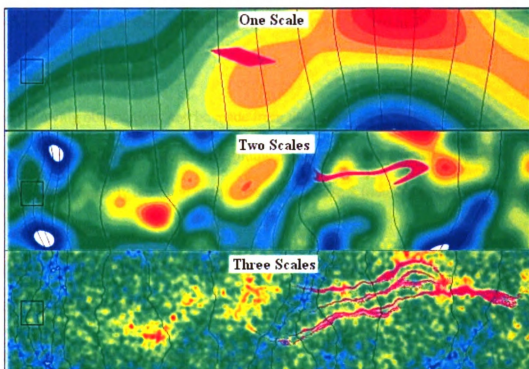


Figure 6.1 Snapshot of the visualization

For a detailed visualization, access the following address:

URL: <http://www.egr.msu.edu/igw/DL/SSH/SDT/SDT1.htm>

6.2 MACRODISPERSION IN THE PRESENCE OF MULTIPLE SCALES OF HETEROGENEITY

6.2.1 Problem statement

This video compares the spreading of a conservative solute plume in $\ln K$ fields where two different methods of representing the small-scale heterogeneity have been employed; the large scale heterogeneities in both fields are identical. In case 1, the small-scale heterogeneity is represented using equivalent macrodispersivities; in case 2, the small-scale heterogeneity is modeled using a random field with pore-scale dispersivities. The modeling domain consists of constant head boundaries on the left and right extremes, and no-flow boundaries at the top and bottom. Details are provided in Table 6.2.

6.2.2 Key observations

The following observations can be made from the video:

- The position and extent of the plume predicted in case 1 (macrodispersion) is approximately the same as that observed in case 2 (random field with pore-scale dispersion).
- The macrodispersion model smoothes the detailed interior structure of the plume observed in case 2.

6.2.3 Additional observations and discussion

Case 1: The small scale of heterogeneity is represented by equivalent macrodispersivities ($A_{11} = 10$ m, $A_{22} = 0.001625$ m) using Gelhar's asymptotic macrodispersion model that is discussed in detail in the next section. The correlation scales (λ) of heterogeneity of the

large scales are 500 m and 100 m respectively. The initial size of the plume is of the order of 100 m.

Case 2: The small scale of heterogeneity is represented by a random field model ($\ln K$ variance = 1.0, $\lambda = 10$ m, $\alpha_L = 0.01$ m, $\alpha_T = 0.001$ m). The correlation scales (λ) of heterogeneity of the large scales are 500 m and 100 m respectively. The third scale of heterogeneity is smaller than the initial size of the plume.

The macrodispersion model in case 1 is able to predict spreading of the plume in case 2. In the absence of high-resolution data, a “coarse” heterogeneous field that incorporates macrodispersion can be used to predict the position and extent of plume spreading approximately. However, the macrodispersion model only predicts the general shape of the plume, and not the peaks and valleys of the plume.

Lack of data limits the ability to model small scales of heterogeneity. In such cases, an effective macrodispersion model with a large-scale trend can be used to obtain better results. From Section 4.1 it is obvious that eliminating smaller scales of heterogeneity from the model underestimates plume spreading. Incorporating smaller scales requires higher-resolution data, which is costly, and perhaps infeasible. When only larger scales are modeled, the detailed structure of the aquifer represented by the smaller scales of heterogeneity is averaged. In this process of averaging, considerable amount of detail is lost. These details are critical, and make a huge difference in the prediction of plume

spreading. However, it is possible to “retrieve” some of the detail using models such as Gelhar’s macrodispersion model.

6.2.4 Mathematical interpretation

The following equations show the relationship between pore-scale dispersion and macrodispersion:

$$\frac{\partial C}{\partial t} + \frac{\partial u_i C}{\partial x_i} = \frac{\partial}{\partial x_i} \left(D_{ij} \frac{\partial C}{\partial x_j} \right), \quad (6.2.1)$$

$$\frac{\partial \bar{C}}{\partial t} + \frac{\partial \bar{u} \bar{C}}{\partial x_i} = \frac{\partial}{\partial x_i} \left(D_{ij} \frac{\partial \bar{C}}{\partial x_j} + \left(-\overline{u_i' C'} \right) \right), \quad (6.2.2)$$

where:

C – Concentration

u_i – Seepage velocity

D_{ij} – Dispersion coefficient.

It can be shown (*Gelhar and Axness, 1983a*) that:

$$-\overline{u_i' C'} \approx A_{ii} \bar{u} \frac{\partial \bar{C}}{\partial x_i}. \quad (6.2.3a)$$

The coefficient A_{ii} is called macrodispersivity and is given by (*Gelhar, 1993*):

$$A_{11} = \sigma_{\ln K}^2 \lambda; \quad A_{22} = \frac{\sigma_{\ln K}^2}{8} (\alpha_L + \alpha_T), \quad (6.2.3b)$$

where:

$\sigma_{\ln K}^2$ – $\ln K$ variance

λ – Correlation scale

A_{11} – Longitudinal macrodispersivity

A_{22} – Transverse macrodispersivity

α_L – Longitudinal dispersivity

α_T – Transverse dispersivity.

Equation (6.2.3b) shows that the longitudinal macrodispersion is unaffected by pore-scale dispersion, whereas transverse macrodispersion is affected. Therefore, the magnitude of longitudinal macrodispersion is many orders of magnitude larger than the transverse macrodispersion. Substituting (6.2.3a) into (6.2.2):

$$\frac{\partial \bar{C}}{\partial t} + \frac{\partial \bar{u} \bar{C}}{\partial x_i} = \frac{\partial}{\partial x_i} \left(D_{ij} \frac{\partial \bar{C}}{\partial x_j} + \left(A_{ii} \bar{u} \frac{\partial \bar{C}}{\partial x_i} \right) \right), \quad (6.2.4)$$

$$\frac{\partial \bar{C}}{\partial t} + \frac{\partial \bar{u} \bar{C}}{\partial t} = (\alpha_{ij} + A_{ij}) \bar{u} \frac{\partial \bar{C}}{\partial x_i}. \quad (6.2.5)$$

The pore-scale dispersivity, α_{ij} , is typically one-hundredth of a meter, while the macrodispersivity, A_{ij} , is approximately one meter. Therefore, macrodispersion is the dominant process and controls the total spreading of the plume.

Equation (6.2.5) simplifies the complex heterogeneous field, represented by (6.2.2). A simple mean macrodispersion model is obtained by replacing the dispersion coefficient with a macrodispersivity value. This model can predict the mean spreading of the plume.

Table 6.2 Model parameters and inputs

Parameter	Case 1	Case 2
Mean hydraulic conductivity, K_g (m/day)	10	10
ln K variance (for all scales)	1.0	1.0
Scale 1 correlation scale, λ (m)	500	500
Scale 2 correlation scale, λ (m)	100	100
Scale 3 correlation scale, λ (m)	-	10
Porosity, n	0.3	0.3
Longitudinal pore-scale dispersivity (m)	NA	0.01
Transverse pore-scale dispersivity (m)	NA	0.001
Longitudinal macrodispersivity (m)	10	NA
Transverse macrodispersivity (m)	0.001625	NA
Head difference (m)	1	1
Size of model (m)	2000 x 500	2000 x 500
Covariance function	Gaussian	Gaussian
Approximate initial plume size (m)	100	100
Grid	801 x 201	801 x 201
Cell size, Δx (m)	2.5 x 2.5	2.5 x 2.5
Time step, Δt (days)	100	100

The model parameters and inputs are explained below:

- The ln K field is a normally distributed random field. Therefore, there is an equal probability of the plume encountering a ‘low’ K zone or a ‘high’ K zone.
- The heterogeneous conductivity field is uniquely characterized by the following set of statistical parameters: geometric mean (K_g) of K , correlation scale, variance and covariance.
- The geometric mean and ln K variance are constant for both cases.
- The first and second scales of heterogeneity are common to both cases, and have a correlation scale of 500 m and 100 m respectively.
- The third scale of heterogeneity is applicable only to cases 1 and 2, and has a correlation scale of 10 m.
- The covariance function for all cases is Gaussian.

- The cell size, Δx , is selected such that the correlation scale, λ , is resolved.
Typically, Δx is at least 3 to 4 times smaller than the correlation scale.
- The time step, Δt , is selected such that a particle of the plume travels a distance that is less than λ in one time step.

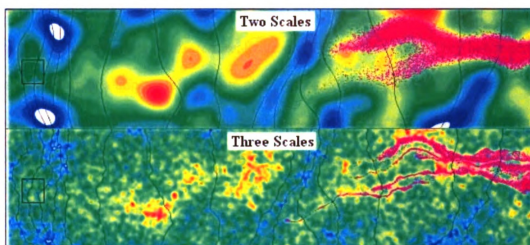


Figure 6.2 Snapshot of the visualization

For a detailed visualization, access the following address:

URL: <http://www.egr.msu.edu/igw/DL/SSH/SDT/SDT2.htm>

7 MONTE CARLO SIMULATIONS

7.1 EFFECTS OF HYDRAULIC CONDUCTIVITY HETEROGENEITY – DIFFERENT REALIZATIONS

7.1.1 Problem statement

This video demonstrates 4 different realizations of hydraulic conductivity heterogeneity. The spreading of a conservative solute plume through these realizations is shown. The modeling domain consists of constant head boundaries on the left and right extremes, and no-flow boundaries at the top and bottom. Details are provided in Table 7.1.

7.1.2 Key observations

The following observations can be made from the video:

- Despite the plume being larger than the scale of heterogeneity, different realizations cause significantly different plume spreading.
- The different plumes vary in all aspects, such as size, shape, mean displacement, and overall extent of spreading.

7.1.3 Additional observations and discussion

Even though all the realizations have the same set of statistical parameters, the eventual patterns of spreading exhibited by the plumes are significantly different. The plumes differ not only in their eventual extents of spreading, but also in their shape, size, and mean displacement. There is no way to compare the patterns of spreading of the different realizations using a generalization. However, if a large number of such realizations are considered, the mean of all those realizations will be a Gaussian distribution.

Uniquely characterizing the plume's behavior from a single realization is difficult. This uncertainty in plume behavior is a result of uncertainty in aquifer properties. Therefore, stochastic methods such as Monte Carlo simulations need to be used in order to perform a systematic probabilistic analysis that can be used for risk-estimation.

Table 7.1 Model parameters and inputs

Parameter	All Realizations
Geometric mean hydraulic conductivity, K_g (m/day)	10
$\ln K$ variance	2.0
Correlation scale, λ (m)	2
Porosity, n	0.3
Local dispersivity	0
Head difference (m)	1
Covariance function	Exponential
Approximate initial size of plume (m)	10
Grid	401 x 407
Cell size, Δx (m)	0.5 x 0.5
Time step, Δt (days)	1

The model parameters and inputs are explained below:

- The $\ln K$ field is a normally distributed random field. Therefore, there is an equal probability of the plume encountering a 'low' K zone or a 'high' K zone.
- The heterogeneous conductivity field is uniquely characterized by the following set of statistical parameters: geometric mean (K_g) of K , correlation scale, variance and covariance.
- The geometric mean, $\ln K$ variance, correlation scale (λ), and covariance function are constant for all cases.
- The cell size, Δx , is selected such that the correlation scale, λ , is resolved.

Typically, Δx is at least 3 to 4 times smaller than the correlation scale.

- The time step, Δt , is selected such that a particle of the plume travels a distance that is less than λ in one time step.

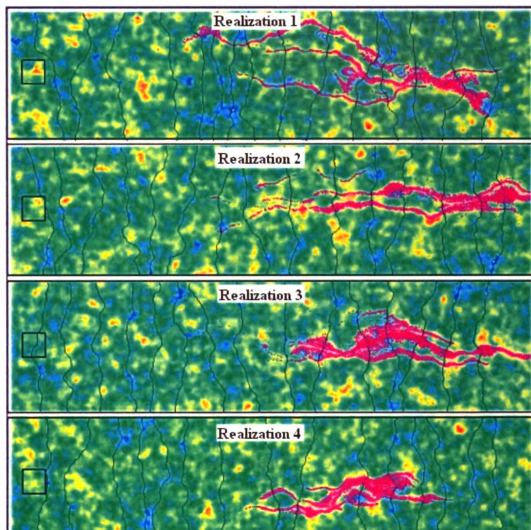


Figure 7.1 Snapshot of the visualization

For a detailed visualization, access the following address:

URL: <http://www.egr.msu.edu/igw/DL/SSH/IMCFTS/IMCFTS1.htm>

7.2 EFFECTS OF HYDRAULIC CONDUCTIVITY HETEROGENEITY – DIFFERENT REALIZATIONS

7.2.1 Problem statement

This video demonstrates 4 different realizations of hydraulic conductivity heterogeneity. The spreading of a conservative solute plume through these realizations is shown. The modeling domain consists of constant head boundaries on the left and right extremes, and no-flow boundaries at the top and bottom. Details are provided in Table 7.2.

7.2.2 Key observations

The following observations can be made from the video:

- The plume is of the same order as the scale of heterogeneity, different realizations cause drastically different plume spreading.
- The different plumes vary in all aspects, such as size, shape, mean displacement, and overall extent of spreading.

7.2.3 Additional observations and discussion

Even though all the realizations have the same set of statistical parameters, the eventual patterns of spreading exhibited by the plumes are drastically different. The plumes differ not only in their eventual extents of spreading, but also in their shape, size, and mean displacement. There is no way to compare the patterns of spreading of the different realizations using a generalization. However, if a large number of such realizations are considered, the mean of all those realizations will be a Gaussian distribution. Comparing the plume behavior with Section 7.1, it is obvious that the plumes become increasingly different with increasing correlation scale.

Uniquely characterizing the plume's behavior from a single realization is difficult. This uncertainty in plume behavior is a result of uncertainty in aquifer properties. Therefore, stochastic methods such as Monte Carlo simulations need to be used in order to perform a systematic probabilistic analysis that can be used for risk-estimation.

Table 7.2 Model parameters and inputs

Parameter	All Realizations
Geometric mean hydraulic conductivity, K_g (m/day)	10
$\ln K$ variance	2.0
Correlation scale, λ (m)	10
Porosity, n	0.3
Local dispersivity	0
Head difference (m)	1
Covariance function	Exponential
Approximate initial size of plume (m)	10
Grid	401 x 407
Cell size, Δx (m)	0.5 x 0.5
Time step, Δt (days)	1

The model parameters and inputs are explained below:

- The $\ln K$ field is a normally distributed random field. Therefore, there is an equal probability of the plume encountering a 'low' K zone or a 'high' K zone.
- The heterogeneous conductivity field is uniquely characterized by the following set of statistical parameters: geometric mean (K_g) of K , correlation scale, variance and covariance.
- The geometric mean, $\ln K$ variance, correlation scale (λ), and covariance function are constant for all cases.
- The cell size, Δx , is selected such that the correlation scale, λ , is resolved.

Typically, Δx is at least 3 to 4 times smaller than the correlation scale.

- The time step, Δt , is selected such that a particle of the plume travels a distance that is less than λ in one time step.

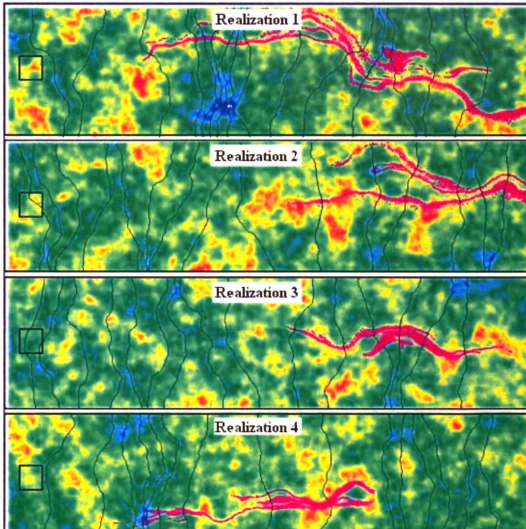


Figure 7.2 Snapshot of the visualization

For a detailed visualization, access the following address:

URL: <http://www.egr.msu.edu/igw/DL/SSH/IMCFTS/IMCFTS2.htm>

7.3 MONTE CARLO SIMULATION – MEAN, VARIANCE AND COVARIANCE

7.3.1 Problem statement

This video illustrates the statistical results (mean concentration, concentration variance, and the covariance structure of concentration at a point) obtained from a set of 500 realizations of a Monte Carlo simulation. The Monte Carlo simulation is generated for a random K field. The modeling domain consists of constant head boundaries on the left and right extremes, and no-flow boundaries at the top and bottom. Details are provided in Table 7.3.

7.3.2 Key observations

The following observations can be made from the video:

- Each realization is very different from other realizations; yet, the mean concentration after 500 realizations is predominantly uniform.
- The concentration variance obtained over 500 realizations is non-stationary, exhibits the “double peak” structure (*Graham and McLaughlin, 1989*).
Concentration variance increases with concentration gradient.
- The covariance structures are strongly “non-stationary,” since they are very different from each other at different points.

7.3.3 Additional observations and discussion

Mean concentration: Although each realization is dramatically different from other realizations, the statistical best estimate of concentration is given by the mean concentration obtained from all realizations. During the first few realizations, the mean concentration is strongly controlled by the concentration obtained from the realizations.

After ~50 realizations, the mean concentration approaches a uniform distribution.

Additional realizations cause little change to the mean concentration. At the end of 500 realizations, the mean concentration is predominantly uniform.

Concentration variance: The concentration variance during the initial realizations changes drastically with each realization, since the concentration for that realization has a significant impact on the variance. With increasing number of realizations, the variance begins to exhibit the “double-peak” structure (*Graham and McLaughlin, 1989*).

Downstream of the concentration source, the chance of obtaining a mean concentration away from the centerline of the source is low compared to along the centerline of the source. Therefore, the variance along the centerline is low, and higher away from the centerline, resulting in the double peak.

Covariance structure: Typically, a single covariance structure is used for a site. Such a procedure can lead to inaccuracies because the covariance is strongly non-stationary; i.e. it is dependent on the location. This can be seen from the covariance structure which is shown for 6 different points: (50,15), (50,25), (50,35), (70,15), (70,25), and (70,35).

Table 7.3.1 Model parameters and inputs

Parameter	All realizations
Geometric mean hydraulic conductivity, K_g (m/day)	10
ln K variance	2.0
Correlation scale, λ (m)	4
Porosity, n	0.3
Longitudinal pore-scale dispersivity (m)	0.01
Transverse pore-scale dispersivity (m)	0.001
Head difference (m)	1
Size of model (m)	150 x 50
Covariance function	Gaussian

Approximate initial plume size (m)	10
Grid	301 x 101
Cell size, Δx (m)	0.5 x 0.5
Time step, Δt (days)	2

The model parameters and inputs are explained below:

- The $\ln K$ field is a normally distributed random field. Therefore, there is an equal probability of the plume encountering a 'low' K zone or a 'high' K zone.
- The heterogeneous conductivity field is uniquely characterized by the following set of statistical parameters: geometric mean (K_g) of K , correlation scale, variance and covariance.
- The geometric mean and $\ln K$ variance are constant for all realizations.
- The correlation scale of heterogeneity is common for all realizations.
- The covariance function for all cases is Gaussian.
- The cell size, Δx , is selected such that the correlation scale, λ , is resolved.

Typically, Δx is at least 3 to 4 times smaller than the correlation scale.

- The time step, Δt , is selected such that a particle of the plume travels a distance that is less than λ in one time step.

Table 7.3.2 Maximum and minimum values for plotting

Parameter	Minimum	Maximum
Concentration covariance (ppm^2)	-350	1400
Concentration variance (ppm^2)	0	2000
Transmissivity (m^2/day)	1.5	5000

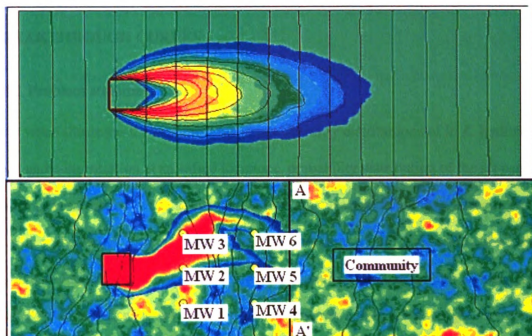


Figure 7.3 Snapshot of the visualization

For a detailed visualization, access the following address:

URL: <http://www.egr.msu.edu/igw/DL/SSH/IMCFTS/IMCFTS3.htm>

7.4 MONTE CARLO SIMULATION – PROBABILITY DISTRIBUTIONS AND BREAKTHROUGH CURVES

7.4.1 Problem statement

This video illustrates the statistical results (probability distributions of $\ln K$, hydraulic head and concentration at specified locations, probability distribution of the seepage flux across a cross-section of the aquifer, breakthrough curves of solute flux across a cross-section and concentration at a point) obtained from a set of 500 realizations of a Monte Carlo simulation. The Monte Carlo simulation is generated for a random K field. The modeling domain consists of constant head boundaries on the left and right extremes, and no-flow boundaries at the top and bottom. Details are provided in Table 7.4.

7.4.2 Key observations

The following observations can be made from the video:

- Although the $\ln K$ probability distribution function (PDF) over the modeling domain is Gaussian, the hydraulic head PDF at MW 6 is approximately Gaussian, though it is skewed.
- The concentration PDFs at MW 1, MW 2, MW 3, and MW 5 are very different from each other. All of them are skewed in different directions to varying degrees. While the PDF at MW 1, MW 3, and MW 5 are skewed towards low concentrations, MW 2 is skewed towards the higher concentration. This drastic difference means that MW 2 has a greater probability of a high concentration compared to MW 1, MW 3, and MW 5. It is more likely that the concentrations at MW 1 and MW 3 are low compared to MW 5.

- The seepage flux PDF at cross-section AA' obtained over 500 realizations is predominantly Gaussian.
- The solute flux breakthrough curve at cross-section AA' obtained over 500 realizations indicates that the average solute flux across AA' is ~ 2000 g/day, with a standard deviation of ~ 1000 g/day.
- The concentration breakthrough curve at Monitoring Well (MW 2) obtained over 500 realizations indicates that the average concentration at MW 2 is ~ 60 ppm, with a standard deviation of ~ 40 ppm.

7.4.3 Additional observations and discussion

Hydraulic head PDF: Since hydraulic head is almost linearly related to $\ln K$, hydraulic head PDF is also Gaussian.

Concentration PDFs: Concentration PDFs are strongly skewed, in either direction (low or high concentrations). Concentration is neither Gaussian nor lognormal. A normal distribution is characterized by a mean and a variance. Therefore, a mean and variance cannot be used to characterize uncertainty of concentration. In addition, concentration PDF is non-stationary, in the sense that it varies with respect to location.

Seepage flux PDF: Seepage flux PDF is almost Gaussian, though it appears to have a “flat peak.”

Solute flux breakthrough curve: The solute flux breakthrough curve obtained from 500 realizations, predicts a mean solute flux of ~ 2000 g/day with a standard deviation of ~ 1000 g/day.

Concentration breakthrough curve: The concentration breakthrough curve obtained from 500 realizations, predicts a mean concentration ~ 60 ppm with a standard deviation of ~ 40 ppm.

Table 7.4 Model parameters and inputs

Parameter	All realizations
Geometric mean hydraulic conductivity, K_g (m/day)	10
$\ln K$ variance	2.0
Correlation scale, λ (m)	4
Porosity, n	0.3
Longitudinal pore-scale dispersivity (m)	0.01
Transverse pore-scale dispersivity (m)	0.001
Head difference (m)	1
Size of model (m)	150 x 50
Covariance function	Gaussian
Approximate initial plume size (m)	10
Grid	301 x 101
Cell size, Δx (m)	0.5 x 0.5
Time step, Δt (days)	2

The model parameters and inputs are explained below:

- The $\ln K$ field is a normally distributed random field. Therefore, there is an equal probability of the plume encountering a 'low' K zone or a 'high' K zone.
- The heterogeneous conductivity field is uniquely characterized by the following set of statistical parameters: geometric mean (K_g) of K , correlation scale, variance and covariance.
- The geometric mean and $\ln K$ variance are constant for all realizations.

- The correlation scale of heterogeneity is common for all realizations.
- The covariance function for all cases is Gaussian.
- The cell size, Δx , is selected such that the correlation scale, λ , is resolved.
Typically, Δx is at least 3 to 4 times smaller than the correlation scale.
- The time step, Δt , is selected such that a particle of the plume travels a distance that is less than λ in one time step.

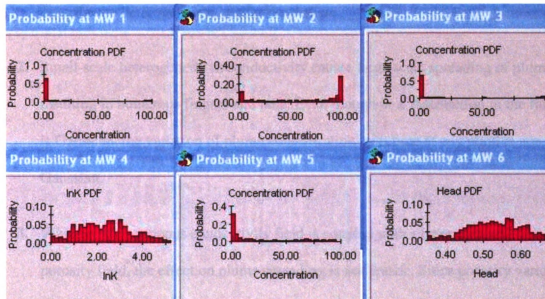


Figure 7.4 Snapshot of the visualization

For a detailed visualization, access the following address:

URL: <http://www.egr.msu.edu/igw/DL/SSH/IMCFTS/IMCFTS4.htm>

8 CONCLUSIONS

1. The subsurface environment is inherently heterogeneous, exhibiting dramatic variations over surprisingly small distances. Since it is practically impossible to measure these detailed point-to-point variations, heterogeneity translates into uncertainty. A random field representation characterized by statistics such as mean, variance, and covariance derived from data provides a systematic way to describe the heterogeneous aquifer properties.
2. Small-scale heterogeneity in conductivity causes large scale spreading of plume resulting in numerous fingers and tails. Even though $\ln K$ distribution in the field is Gaussian, the variation of plume concentration with time at any point is non-Gaussian.
3. When a heterogeneous conductivity field is coupled with a heterogeneous porosity field, the effect on plume spreading is not drastic. Since porosity varies over a small range of values compared to conductivity, the impact on velocity variability is minimal. When n and K are positively/negatively correlated, the plume is slightly smaller/larger compared to when n and K are not correlated.
4. When a heterogeneous conductivity field is coupled with partitioning coefficient, the effect on plume spreading is drastic. Since partitioning coefficient variability is comparable to that of conductivity, the impact on velocity variability is significant. When K_d and K are positively/negatively correlated, the plume is significantly smaller/larger compared to when K_d and K are not correlated.

5. Depending on the scale of the heterogeneity with respect to the initial size of the plume, the type of plume transport is significantly different. Usually, when the plume is larger than the scale of heterogeneity, plume spreading is considerably higher. However, when the plume is much smaller than the scale of heterogeneity, the plume travels predominantly along preferential channels, while not spreading by a great extent. When the plume is extremely small compared to the scale of heterogeneity, the plume undergoes “negative transverse dispersion.”
6. Temporal variability caused by seasonal fluctuations, in the absence of spatial heterogeneity, causes to and fro motion of the plume, which is reversible. Generally, the plume does not undergo extensive spreading. When temporal variability interacts with spatial heterogeneity, the effect on plume transport is drastic as the plume is shred into fingers and tails. In addition, the process cannot be reversed because the plume may get trapped in a low conductivity zone, which causes enhanced spreading of the plume. When additional heterogeneities, such as partitioning coefficient, are coupled together with temporal variability and spatial heterogeneity, the effect on plume spreading is compounded.
7. Heterogeneity in the real world is practically not deterministic. In order to model this highly complex variable conductivity field, a stochastic approach is used. In this approach, the aquifer structure is represented using a set of statistical parameters, such as mean, correlation scales, and variance. These statistical parameters are obtained by analysis of the data.

- Mean – Is the geometric mean of the data, which represents the average conditions that exist in the aquifer
- Correlation scales – Are a measure of the spatial distance across which the aquifer properties are supposed to be correlated. This parameter can be different in all three directions making the aquifer anisotropic. However, in most cases, the horizontal correlation scales (λ_x and λ_y) are assumed to be constant.
- Variance – Is a measure of how variable the aquifer properties are with respect to the mean. A higher variance means higher variability of aquifer properties and vice versa.

Using these properties, the aquifer can be described stochastically, which allows systematic probabilistic analysis.

8. Macrodispersion models predict the mean plume spreading and the overall extent of the plume. However, these models do not provide information on the maximum concentration, concentration variance and the degree of dilution.
9. Multiple scales of heterogeneity have a significant impact on plume spreading. Large scales of heterogeneity provide only a “trend” for plume transport, while the smaller scales spread the plume. If the smaller scales are not modeled, the spreading of the plume is significantly less. When the smaller scales are modeled using an effective macrodispersion model the model is able to predict the overall extent of the plume. However, this model does not provide information on the maximum concentration, concentration variance and the degree of dilution.

- 10.** Stochastic methods such as Monte Carlo simulations provide information on the mean plume behavior by statistically analyzing the plume characteristics obtained from an infinite number of realizations. Monte Carlo simulations can also provide information on the probability distribution function (PDF) of any parameter of interest, such as head, $\ln K$, concentration at a monitoring well, and seepage and solute flux across a cross-section of the aquifer.
- 11.** Although a Gaussian distribution of $\ln K$ characterizes the random field, the concentration PDF and solute flux PDF are strongly skewed. However, the head and seepage flux PDF across a cross-section are predominantly Gaussian. In the vicinity of stresses such as pumping wells, head and seepage flux PDF may not be Gaussian.
- 12.** If the concentration PDF is assumed to be Gaussian, a mean and variance will be sufficient to estimate the probability distribution. Since concentration PDF is strongly skewed, characterizing the uncertainty is difficult. If the concentration PDF is lognormal, it can be characterized using a mean and a variance. However, concentration is strongly location dependent, and a lognormal distribution does not hold good always. Therefore, variance is not a good measure of uncertainty for concentration PDF. Hence, the actual concentration PDF is needed to determine the variability at each point of interest.

9 REFERENCES

1. Bouwer, H., *Groundwater hydrology*, McGraw-Hill, Inc., 1978.
2. Ferris, J.G., Cyclic fluctuations of water level as a basis for determining aquifer transmissibility. *International Association of Hydrological Sciences*, Wallingford, UK, 33(2), 148–155, 1951.
3. Freeze, R.A., and J.A.Cherry, *Groundwater*, Prentice-Hall, Englewood Cliffs, NJ, 1979.
4. Gelhar, L.W., *Stochastic subsurface hydrology*, Prentice-Hall, Englewood Cliffs, NJ, 1993.
5. Gelhar, L.W., and C.L. Axness, Three-dimensional stochastic analysis of macrodispersion in aquifers, *Water Resources Research*, 19(1), 161-180, 1983a.
6. Graham, W. and D. McLaughlin, Stochastic analysis of nonstationary subsurface solute transport, 1. Unconditional moments, *Water Resources Research*, 25(2), 215-233, 1989.
7. Li, S. G. and Q. Liu, Interactive Ground Water (IGW): An Innovative Digital Laboratory For Groundwater Education and Research, *Computer Applications in Engineering Education*, 2003, 11(4), 179-202, 2003.
8. Li, S. G. and Q. Liu, "A New Paradigm for Groundwater Modeling" (In review)
9. Paulson, K.J., and S.G. Li, *Interactive Groundwater Users Manual*, Department of Civil and Environmental Engineering, Michigan State University, 2002.
10. Sudicky, E. A., A natural gradient experiment on solute transport in a sand aquifer: Spatial variability of hydraulic conductivity and its role in the dispersion process, *Water Resources Research*, 22(13), 2069-2082, 1986.

MICHIGAN STATE UNIVERSITY LIBRARIES



3 1293 02845 2369